N° d'ordre :
N° de série :

A thesis submitted in fulfillment of the requirements for the degree of

MASTER

Domain: *Sciences and Technologies*

Branch: *Mechanical Engineering*

Specialty: *Renewable Energies in Mechanics*

Theme

Design and Optimization of a New Passive Building Cooling System Using Water Evaporation: A Numerical and Experimental Approach Guided by Artificial Intelligence

By :

BEN KINA Nesrine

Defended publicly on /06/2025

In front of the jury:

Name	Rank	Univ. Ghardaïa	President
Name	Rank	Univ. Ghardaïa	**Examiner**
Name	Rank	Univ. Ghardaïa	**Examiner**
AISSAOUI Fares	MCA	Univ. Ghardaïa	**Supervisor**
HACENE Nacer	MCA	Univ. Ghardaïa	**Co-Supervisor**

Academic year 2024/2025

Dedication

To my first refuge, my first admirer, and my first support...
To myself—the one who stood firm despite everything.

To my family, my source of warmth and safety, my eternal shelter in moments of fragity.

To those who were the light when the path darkened,
The support when my steps faltered,
To those who believed in me before I believed in myself...

To everyone who taught me a letter, and to those who planted unforgettable lessons within me,
To all my professors and mentors, who gifted me the light of knowledge and boundless horizons.

To my dearest friend, my solace in solitude, my companion on this journey:
Hiba
You were home when cities felt like a maze.

To every station I've passed through,
To every doubt I've fought,
And every thought that lit the darkness of questioning...

To knowledge,
That steadfast companion,
Who grants its gifts only to the worth

Acknowledgment

Praise and gratitude be to Allah until praise reaches its utmost end… To Him belongs all glory, from beginning to end.

Praise be to Allah for the people who were our support in stumbles, And our refuge in moments of fading light.

To all my family members, my brothers and sisters, To my friends who were the light on this long path— My sincere and deepest gratitude.

To my honorable teachers who illuminated my path of knowledge, And to my university, which embraced me and gifted me The learning and opportunities I cherish…

A special and heartfelt thank you to my esteemed supervisors: Dr. Issaoui Farès, my principal advisor, and Dr. Hacen Nacer, my assistant advisor— who were the guiding light in every step I took, the steady support in every moment of doubt. Without their unwavering encouragement and wisdom, this work would not have come to completion.

"For gratitude is the most beautiful thing one can say When words fail to repay kindness."

Thank you, from the depths of my heart.
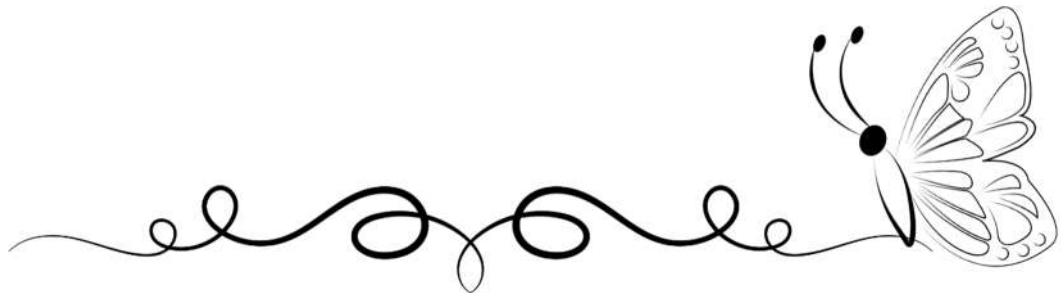
Abstract

This thesis presents the design, optimization, and experimental validation of a passive evaporative cooling system for buildings, utilizing natural plant fibers, specifically cotton and sisal as eco-friendly evaporative pads. The study aims to provide a sustainable, low-energy alternative to conventional cooling technologies by combining traditional passive cooling principles with modern analytical tools and artificial intelligence.

Two system configurations were evaluated: a basic prototype and an improved model featuring enhanced thermal insulation, water recovery, and real-time performance monitoring. Experimental tests were conducted under varying airflow rates and pad thicknesses to assess thermal performance, cooling effectiveness, and water consumption. Cotton demonstrated superior water retention and cooling performance, while sisal offered greater airflow permeability and structural durability.

Numerical analysis using Python and psychrometric modeling enabled detailed evaluation of heat and mass transfer within the system. Additionally, preliminary AI models based on Random Forest regression were developed to predict system behavior under changing conditions, supporting the feasibility of intelligent, adaptive cooling solutions.

The results confirm that material properties, pad geometry, and airflow significantly affect system efficiency. The final prototype represents a low-cost, scalable solution for passive building cooling, with potential for integration into smart building infrastructures. This work contributes to the advancement of environmentally responsible cooling technologies and lays the groundwork for future AI-driven passive systems.

Keywords: Passive cooling, Evaporative cooling, Natural fibers, Artificial intelligence, Sustainable buildings

Résumé

Ce mémoire présente la conception, l'optimisation et la validation expérimentale d'un système de refroidissement passif par évaporation destiné aux bâtiments, en utilisant des fibres végétales naturelles, principalement le coton et le sisal comme matériaux écologiques pour les panneaux évaporatifs. L'objectif est de proposer une alternative durable et à faible consommation énergétique aux systèmes de refroidissement classiques, en combinant les principes du refroidissement passif avec des outils modernes d'analyse numérique et l'intelligence artificielle.

Deux configurations du système ont été évaluées : un prototype de base et une version améliorée intégrant une isolation thermique renforcée, un système de récupération d'eau et un dispositif de surveillance en temps réel. Des tests expérimentaux ont été menés sous différentes vitesses d'air et épaisseurs de panneaux afin d'évaluer les performances thermiques, l'efficacité de refroidissement et la consommation en eau. Le coton s'est distingué par sa capacité supérieure de rétention d'eau et de refroidissement, tandis que le sisal a offert une meilleure perméabilité à l'air et une durabilité structurelle.

Une analyse numérique basée sur le langage Python et des calculs psychrométriques a permis une modélisation détaillée des transferts de chaleur et de masse. Par ailleurs, des modèles

d'intelligence artificielle, utilisant la régression par forêts aléatoires, ont été développés pour prédire le comportement du système en fonction des variations environnementales, renforçant ainsi la faisabilité de solutions de refroidissement intelligentes et adaptatives.

Les résultats confirment que les propriétés des matériaux, la géométrie des panneaux et le débit d'air influencent fortement l'efficacité du système. Le prototype final constitue une solution économique et évolutive pour le refroidissement passif des bâtiments, avec un fort potentiel d'intégration dans les infrastructures intelligentes. Ce travail apporte une contribution significative à l'évolution des technologies de refroidissement respectueuses de l'environnement et ouvre la voie à de futurs systèmes passifs guidés par l'intelligence artificielle.

Mots-clés : Refroidissement passif, Refroidissement par évaporation, Fibres naturelles, Intelligence artificielle, Bâtiments durables

ملخص

تتناول هذه المذكرة تصميم وتحسين وتقييم نظام تبريد سلبي بالتبخر مخصص للمباني، باستخدام ألياف نباتية طبيعية، تحديدًا القطن والسيزال، كمكونات صديقة للبيئة في وسائط التبريد. يهدف هذا العمل إلى تقديم بديل مستدام ومنخفض الاستهلاك للطاقة مقارنة بأنظمة التبريد التقليدية، وذلك من خلال الجمع بين مبادئ التبريد السلبي التقليدي وأدوات التحليل الحديثة وتقنيات الذكاء الاصطناعي.

تم اختبار نسختين من النظام: النموذج الأساسي، ونموذج مطور يتميز بعزل حراري محسّن، ونظام لاسترجاع المياه، وآلية لمراقبة الأداء في الزمن الحقيقي. أُجريت تجارب عملية تحت معدلات مختلفة لتدفق الهواء وسماكات متنوعة لوسادة التبريد، لتقييم الأداء الحراري وفعالية التبريد ومعدل استهلاك المياه. وقد أظهر القطن أداءً أفضل في امتصاص المياه والترطيب، بينما تميز السيزال بقدرة نفاذية أعلى للهواء ومتانة ميكانيكية وتبريد أفضل.

كما أُجري تحليل عددي باستخدام لغة Python ومعادلات نفسية حرارية لدراسة انتقال الحرارة والكتلة داخل النظام. وتم أيضًا تطوير نماذج أولية باستخدام خوارزمية "الغابات العشوائية" من الذكاء الاصطناعي للتنبؤ بأداء النظام تحت ظروف مناخية متغيرة، مما يبرز إمكانية تطوير أنظمة تبريد ذكية وقابلة للتكيف.

أكدت النتائج أن خصائص المواد، وهندسة الوسادة، ومعدل تدفق الهواء، لها تأثير كبير على كفاءة التبريد. ويمثل النموذج النهائي نظامًا منخفض التكلفة وقابلًا للتوسعة لتبريد المباني بطريقة سلبية، مع إمكانية دمجه في بنى تحتية ذكية. يسهم هذا العمل في تطوير تقنيات التبريد البيئية، ويمهد الطريق نحو أنظمة تبريد مستقبلية تعتمد على الذكاء الاصطناعي.

الكلمات المفتاحية: التبريد السلبي، التبريد بالتبخر، الألياف الطبيعية، الذكاء الاصطناعي، المباني المستدامة

Table of Contents

List of Figures

List of Tables

Common Heat Transfer Equations and Symbols

Symbol	Description	Equation
Q (convection)	Heat transfer by convection	$Q = h \times A \times (T_s - T\infty)$
h	Convective heat transfer coefficient	—
A	Surface area	—
T_s	Surface temperature	—
$T\infty$	Ambient temperature	—
Q (conduction)	Heat transfer by conduction	$Q = \lambda \times A / L \times (T_1 - T_2)$
λ	Thermal conductivity	—
L	Thickness or length of material	—
Q (radiation)	Heat transfer by radiation	$Q = \varepsilon \times \sigma \times A \times (T_s^4 - T\infty^4)$
ε	Emissivity of the surface	—
σ	Stefan-Boltzmann constant	5.67×10^{-8} W/m²·K⁴
Q (evaporation)	Heat from phase change	$Q = m \times L$ or $Q = \dot{m} \times L$
L	Latent heat of vaporization	—
m / $\dot{m}$	Mass or mass flow rate of evaporated liquid	—

General Technical and Thermal Terms

Acronym	Full Form
DEC	Direct Evaporative Cooling
InDEC	Indirect Evaporative Cooling
RH	Relative Humidity
SEER	Seasonal Energy Efficiency Ratio
EER	Energy Efficiency Ratio
HVAC	Heating, Ventilation, and Air Conditioning
$\dot{m}$	Mass Flow Rate
Tout	Outlet Temperature
Tin	Inlet Temperature
Hin	Outlet relative humidity
Hout	Inlet relative humidity
Tv	Water temperature
Vv	Water volume
tp	Pad Thickness
Qair	Heat Absorbed by Air
LHV	Latent Heat of Vaporization
Cpa	Specific Heat Capacity of Air
Cpg	Specific Heat Capacity of Vapor
ΔP	Pressure Difference
CAD	Computer-Aided Design
3D	Three-Dimensional

AI, Modeling, and Prediction Terms

Acronym	Full Form	Description
AI	Artificial Intelligence	Simulation of human intelligence by machines.
ML	Machine Learning	A subset of AI that involves learning patterns from data.
RF	Random Forest	A machine learning algorithm using ensemble decision trees.
R^2	Coefficient of Determination	Indicates how well data fits a regression model.
MAE	Mean Absolute Error	Average of absolute errors between predicted and actual values.
MSE	Mean Squared Error	Average of the squares of errors.
RMSE	Root Mean Square Error	Square root of MSE; commonly used to measure prediction accuracy.

INTRODUCTION

Introduction

In the impact of carbon dioxide emissions and the increasing trend towards renewable energies, passive cooling systems have also received their share of this attention despite the presence of old environmentally friendly cooling technologies due to the demand for alternative solutions with the increasing climate change. This is due to the environmental impacts of common cooling systems from carbon dioxide emissions and energy consumption. Today, the world is moving towards using technologies with a friendly environmental impact and lower energy consumption. Artificial intelligence has also received its share in the field of renewable energies in general.

Passive cooling means using building design and materials to control temperature in hot weather. To be comfortable, buildings around the world require some form of cooling at some time of the year, and this need increases as the climate warms. There are two basic components to passive cooling: cooling the building, and cooling the people [1].

Passive cooling uses free renewable energy sources such as the sun and wind to provide cooling, ventilation and lighting needs, and eliminates the need for mechanical cooling. Implementing passive cooling means reducing the differences between outside and inside temperatures, improving indoor air quality and making a building a better and more comfortable environment to live or work in. It can also reduce energy use levels and environmental impacts such as greenhouse gas emissions. Interest in passive design for both heating and cooling has grown recently as part of the movement towards sustainable architecture [2].

There are several limitations associated with passive cooling technologies in buildings. These may be the main reason for abandoning these technologies. The limitations depend on the criteria governing the good performance of passive cooling technologies and the challenges of each passive cooling device are proposed according to the incompatibility with spatial availability (availability of sources, topography, soil characteristics, allowed built-up area, etc.), economic barriers (high cost of the passive technology itself, durability of the passive technology over time, maintenance cost, etc.), or planning and architectural legislation [4].

With the increasing convergence of smart buildings and the use of AI, there is great value in developing a centralized analytics platform to provide more insights from the collected data. AI monitors, collects information, controls, assesses, and manages energy consumption in buildings;

controls and reduces energy use during peak hours, identifies and flags problems, and detects equipment failures before they occur. AI-based approaches can facilitate active customer engagement in demand response programs using machine learning algorithms and leveraging blockchain to protect data. While heating, ventilation, and air conditioning (HVAC) systems provide indoor comfort, they also contribute to staggering levels of energy consumption. AI-driven passive cooling provides an indispensable element of resilience to the world's new energy system of the future [5].

Python is a high-level, open-source programming language that is widely recognized for its simplicity, readability, and versatility. It was first developed in 1991 by Guido van Rossum [6]. Python's clear and concise syntax, resembling natural language, makes it accessible to both beginners and professionals. It is extensively used in scientific research, data analysis, artificial intelligence, and software development [7]. Additionally, Python has a rich ecosystem of libraries and frameworks that support a wide range of technical and scientific applications.

Among its key features are:

- Easy-to-read and maintain code
- Support for multiple programming paradigms (object-oriented, functional, procedural)
- A vast and active developer community
- Compatibility and integration with other languages and tools
- A broad set of libraries for specialized tasks [8].
- Python's main functions and applications include:
- Data analysis and manipulation, using libraries like Pandas and NumPy
- Machine learning and artificial intelligence, via Scikit-learn, TensorFlow, and Keras
- Computer vision and image processing, through OpenCV
- Simulation and numerical modeling of complex physical or engineering systems
- Data visualization, with tools like Matplotlib, Seaborn, and Plotly
- Automation of repetitive tasks and scripting

Web application development, using frameworks like Flask and Django

Embedded systems and Internet of Things (IoT) projects, using platforms such as Raspberry Pi

- Statistical analysis and experimental data processing
- Desktop application development with graphical user interfaces (Tkinter, PyQt)
- Automated testing and quality assurance, through tools like pytest
- Big data processing with tools integrated into environments like Hadoop and Spark [9].

The integration of Python in scientific research and technical projects significantly enhances the modeling, simulation, prediction, and optimization processes, making it an essential tool for modern engineering and intelligent system development [10].

Although passive cooling systems using water vapor provide an alternative solution for low energy, they suffer from numerous limitations, such as dependency on environmental conditions and the inability to dynamically control performance. In addition, these systems lack smart technologies for data analysis and performance adjustment in line with climate changes. Therefore, through this project, we aim to renew and innovate a passive cooling system based on artificial intelligence.

To solve these problems, several hypotheses were proposed to design a new evaporative cooling system for buildings. These hypotheses included:

- Airflow potential to affect device performance
- Evaporative pad characteristics and type
- Evaporative pad thickness and size
- Random device performance without control or monitoring

High water consumption, resulting in longer operation of the water pump and consequently greater consumption of both energy and water

To examine these hypotheses, in this thesis, we have studied an evaporative cooling system for buildings as follows:

Chapter One: A theoretical study of passive evaporation systems and the physics of heat transfer. In this chapter, we have discussed the known traditional passive cooling techniques, focusing on evaporative cooling, in addition to the basics of heat transfer associated with cooling systems, including evaporation.

Chapter Two: We will discuss the properties of cellulosic plant fibers as a cheap and readily available alternative that can be used as evaporative pads. We will learn about the various known plant fibers that can be used as evaporative pads and which families their chemical and physical properties belong to.

Chapter Three: A practical experiment with a evaporative air cooler. We will conduct In the innovation space at the University of Ghardaia, in order to verify the validity of the hypotheses that we have put forward, we will measure the temperature, humidity, air pressure, and evaporated water mass and record them in a table to apply mathematical modeling and apply the laws used for cooling and heat transfer systems.

Chapter Four: Numerical analysis of previously recorded measurements. We will first calculate the results using Python libraries such as Pandas and Numpy. Then, based on them, we will develop solutions to design a new passive evaporative cooling system for buildings.

Chapter Five: Based on the obtained data and the AI prediction algorithms Random Forest Regressor, in order to adapt to the data and provide fully hand-coded solutions, the performance of the new system was verified in different environments in order to know the future behavior of the new system and thus a new realistic prototype was created.

Finally, a comprehensive conclusion will synthesize the key findings of this study, highlight their significance, and outline potential avenues for future research or practical application.

Chapter 1

Mechanisms of Heat Transfer and Passive Cooling in Sustainable Building Design

Chapter 1

Mechanisms of Heat Transfer and Passive Cooling in Sustainable Building Design

1.1 Introduction

Passive cooling is a comfortable, cheap, and energy-efficient way tokeep the indoor environment within the comfortable temperature range in many climates, particularly in continental locations.[11]

It is a building design approach that allows the temperature of the building to be controlled, improving indoor thermal comfort with little or no energy consumption. It typically prevents heat from entering the building or removes unnecessary heat from the building.

the use of shade and blinds and night air. Common building components, such as insulation, overhangs and energy-efficient windows are other factors that work in the case of passive cooling. Today, many people prefer to build a new home with a passive cooling design.

In this chapter, we will review the main heat transfer mechanisms, including evaporation, and the types and techniques of passive cooling..

1.2 passive cooling technics

Passive cooling strategies can reduce the load on air conditioning by as much as 80%, report researchers [12].

Water vapor cooling, radiant cooling, floor cooling, shade cooling, natural ventilation cooling are all basic passive building cooling technologies.

1.2.1 Radiative cooling

is known as a passive cooling technology with minimal energy consumption, compared to traditional cooling technologies that require energy sources and discharging waste heat into the surrounding areas.It is a thermal radiation process that carries heat energy. When a hot object and a cold object undergo radiative exchange, there is a net heat flow from the hot to the cold object [13]. Such a heat flow by thermal radiation leads to radiative cooling ; Radiative cooling happens in our everyday life.
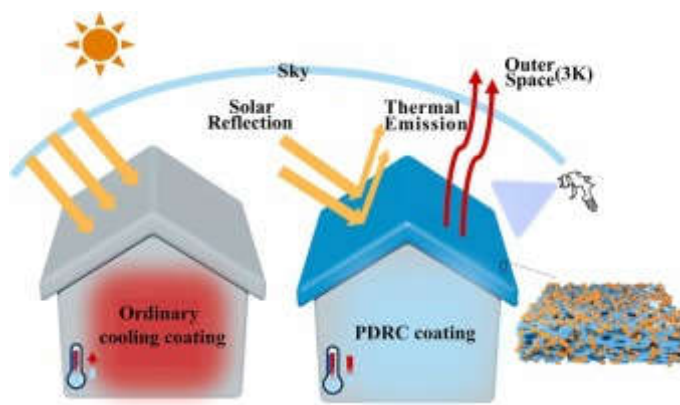
Figure 0-1 Illustration of Radiative Cooling Mechanism [09]

1.2.2 Shading cooling

Shading systems are part of the solar control systems specified in the same standards. A common shading device is one that, by regulating or blocking incoming solar radiation appropriately, creates a pleasant indoor environment, thereby reducing the cooling or heating load of a room and selectively allowing natural light and landscape. Sunlight can create a significant increase in cooling loads in the summer due to internal heat gain from solar radiation, although through window glass it helps reduce heating requirements in the winter. As a result, by using shading devices and supplementing weaker sections of windows in the summer, it is possible to reduce energy consumption while still creating a comfortable indoor environment ; one of the means of shade cooling is trees [14].
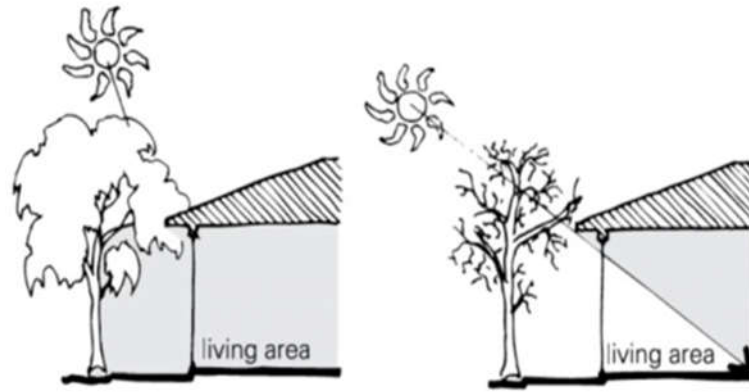
Figure 0-2 Types of Shading Devices for Passive Cooling [15]

1.2.3   Thermal mass

Thermal mass is the ability of a material to absorb and release heat after storing it. Materials such as concrete, bricks, and tiles absorb and store heat.Thermal mass can be used to keep the house cool in the summer. If the sun is blocked from reaching the block through shading, for example, the block will instead absorb heat from inside the house. You can then allow cool breezes and convection currents to pass over the thermal mass throughout the night to draw out the stored energy [16].
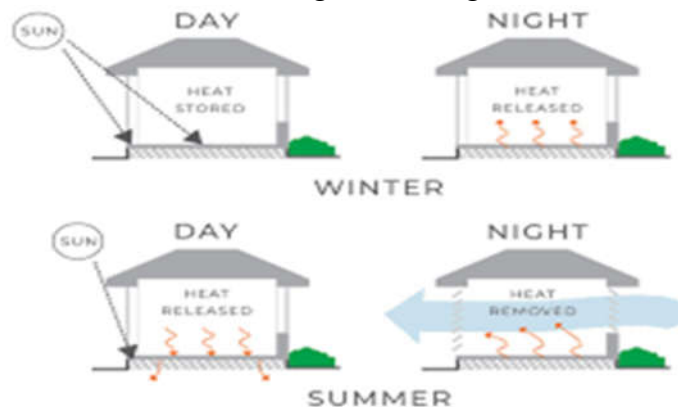
Figure 0-3 Thermal Mass Operation in Heat Storage and Release [17]

1.2.4 Earth cooling

It is also called heat exchangers; it is known that the temperature of the earth's interior remains constant, as in the summer the temperature of the earth's surface is higher than the temperature of the earth's interior, so a certain depth is dug and pipes are provided underground and connected to the buildings. The heat exchange resulting between the temperature of the earth's surface and the temperature of the earth's interior allows the buildings to be cooled in the summer [18].
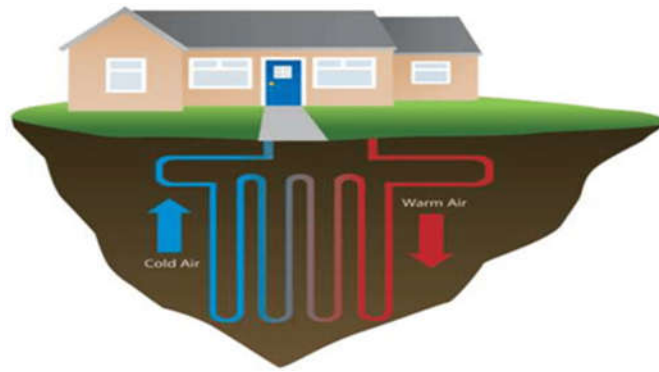
Figure 0-4 Earth Tube Cooling System Concept [19]

.

1.2.5   Evaporative Cooling

Evaporative cooling is the process by which the air temperature is lowered by the evaporation of water within the air stream. During the evaporation process, the water requires a relatively high temperature that is obtained from the surrounding air. This results in a decrease in the air temperature after this process.[20]
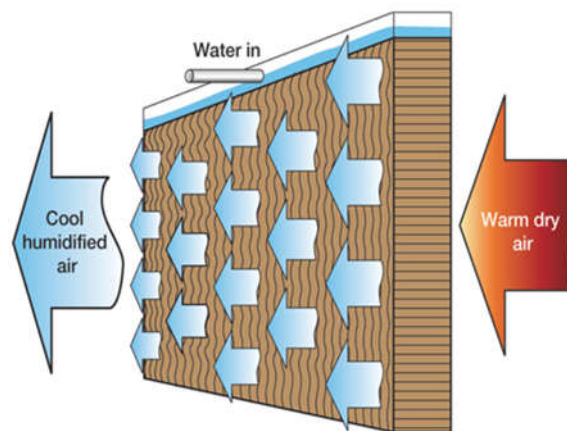
Figure 0-5 Direct Evaporative Cooling Process [21]

1.2.6 Natural ventilation

Natural ventilation is a method of supplying fresh air to a building or room by passive forces, usually by wind speed or differences in pressure inside and outside.[22]
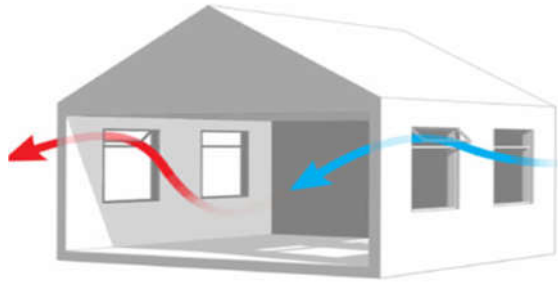
Figure 0-6 Natural Ventilation Diagram in Building Design [23]

1.3 Evaporative Cooling System :

Evaporative cooling is a natural and energy-efficient method of reducing air temperature by evaporating water into the air. When water evaporates, it absorbs heat from the surrounding environment, which results in a noticeable drop in temperature. This method is particularly effective in hot and dry climates, where the low humidity allows for maximum evaporation .

1.3.1 Definition of Evaporative Cooling

Evaporation is the process by which a fluid changes from a liquid state to a gaseous state; evaporative cooling is the process by which a liquid changes from a liquid to a vapor by absorbing high heat in the surrounding air and thus cooling it [24].

1.3.2 Principle of work

The working principle of evaporative cooling is based on the natural process of water evaporation. When hot, dry air passes over or through a wet surface, the water absorbs heat from the air to evaporate. This absorption of heat causes the temperature of the air to drop. The cooled, moist air is then circulated into the space that needs to be cooled. The effectiveness of this process depends on the air's initial temperature and humidity level—the drier and hotter the air, the more effective the cooling.

1.3.2.1 Direct Evaporative Cooling

In this system , there is direct contact between the ambient air and water , the moisture on the surface evaporates and the temperature of the ambient air decreases. The cooling efficiency of this system increases as the ambient temperature increases and the relative humidity decreases [25].
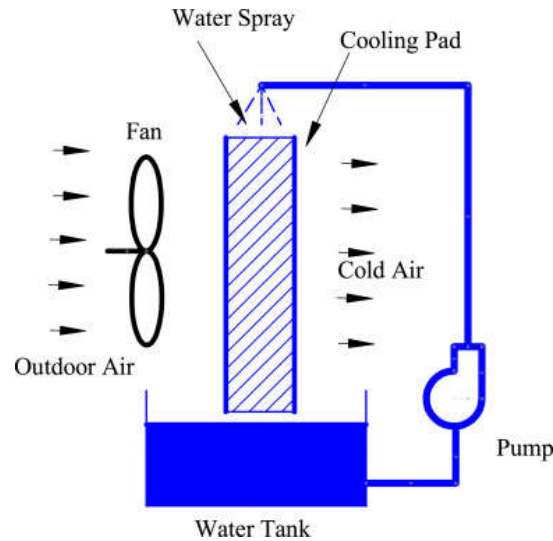
Figure 0-8 DEC chematic device[26]
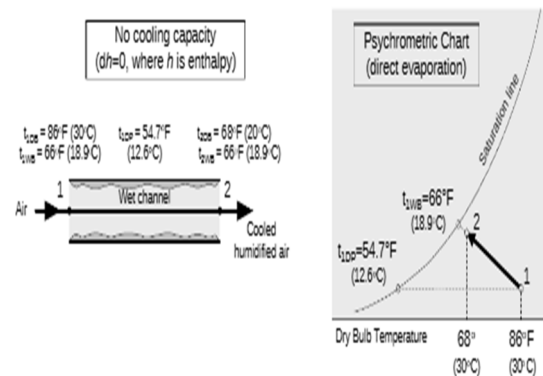
Figure 0-7 DEC psychrometric chart [27]

1.3.2.2   Indirect Evaporative Cooling :

Indirect evaporative cooling works on the same principle as direct evaporative cooling by reducing the air temperature by causing water to evaporate by adding a heat exchanger to cool the outside air, Instead, thermal change is produced between two air flows, not one [28].
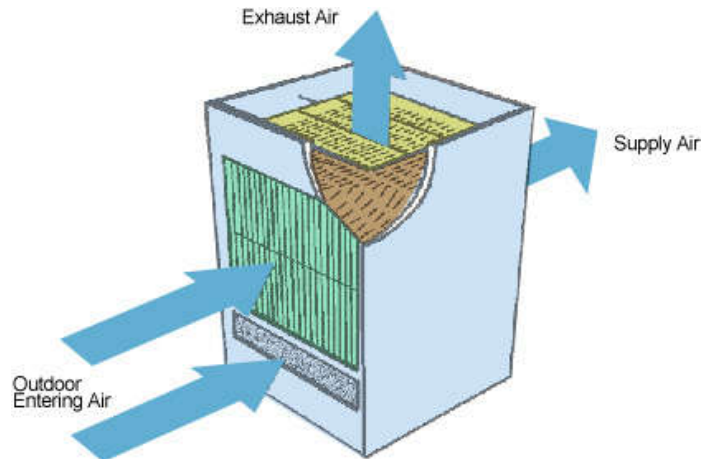
Figure 0-10 InDEC chematic device [29]
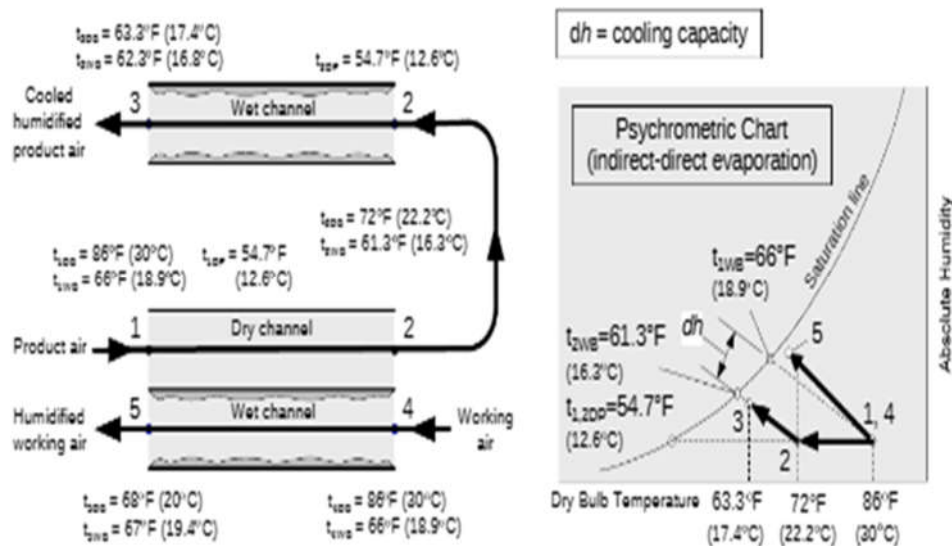
Figure 0-11 indirect EC psychcrometric chart [27]

1.3.2.3   Mixed evaporative cooling

Due to the shortcomings of both direct and indirect evaporative cooling systems, they are often marketed as "hybrid" systems that use a secondary VCS stage to address this capacity limitation, with an additional increase in operating and installation costs. Despite the efficient design, fully indirect evaporative systems are more energy efficient, providing significant energy savings with temperatures lower than the inlet fluid temperature [30].
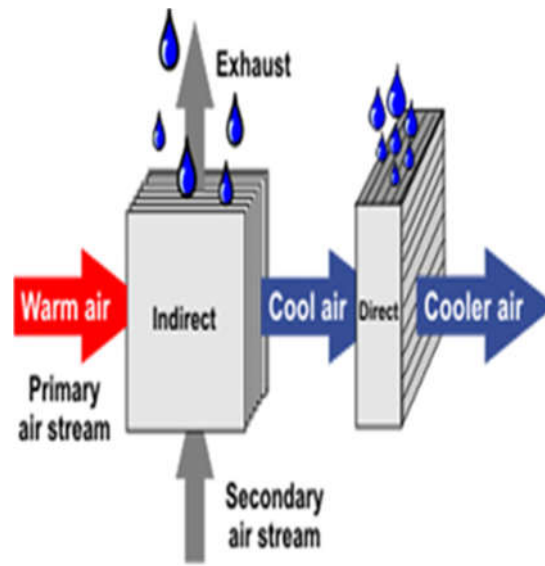
Figure 0-14 Mixed evaporative cooling chematic diagram [31]
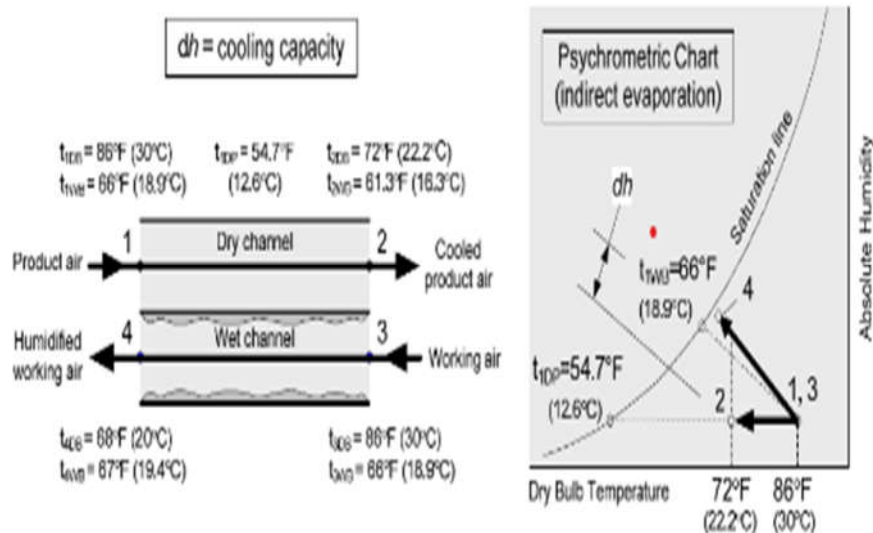
Figure 0-13 Mixed evaporative cooling psychcrometric chart [27]

1.3.2.4 Dew point evaporative cooling

Dehumidification – increasing the evaporative cooling potential of the working air upstream of the direct and/or indirect evaporator, using a desiccant and/or selective membrane. , can be achieved using a novel heat exchanger and flow path arrangement, delivering unhumidified air below wet bulb temperatures while consuming less water than other evaporative coolers. In some cases, supply air temperatures approaching the dew point temperature are achieved in a single-stage unit with cooling capacity independent of the ambient air dry bulb temperature.[32].
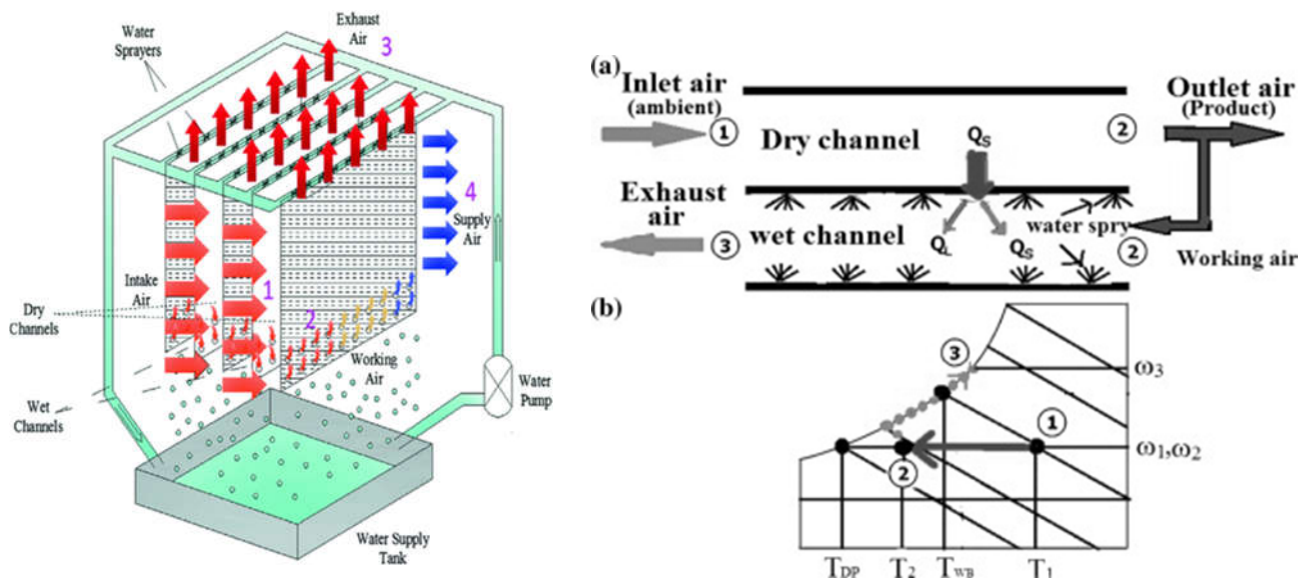
Figure 0-15 Dew point evaporative cooling system [33][27]

1.3.3   Evaporating fluid properties

Water is the best choice for evaporative cooling due to its abundance in nature and its chemical and physical properties, which are:

- 1Chemically, water consists of two hydrogen atoms and one oxygen atom. It is an odorless and colorless liquid, which makes it a better choice for this process.
- One of the physical properties of water is that it freezes at 0 degrees and boils at 100 degrees.
- Specific heat capacity can be described as the amount of heat required for raising the temperature of any substance. The specific heat capacity of water is 4.2 joules per gram at a temperature of 25°C. The specific heat capacity of water is very high.

- 1 gm/cc is the density of the water. Although, the density of water differs with temperature and is different for various states. In the solid-state, it is density remains 0.9gm/cc.

- Viscosity can be described as an amount of resistance used for deformation at the given rate. If explained in other words, it can be defined as the thickness of any substance. The viscosity of water is 0.89 cP (centipoise).

- . The surface tension of water is high and equals 72 mN/m at the temperature of 25°C. Due to the water's high surface tension, any insect cannot walk on it without hindrance.

- . At the temperature of 20°C, the refractive index of water is 1.333 [34].

1.4   Heat transfer from the refroidissement process

Heat transfer includes any or all of the many types of phenomena and mechanisms that transfer energy and entropy from one place to another. These are commonly referred to as convection, thermal radiation, and conduction [35].

1.4.1 convection

Convection is the method of transferring energy resulting from moving materials in the environment. A more precise concept is the flow of thermal energy from an area of high temperature to an area of low temperature through the movement of fluid. [36]
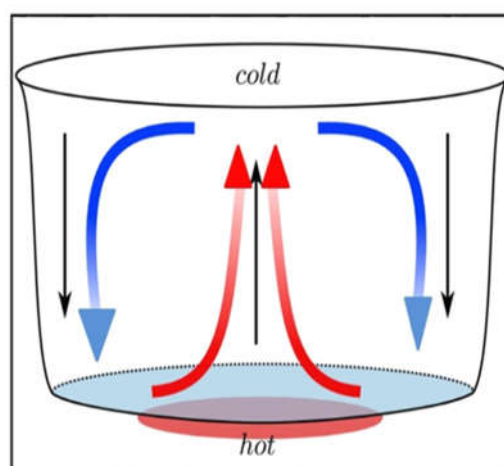
Figure 0-16 Diagram of convection[37]

1.4.1.1   Convection equation's :

$$Q = h.s.(t_1 - t_0)$$

Q : heat transfer rate (W) ;

h : the heat transfer coefficient (w/m².k) ;

S : Surface (m²) ;

T_1 is the surface temperature and T_0 is the ambient temperature(K) ;

1.4.1.2   Natural Convection

In a natural thermal convection , fluid movement occurs by natural means given that the speed of liquid associated with natural thermal pregnancy is relatively low, the heat transfer coefficient that it faces in the natural thermal load is also low.

When something or a warm person we call "A" is exposed to cold air, for example, the "A" temperature will decrease as a result of the heat transportation with cold air while we will increase the temperature of the adjacent thing to "A"; it means that "A" is surrounded by a thin layer of warm air that changes By thermal convection. The temperature adjacent to "A" is higher and therefore its density is lower. We call the rise of hot air natural convection [38].
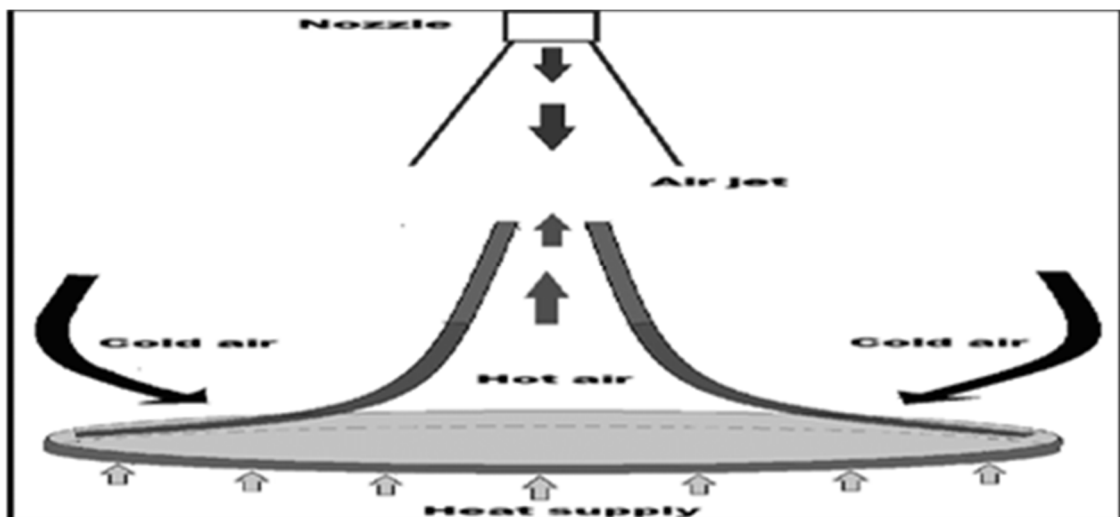
Figure 0-17 Natural convection heat transfer from a hot body to the surrounding cool [39]

1.4.1.3   Forced convection

Forced convection is a special type of heat transfer , An external force is applied that forces the fluid to move and exchange heat Forced heat transfer is adopted to increase the efficiency of heatxchange and speed up the process [40] .
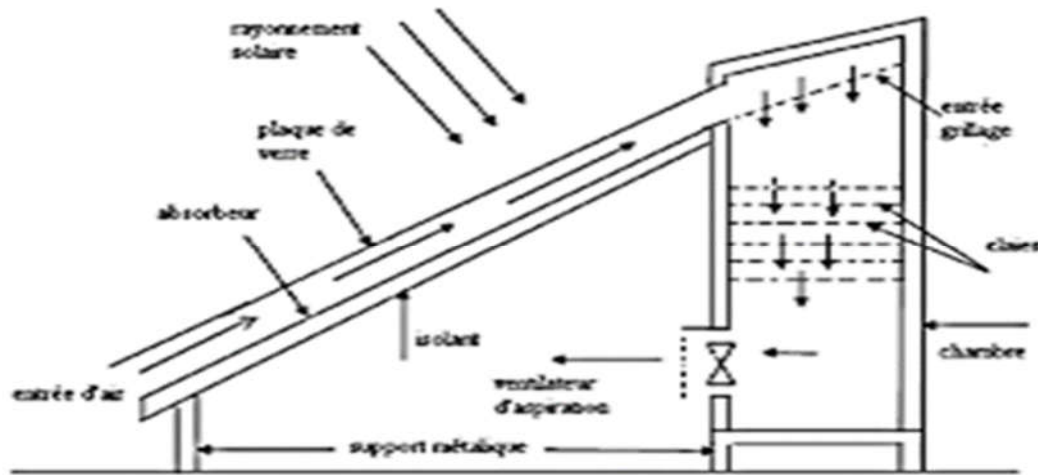
Figure 0-18   Illustration of a solar dryer [41]

1.4.2 Conduction

Conduction is one of the three main ways that heat energy is transferred from one place to another. Conduction is the process by which heat energy is transferred through collisions between neighboring atoms or molecules. This type of heat exchange occurs more easily in solids and liquids, where the molecules are closer together, than in gases, where the molecules are farther apart. The rate of energy transfer by conduction is highest when there is a large temperature difference between the materials in contact [42].
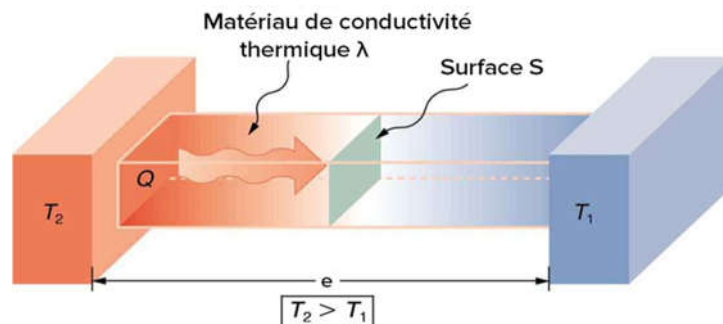
Figure 0-19 Conduction chematic diagram[43]

$$Q = (Ƙ.s \ / \ L) * (t_1 - t_0)$$

Q : heat transfer rate (W) ;

Ƙ : the heat transfer coefficient (w/m.k) ;

S : Surface (m²) ;

L : Lenth (m)

T_1 is the surface temperature and T_0 is the ambient temperature(K) ;

1.4.3 Radiation

Radiation is a major type of heat transfer in which thermal energy is transferred from a hot surface to a cold surface by electromagnetic waves, often through infrared radiation. In contrast to conduction and convection, radiation can occur in a vacuum or through matter. One of the common examples that occurs in our daily lives is the transfer of heat from fire to the body or from the sun to the earth. This process does not occur through direct contact, but rather through electromagnetic waves [44] .
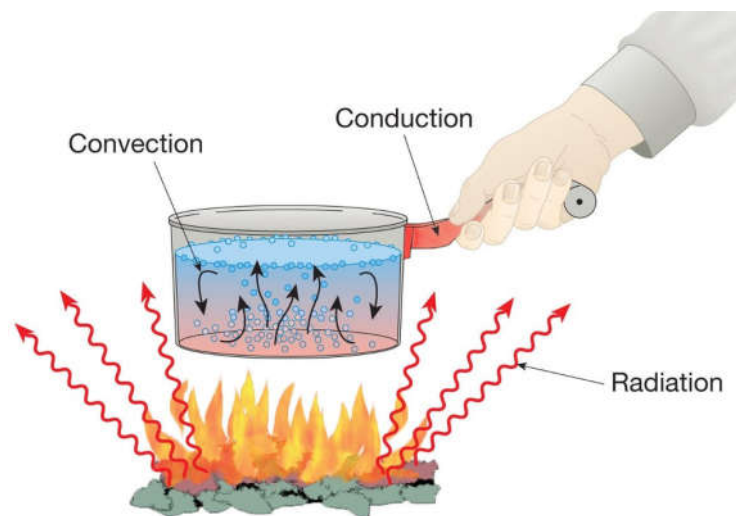
Figure 0-20 Heat transfer mecanisms diagram [45]

1.4.4 Heat transfer by evaporation

Heat transfer by evaporation is a type of heat transfer known as "latent heat transfer" or "phase change heat transfer". This type of heat transfer occurs when a substance changes phase from a liquid to a gas and absorbs or releases heat as a result. In the case of evaporation, thermal energy is absorbed

from its surroundings in order to be transformed into a gas as a result of which heat is absorbed from its surroundings and cooled [46] .

$$\Delta Hvap = Hvapor - Hliquid \quad [47]$$

ΔHvap is the change in enthalpy of vaporization

Hvapor is the enthalpy of the gas state of a compound or element liquid is the enthalpy of the liquid state of a compound or element .

$$Q = m.LHV \quad [48]$$

Where

Q is the heat required for vaporization;
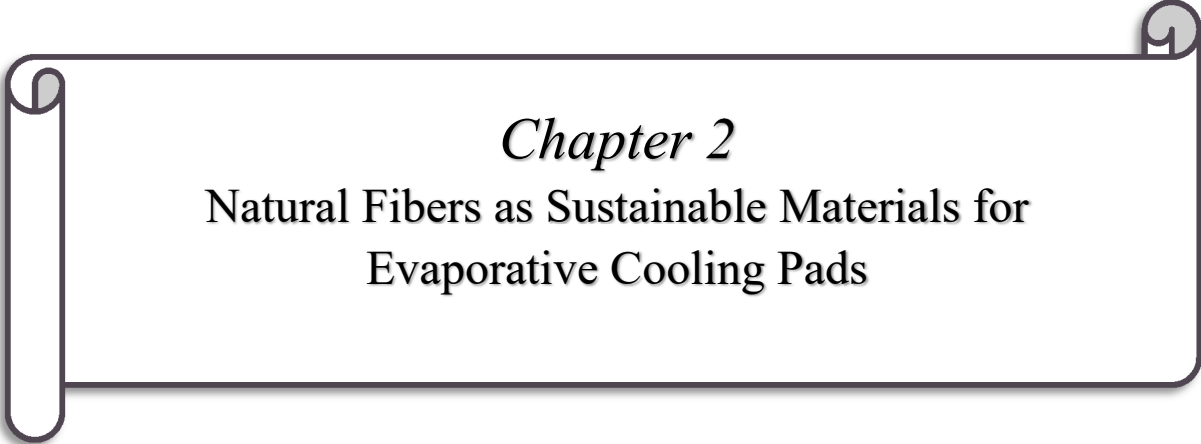
m is the mass of the liquid and LHV is the latent heat of vaporization

Psychrometric formulas:

- Enthalpy of saturated liquids (hfg): **hfg = LHV**
- Enthalpy of saturated vapors (hgs): $hgs = hfg + Cpg(Tsat - Tref)$
- Specific heat capacity of air (Cpa): **Cpa = 1.005 kJ/kg.K**
- Specific heat capacity of vapor (Cpg): **Cpg = 2.04 kJ/kg.K**
- Humidity ratio **(w): w** $=\frac{mvapor}{kg\_dry\_air}$
- Saturation pressure (esat): $esat = 6.11 * exp(17.27 * Tair / (Tair + 273.3))$
  - Vapor pressure (evapor): $evapor = Cpa . \frac{(Tdry\_air - Twet\_bulb)}{LHV}$

1.5 Conclusion

Passive cooling with its various techniques such as shade cooling, natural cooling and evaporative cooling provides environmentally friendly energy efficiency through various heat transfer mechanisms such as radiation, convection and evaporation, of which water is known to be one of the most important elements due to its unique physical and chemical properties.

Chapter 2
Natural Fibers as Sustainable Materials for Evaporative Cooling Pads

Natural Fibers as Sustainable Materials for Evaporative Cooling Pads

2.1 Introduction :

Evaporative pads of various types play the most important role in an evaporative cooling system. The effectiveness of the pad depends on the material it is made of, which must have properties such as high water absorption, good ventilation, and resistance to mold and corrosion. Cellulose evaporative pads have always been a good choice for evaporative cooling systems. When we talk about cellulose evaporative pads, we are talking about natural plant fibers. In this chapter, we will learn about the different organic evaporative pads made from natural fibers and learn about their composition and properties, in addition to their performance. When we talk about cellulose fibers manufactured for evaporative pads, we are talking about natural plant fibers which are also a clean, available and renewable source of energy; wool, palm, coconut fibers... all with different properties and compositions are raw materials for manufacturing organic evaporative pads for passive cooling system.

2.2 Natural plant fiber

Natural fiber composites offer a unique combination of properties that make them attractive for various applications. Natural fiber composites are a class of materials that combine natural fibers with a polymer matrix. These composites aim to create a composite material with unique properties [42]. Natural fibers are sometimes referred to as plant fibers or biomass, where natural fibers refer to fibrous plant materials that are produced as a result of photosynthesis [49].

2.2.1 Natural plant fiber groups

Plant cells are surrounded by a rigid cell wall, which distinguishes them from animal cells. The dimensions of these so-called fibers vary between different plants, but their general shape is often elongated with lengths ranging from 1-35 mm and diameters ranging from 15-30 μm [50]. From a composite reinforcement perspective, it is best to group the fibers according to their length:

2.2.1.1 Group 1 :

Short fibres (1-5 mm), usually originating from wood and non-wood species and often used to make composites with isotropic properties in plane , meaning composites with random , undefined fibre orientation.

2.2.1.2 Group 2 :

Long fibres **(5-50 mm)** , usually originating from non-woody annual plant species (e.g. flax, hemp, jute) that are often used to make composites with anisotropic properties, meaning the opposite of Group 1; composites with a specific fibre orientation. Natural plant fibres consist of:

a. Seed hairs ; as the name suggests are fibres collected from seeds or seed pods, cotton seeds , kapok , coconut and poplar. The most important of these is cotton, which has properties that allow it to be turned into threads or stuffing.

b. Bark fibres - a group of fibres derived from the bark of dicotyledons, including herbaceous plants , shrubs and trees (softwood , hardwood and recycled wood)

c. Leaf fibres are fibres derived from the vascular bundles of the very long leaves of some monocotyledonous plants. These fibres are also known as "hard" fibres because they are more woody than bast fibres .

d. Grass fibres, another group of monocotyledonous fibres , are extracted from the entire stem with the leaves and used in papermaking. This pulp is composed not only of fibres but also of other cellular elements [51].

These groups are summarized in the figure :
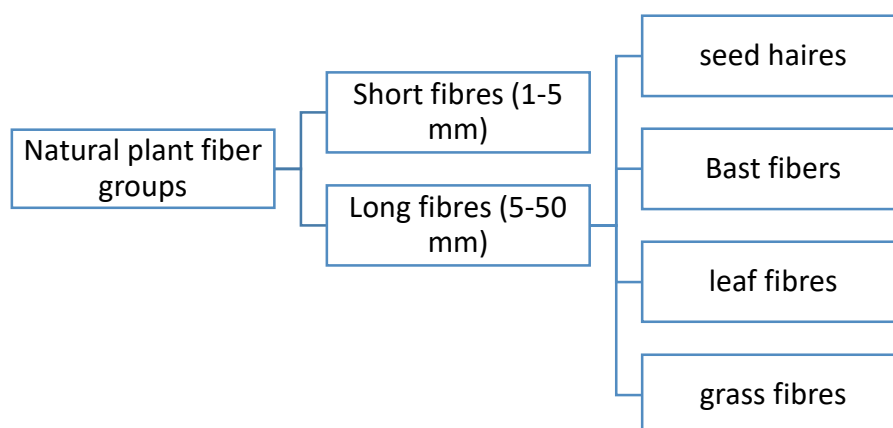
Figure 0-1 Natural plant fiber groups diagram

2.2.2 Structure of natural plant fibers

The structure of plant fibers consists of 3 main components which are cellulose, hemicellulose and lignin. The structure has an outer primary layer and 3 inner layers while the cell wall of plant fibers is made up of cellulose which is in crystalline form and arranged irregularly. The secondary cell wall is made up of cellulose arranged in the direction of the fibers. Generally the properties of these plant fibers depend on various parameters such as the part of the plant from which the fibers are extracted, the geological location, the extraction method and the maturity of the plants [52]. Cellulose is the main structural component of plant cell walls, making up about 33% of all plant material (90% of cotton and 50% of wood is cellulose), making it the most abundant of all naturally occurring organic compounds [53].
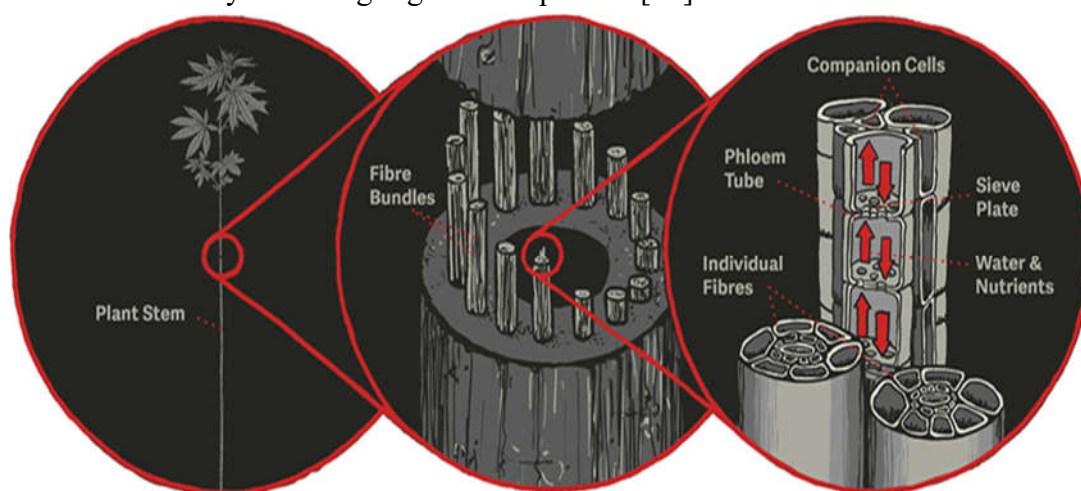
Figure 0-2 Shematic represeanaion of plant fiber structure [54]

2.2.2.1   Cellulose

Cellulose is the most abundant organic compound on earth with a chemical formula (C6H10O5)n ; While the final group is C1-OH, the reducing end with the aldehyde structure; The cellulose consists of a D-glucose unit at one end and a C4-OH group, the non-reducing end, while the final group is C1-OH,Some technical celluloses contain extra carbonyl and carboxy groups, like the bleached wood pulp . The molecular structure is responsible for its significant properties : Chirality , hydrophilicity , degradability and chemical vari-ability due to high reactivity from the donor group—OH .The superior hydrogen bonds add crystalline fibre structures to cellulose to high reactivity from the donor group—OH .The superior hydrogen bonds add crystalline fibre structures to cellulose [55].
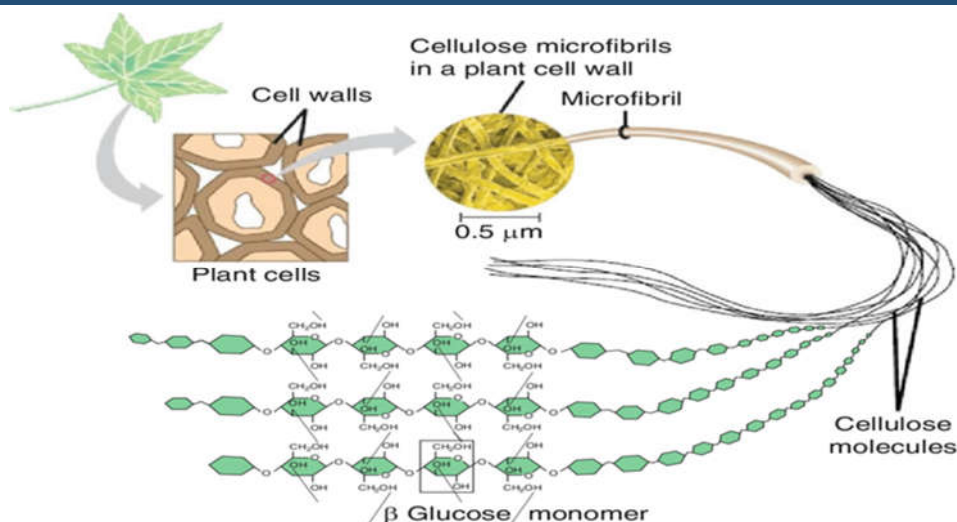
Figure 0-3   Cellulose structure for plant fibers [56]

2.2.2.2   Hemicelluloses

Hemicelluloses are polysaccharides in plant cell walls that contain equatorially arranged backbones linked to β-(1→4)xyloglucans, xylans, mannans, glucomannans, and β-(1→3,1→4)-glucans. These hemicelluloses are found in the cell walls of all land plants, except β-(1→3,1→4)-glucans, which are restricted to oleaginous plants and a few other groups. The composition and abundance of hemicelluloses vary among cell types. Their most important role is to contribute to cell wall strengthening by interacting with cellulose and, in some walls, with lignin. Many of the glycosyltransferases required for the biosynthesis of xylglucan and mannan are located in the known membranes of the Golgi apparatus; hemicellulose is synthesized by them [57].
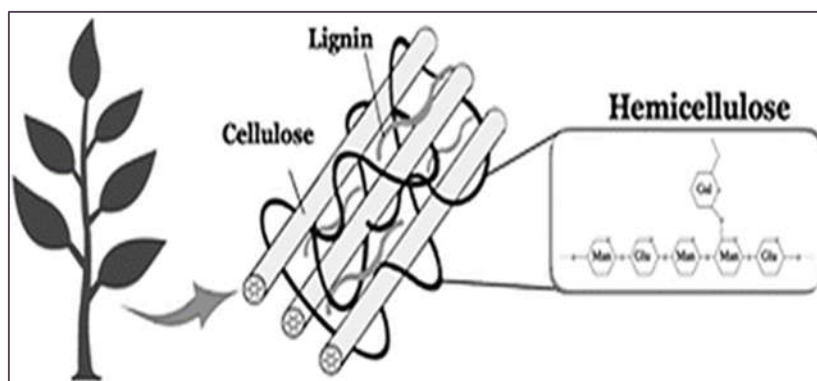
Figure 0-4 plant fiber chemical structure [58]

The various polymers of hemicellulose include xylan, glucuronoxylan, arabinoxylan, glucomannan, and xyloglucan. Xylan is a linear chain of β-1,4-linked xylosyl residues that are usually replaced by glycosyl side chains, such as glucuronosyl/methylglucuronosyl and arabinofuranosyl residues, and are acetylated at O-2 and/or O-3 [59] , while xyloglucan consists of a β-1,4-linked D-glucose skeleton replaced by D-xylos where L-arabinose and D-galactose residues can be attached to the xylose residues and L-fucose is attached to the galactose residues in xyloglucan [60] ; glucomannan is a hydrocolloid polysaccharide of the mannan family consisting of β-1,4-linked D-mannose and D-glucose monomers with acetyl side branches on part of the skeleton units [61]. Beta-glucans are biologically active compounds characterized by a group of polysaccharides with a 1,3-beta-glycoside backbone. Polysaccharides can take many forms depending on the origin [62].
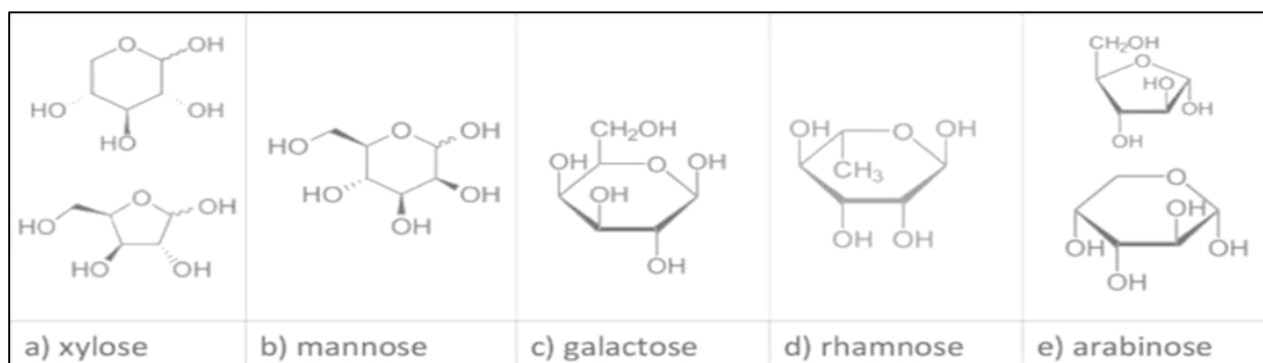
Figure 0-5 Chemical structure of hemicelluloses [63]

2.2.2.3   Lignin

The term lignin refers to a large group of aromatic polymers resulting from the oxidative conformational coupling of 4-hydroxyphenylpropanoids. These polymers will often be deposited in thick cell walls secondarily, making them rigid and impermeable [61]. Lignin biosynthesis can be stimulated under various biotic and abiotic stress conditions in addition to its developmentally programmed deposition. Lignin has a major role in protecting cell wall polysaccharides from microbial degradation. Thus it imparts resistance to degradation and is also one of the most important determinants in the conversion of plant biomass into pulp or biofuel [64]
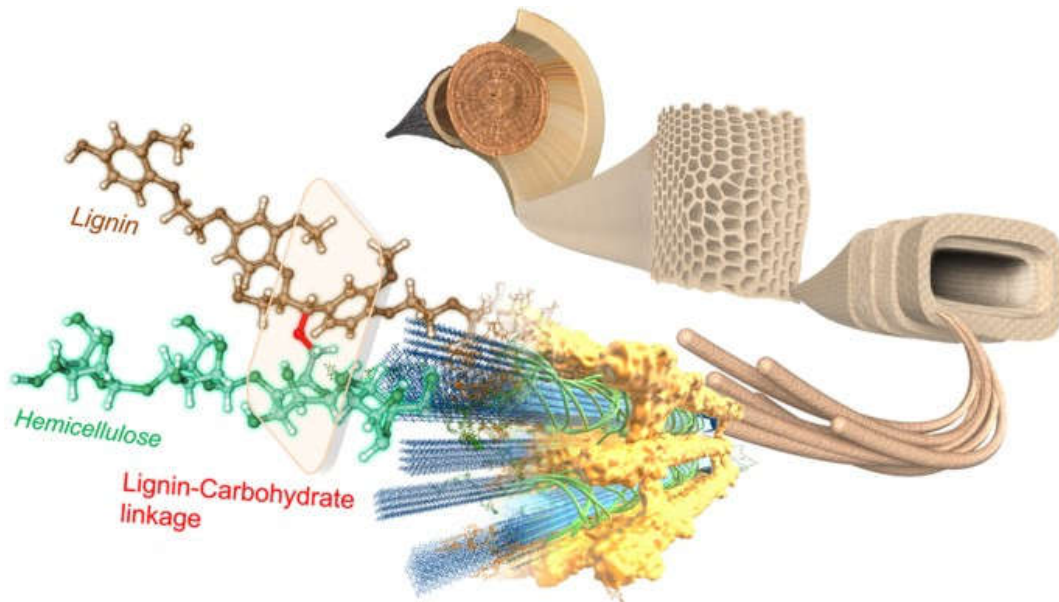
Figure 0-6 plant fiber chemical structur [65]

2.2.3 Types of plant fibres

Plant fibers derived from natural fibers manufactured for the evaporation pad are divided into several types or families, each with its own structure and properties ; Bast fibers, leaf fibres, seed fibres, fruit fibres, wood fibres are all types of natural plant fibres..

2.2.3.1 Bast fibers

Bast fibers are usually long and very strong, such as flax, hemp, jute and ramie. These fibers are often obtained from the outer layer of plant fibers and in the form of fibrous bundles [66].... The primary stems of the plant are covered with an epidermis consisting of thin walls and adhered tightly to it. An outer layer of the epidermis gradually forms from dead cells over time to form what is called the phloem [67]. They are mainly composed of cellulose, hemicellulose and lignin, the proportion of these chemical compositions depending on age, growing conditions, source of fibre and method of fibre extraction [68].
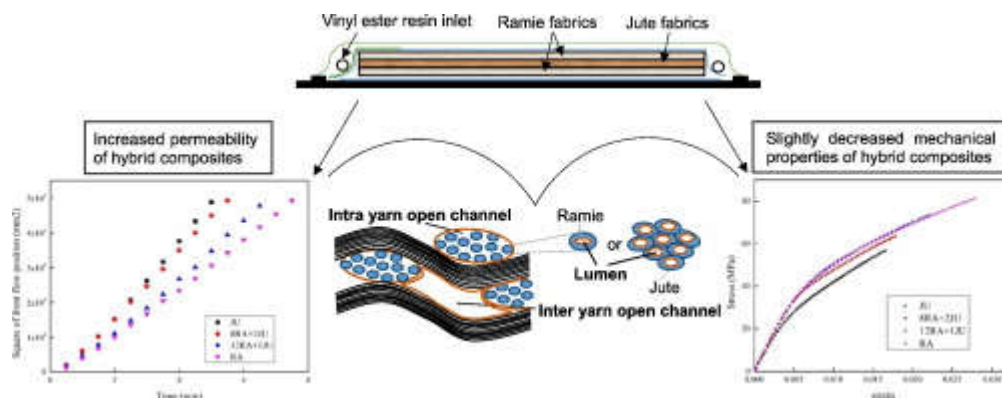
Figure 0-7 Permeability and mechanical properties of plant fiber [69]

Bast fibres have a major structural component, cellulose (60-75%), which provides tensile strength and stability to the plant cell walls and fibres, while the remaining components of bark fibres are hemicellulose, lignin, pectin and ash. Each cell wall has primary and secondary layers S1, S2 and S3. Bark fibres are long and rough (20 mm for hemp, for example) [70].
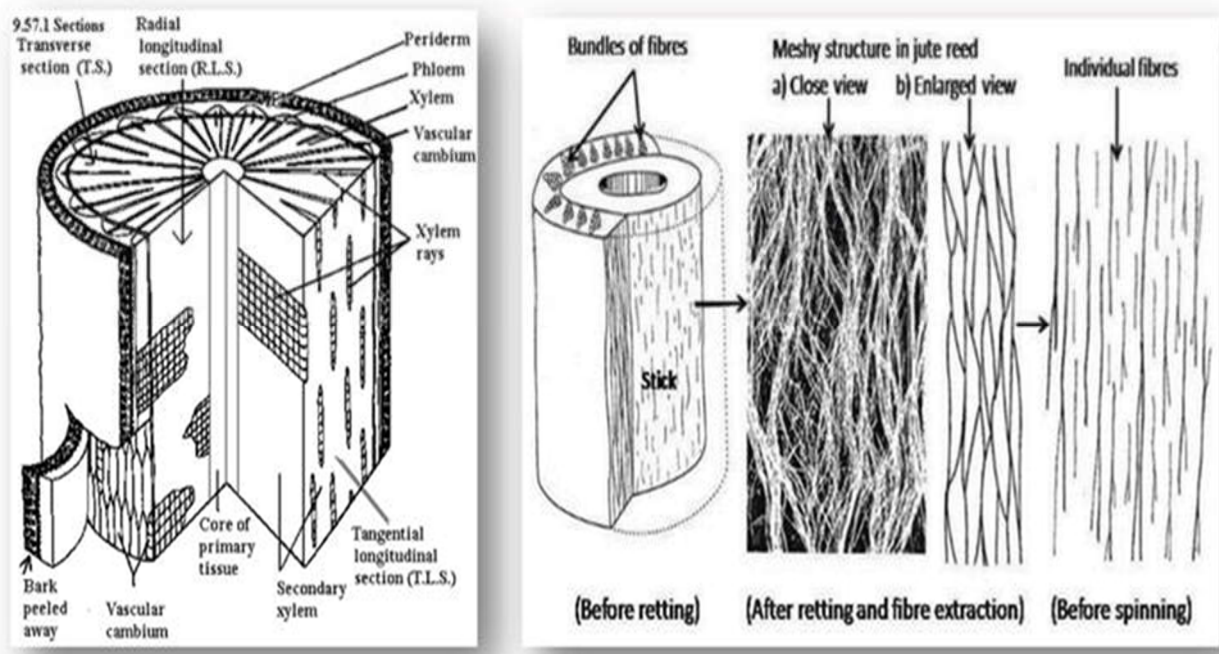
Figure 0-8 Bast fibers composents [71]

2.2.3.1.1 Flax fiber

Flax is one of the strongest natural fibers. It is an annual herbaceous plant that is adaptable to a variety of soils and climates, but grows best in well-drained sandy loam and in temperate climates. Its history dates back 30,000 years. Flax is classified as a bast fiber.... [72].

Plants average 0.9 to 1.2 m (3 to 4 ft) tall, with slender stems 2.5 to 4 mm (about 0.10 to 0.15 in) in diameter with concentrated branches at the top [73]. Plants grown for seed are shorter and multi-branched. The leaves which alternate on the stem are small and lance-like. The flowers, borne on stems, have five petals and are usually blue but sometimes white or pink. They grow from the tips of the branches [74]. The fruits are small dry capsules consisting of five lobes. Flax is a complex group of different polymers, polysaccharides such as cellulose 65-75%, hemicellulos 15-25%, pectin 1-5% ,and phenolic-derived lignin 5-15%. Flax contains a wide range of secondary metabolites derived from the phenylpropanoid pathway which distinguishes it from other fibers and ensures its biological activity [75].

We have two main types of flax fibers: primary (tow) and secondary (flax).

   a. **Primary (tow) flax fiber**: This type of flax fiber is made from the outer part of the flax stalk which is usually shorter, coarser and more flexible than secondary flax fibers and is commonly used in industrial applications, such as the production of ropes and twines and for composite materials such as those used in building construction and vehicles [76].

   b. **Secondary flax fiber (linin):** This type of flax fiber is produced from the inner part of the flax stem which is longer, finer and stronger than the primary flax fiber and is commonly used in textiles such as clothing, linen and upholstery. Linin fiber is soft, shiny and absorbent and is also used in the production of high-quality paper produc .
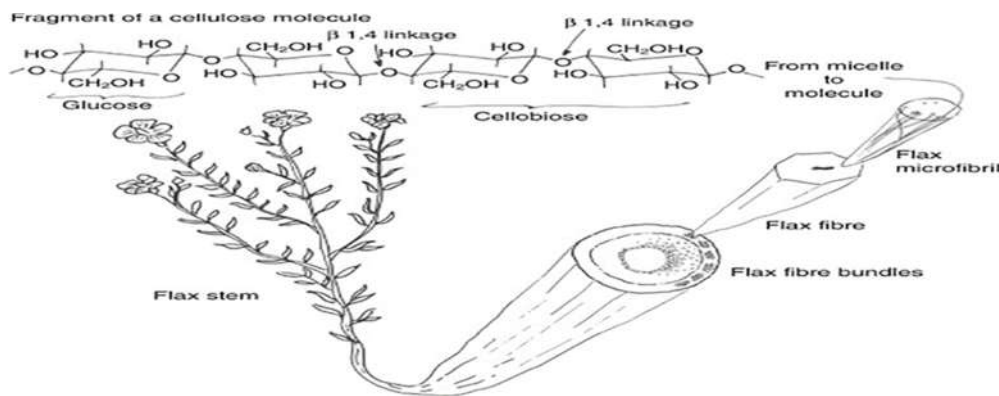
Figure 0-9 Flax Fiber Cellular Structure [77]

2.2.3.1.2   Jute fibre

Jute fibre is obtained from the burlap plant which is a common reinforcement material for green vehicles and belongs to the Tiliaceae family. Jute grows in countries like China, India, Bangladesh and other Asian countries in a height range of 2 to 3.5 metres [78].

Jute is a long, soft, lustrous vegetable fibre of the genus Corchorus that can be spun into coarse, strong yarns produced from plants, of the Malvaceae family, which fall into the category of bast fibres. Jute fibres range from yellowish-white to brown and are 1 to 4 metres long [79]. The length of a single cell is usually short, ranging from 3-6 mm on average, with a large width ranging from 40-80 micrometres; jute is characterized by its roughness and hardness, which makes it difficult to process and can only produce coarse, heavy yarns and fabrics. The longitudinal appearance of jute is straightened with lines and gum, while the cross-section resembles a polygon with a central cavity. Jute fiber contains three main classes of chemical compounds, namely cellulose (58~63%), hemicellulose (20~24%) and lignin (12~15%), in addition to some small amounts of other components such as pectin 0.2-0.5%, fat 1.0-1.4%, aqueous extract, etc. Jute

fiber consists of small units of cellulose surrounded and held together by lignin and hemicellulose10-11 [80].

There are four types of jute fibre :

a. **White jute:** This type of jute is considered the oldest among other types. White jute is known as Corchorus capsularis jute. This type is characterized by the fact that this type of jute is brighter in color than other types, but at the same time it is less durable than many other types [81].

b. **Dark Jute or Tosa Jute:** Tosa jute has a brown colour and long fibres and is used in making burlap bags and purses as the fibres of Tosa jute are soft, silky and stronger than white jute [82].

c. **Jute Mista:** This variety was introduced in India during the year 1947 when India gained its independence and is a mixture of white jute and Tosa jute [83].

d. **Jute scraps:** Jute scraps are the leftovers of jute. Jute scraps are used in making bags, ropes, paper products and basic textile materials. Jute scraps do not show much strength and are rough in texture [84].
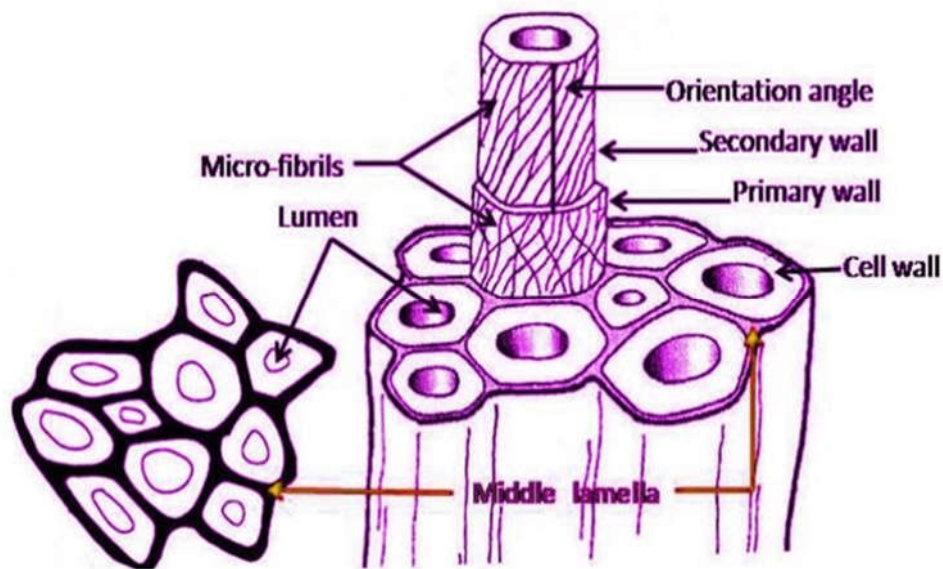
Figure 0-10 Jute Fiber Cross-sectional and Longitudinal View [85]

2.2.3.1.3   Kenaf fiber

Kenaf belongs to the Malvaceae family and the Hibiscus genus. Kenaf is an annual or biennial perennial herb that is mainly grown in Asia, Africa, America and Europe, where it is considered one of the most important and cheapest commercially available bark fibers. It is characterized by strong, hard and durable fibers [86] ; it is grow at a rate of about 10 cm/day and mature in about 90 days. The plant grows to an average height of 3 m and has a diameter of 3-5 cm. The long fibres are light yellow to grey in colour, and are tougher and shinier than jute. The stems consist of two types of fibres: outer fibres (bark) and inner fibres (pith). The bark is similar to softwood fibres in general, while the pith is similar to hardwood fibres. It grows to an average height of 3 m and has a diameter of 3-5 cm. However, it has a low cellulose content (44.0-63.0%) due to its wood-like structure, and is composed of a high proportion of lignin (15.0-19.0%). The pith fibres represent about 60% of the total weight of kenaf and are the main part of the kenaf plant [87].
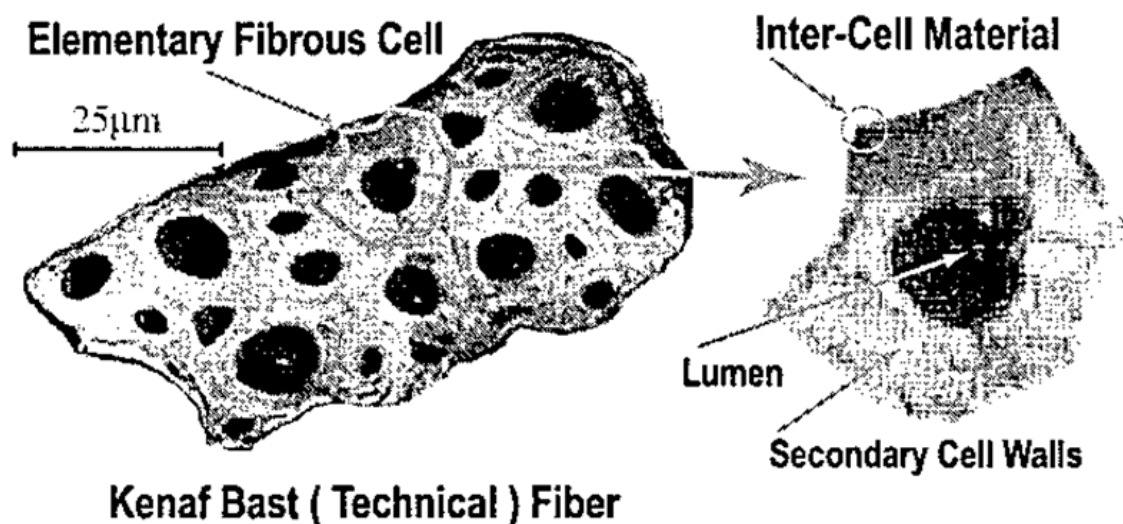
Figure 0-11   Kenaf fiber structure [88]

2.2.3.1.4   Hemp fiber

Hemp is a tall, annual crop plant with a yellowish-gray fiber and a shiny nature, in addition to a cylindrical shape with joints and cracks on the surface of the fibers. The hemp plant reaches a height of more than 3 meters [89].

Hemp stalks contain 25% to 40% bark fibers and 60% to 80% husk with a woody core; the outer part of the stalk is covered with bark, while the inner part of the stalk consists of woody core and bark fibers. Like other plant fibers, hemp fiber contains 5 main components: (1) structural polysaccharides cellulose and hemicellulose; (2) structural protein; (3) other polysaccharides, especially pectin (homogalacturonan); (4) lignin; (5) wax; and (6) minerals. Hemp fiber generally consists of 53-91% cellulose, 4-18% hemicellulose, 1-17% pectin, and 1-21% lignin[90].Schematic representation of different chemical components of hemp fiber derived from the stem of the hemp plant [90].
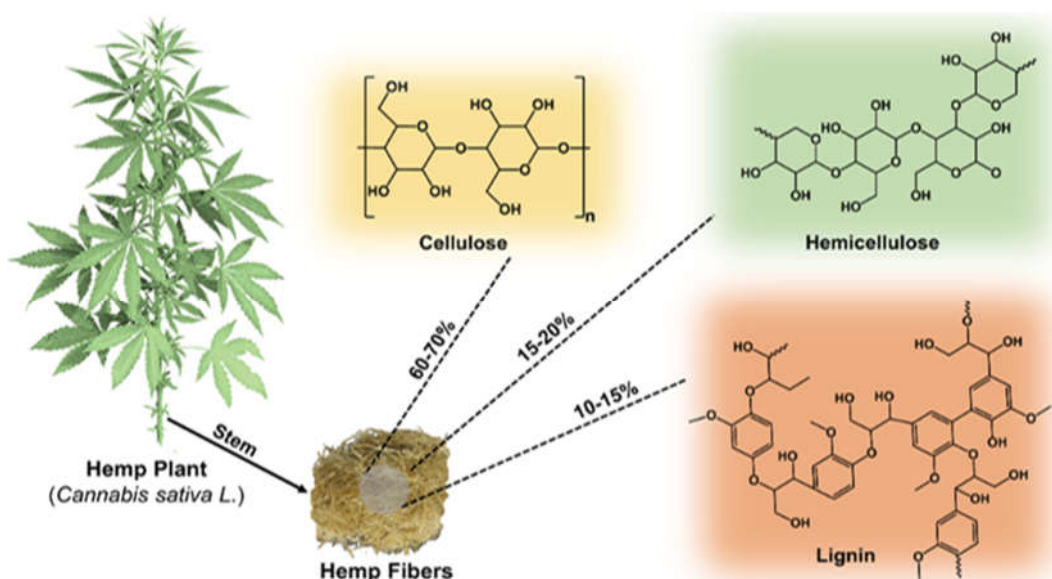
Figure 0-12 Schematic representation of different chemical components of hemp fiber derived from the stem of the hemp plant [91]

2.2.3.1.5 Ramie fibers

around for a long time. It comes from a tall plant in the nettle family that is grown in Asia and Europe.The stems produced by the perennial ramie plant reach a height of 1.9 to 2.4 m and an average diameter of 45 μm. The leaves that grow on the upper part of the stem are somewhat heart-shaped with serrated edges and have bright green upper and lower sides covered with white hairs. The leaves of the green ramie are green on both sides while the greenish-white flowers form pendulous clusters that grow from the angles between the leaf stalks and the stems [92]. Ramie fibers are characterized by their pure white color and luster, which allows them to be easily dyed. Individual fiber cells average 13 to 15 cm (5 to 6 inches) in length. Ramie, like other bast fibers, consists of chemical components, i.e. hemicellulose, cellulose, non-cellulose materials and minerals. It consists of cellulose 68.6 - 76.2%, hemicellulose 13.1 - 16.7%, lignin 0.6 - 0.7%, pectin 1.9%, and wax 0.3% [91].
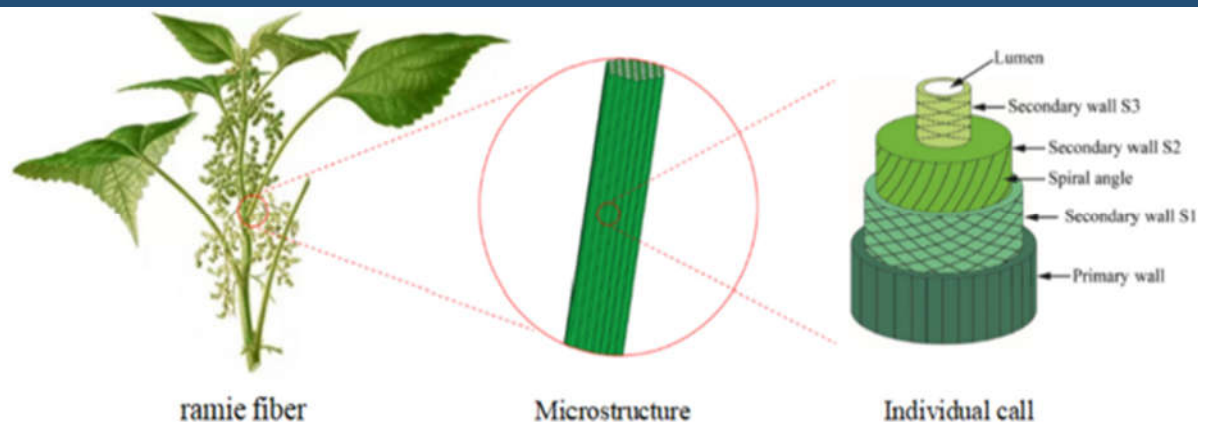
Figure 0-13 Ramie fibers structure [92]

2.2.3.2 Fruit fiber

Fruit fiber is the part of plant-derived food that cannot be completely broken down by human digestive enzymes. Plant fiber consists of non-starch polysaccharides and other plant components such as cellulose, resistant starch, resistant dextrin, inulin, lignin, chitin, pectin, beta-glucan, and oligosaccharides [93]. Cell walls are highly complex networks of various non-starch polymers, structural proteins, and phenolic substances. The most abundant non-starch polymers in plant cell walls are cellulose, hemicellulose, pectin, and lignin. The original complex cell wall material is mainly water-insoluble starches and has a volcanic structure. The composition of this essential cell wall material can vary between different plants and depends on the biological function of the plant's organs and tissues [94].
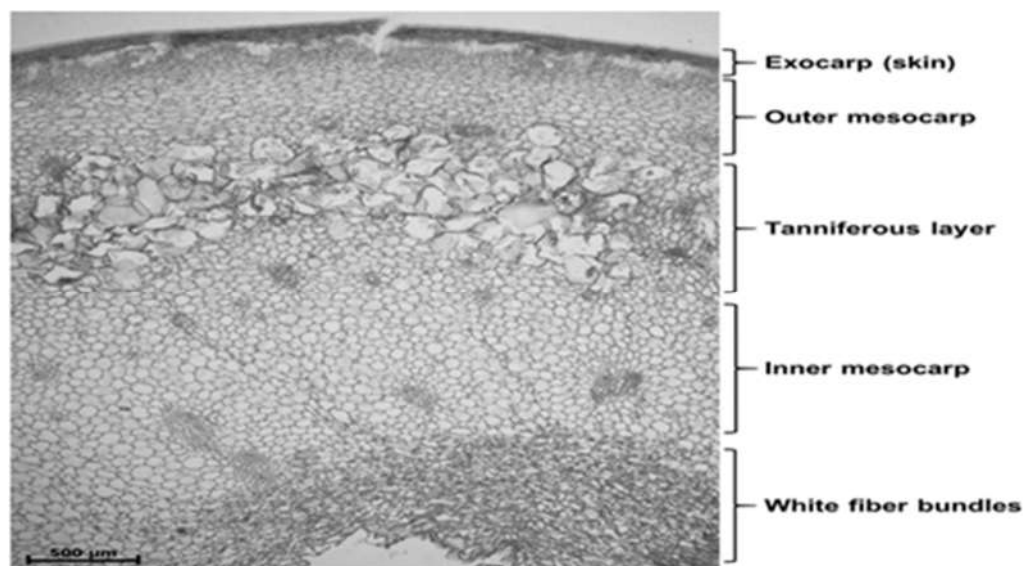
Figure 0-14 Fruit fiber structure [95]

2.2.3.2.1 Coconut fibre

Coconut fibre grows in its native regions Coconut fibre is a fibre native to the Asia-Pacific region, especially India and Sri Lanka. It is a coarse fibre extracted from the fibrous outer husk of the coconut [94]. The individual fibre cells are narrow and hollow, with thick walls made of cellulose. These fibres are pale when immature but later become hard and yellowish with a layer of lignin deposited on their walls [96]. Individual coconut fibre cells are narrow and hollow with thick walls made of cellulose, each cell is about 1 mm long and 10-20 μm in diameter. Coconut fibres range in length from 15 to 35 cm and in diameter from 50 to 300 μm [97]. Plant cell wall material consists of three important components: α-Cellulose36-43, lignin 16.8-18, and hemicellulose. Lignin fills the spaces in the cell wall between the cellulose, hemicellulose, and pectin components, and is covalently bonded to hemicellulose [98].
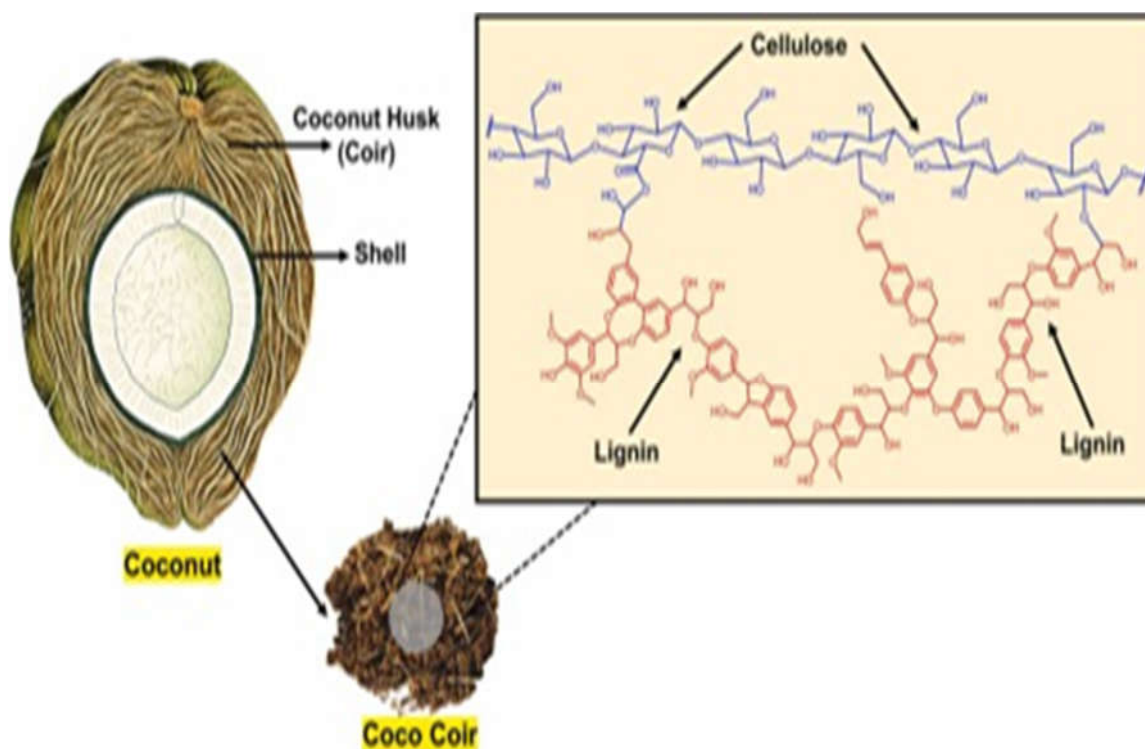
Figure 0-15 Coconut fibre structure [99]

2.2.3.3 Seed fibers

Seed fibers are fibers that are obtained from plants from seeds. These seeds can also grow in winter. Kapok and cotton are plant seed fibers. The chemical composition of seed fibres generally consists of cellulose, which can make up to 67% of the fibre along with smaller amounts of lignin [100] .
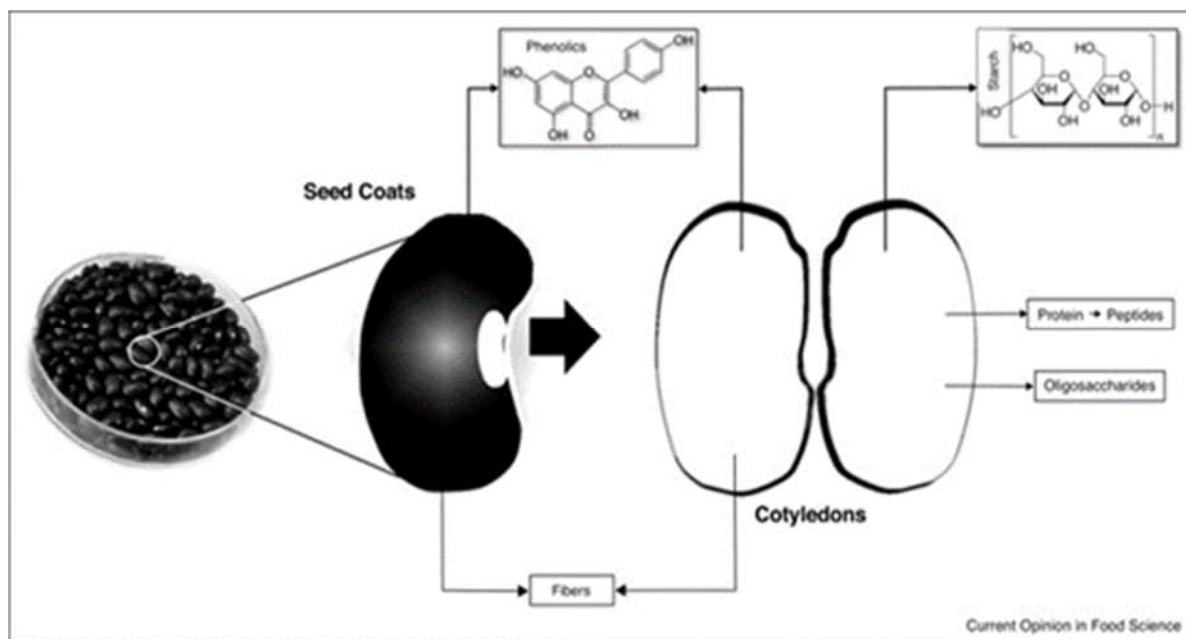
Figure 0-16   Seed fibers structure [101]

2.2.3.3.1 Cotton fiber

Cotton fiber is a fiber harvested from the seed pods of the cotton plant. It is a natural, soft, and delicate fiber. The cotton plant belongs to the genus Gossypium in the Malvaceae family. Cotton fibers have a complex, heterogeneous morphology that is a single-celled seed hair that grows around the seeds of the cotton plant [102].

Cotton fibers vary in length and diameter based on many factors including the growing environment, causing significant differences in fiber properties within bales, and even within a given capsule and on a single seed. While cotton fibers typically range in diameter from 8 to 20 μm, their length ranges from less than 20 mm to 35 mm and above. Cotton is a natural cellulose fiber made of long chains of natural cellulose characterized by a long linear molecular chain of more than 10,000 cellulose units held together by strong molecular forces [103]. It's consist of four main parts in cross-section, a primary wall containing natural impurities and a water-repellent waxy layer. The secondary wall is pure cellulose and contains an open space in the center of the fiber through which nutrients flow called the cavity [104].
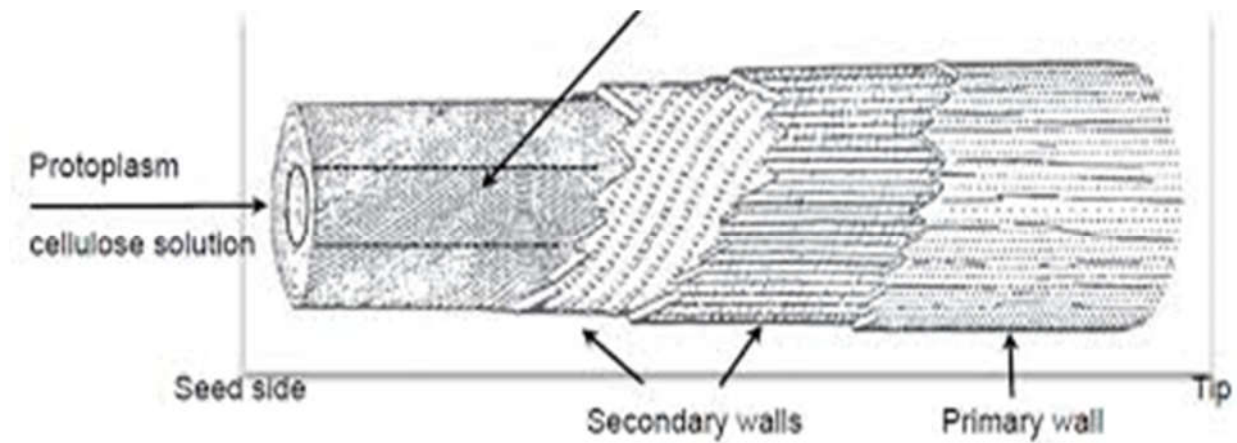
Figure 0-17 Cotton fiber structure [105]

2.2.3.4 Leaf fibres

Leaf fibres consist of many interlocking sclerenchyma cells or true plant fibres held together by a gummy substance. The fibres generally run the length of the leaf and are often denser near the lower surface of the leaf. Leaf fibres consist of cellulose, 43–80%, hemicellulose 10–39%, and lignin 3–15%. Leaf fibres have a tensile strength of 230–1627 MPa, a Young's modulus of **0.2–22 GPa, and a density of 0.8–1.4 g/cm3 [106].**
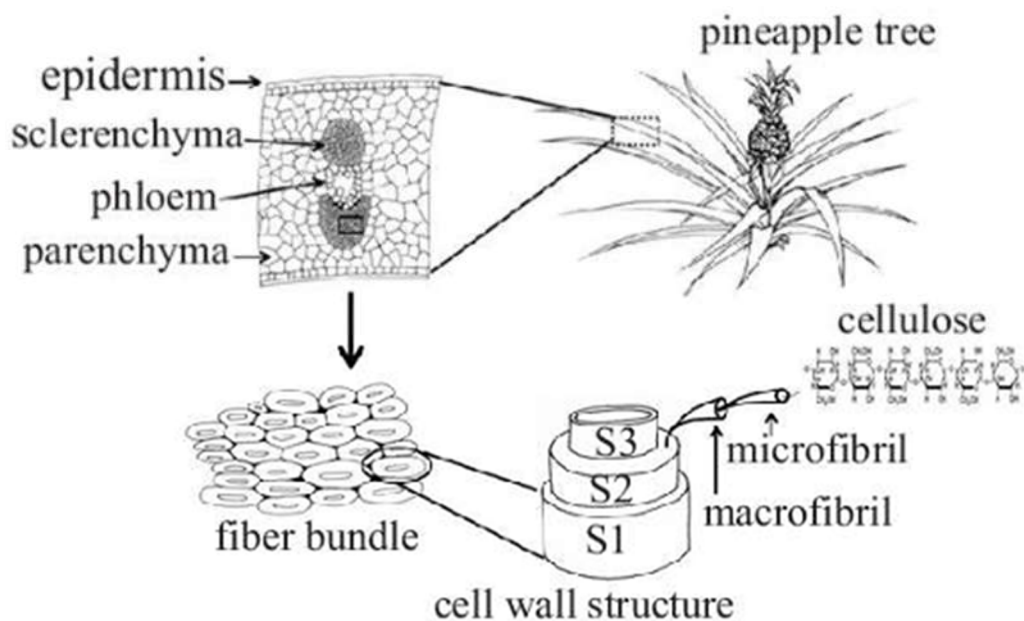
Figure 0-18 Pineapple Plant Fiber Schematic structure [107]

2.2.3.4.1 Sisal fiber

Sisal fiber is a tough fiber extracted from the leaves of the sisal plant. The sisal plant produces between 200 and 250 leaves, each leaf containing between 1000 and 1200 fiber bundles

[108]. In cross-section, the fiber bundles consist of about 100-200 single cells held together by a natural glue. The single cells consist of thick walls with a central cavity. The cavity varies in size in the cross-section of the sisal fiber. In the longitudinal section, the fibers are straight and without curls and their appearance is almost cylindrical. On the surface of the fiber, there are many knots and lines that confirm that the fiber bundle consists of many single cells arranged in straight parallel lines [109] .

Sisal fibers are composed of cellulose (~52.1%), hemicellulose (11.9%), and lignin (15.45%). Sisal fibers have an average tensile strength of 493 MPa and a tensile modulus of 10.7 GPa [110].
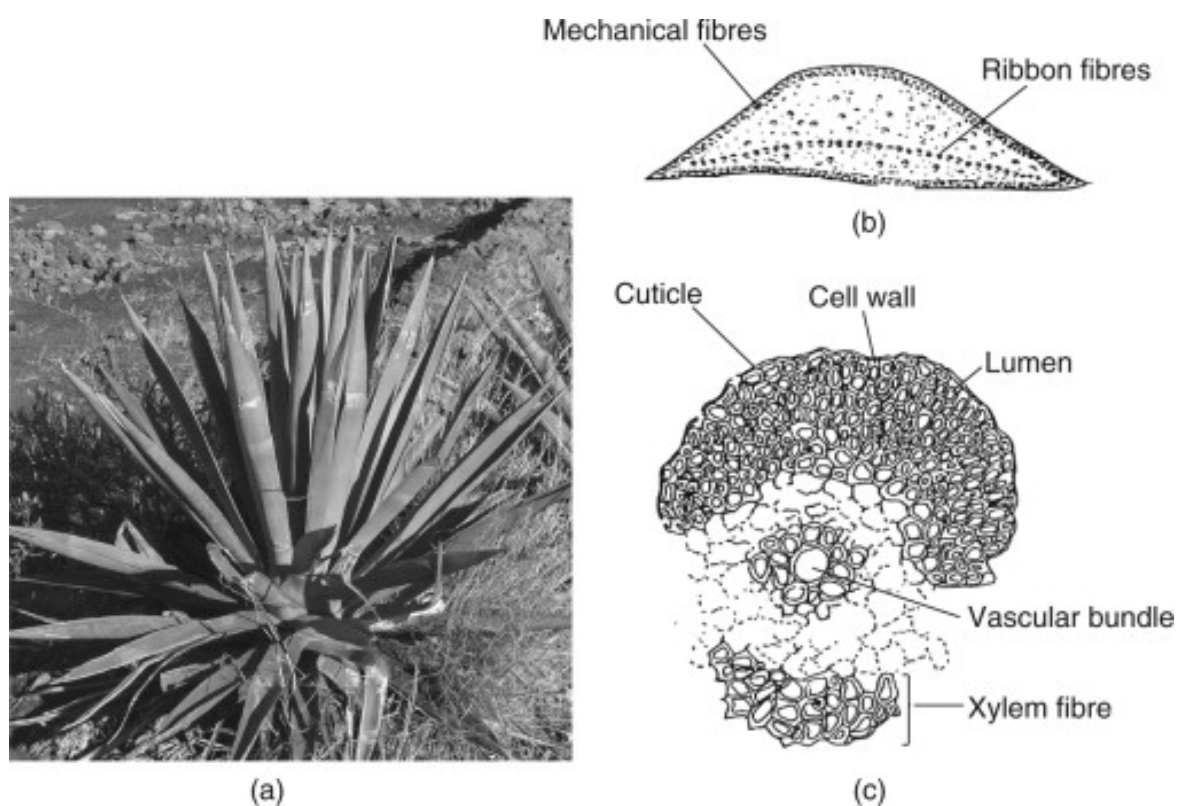
Figure 0-19 (a) The sisal plant leaf ,(b) a leaf cross section, and (c) the different types of fibers in the plant leaf [111]

2.2.4 properties of natural plant fibers

Similar to the water absorption rate, flexibility, and amount of cellulose, each type of plant fiber has its own characteristics that make it different from other types, which explains its uses.

2.2.4.1   chemical properies

Cellulose is the strongest and toughest component of fibers. The chemical composition of cellulose remains the same for all natural fibers while the degree of polymerization changes, affecting the mechanical properties of the fibers. Bark fibers have the highest degree of polymerization compared to most other plant fibers as seen in the table below:

Table 1 Natural fibers chemical properties

Chemical Property	Cotton	Sisal	Flax	Hemp
Cellulose content (%)	88–96	65–76	71–75	70–74
Hemicellulose (%)	5–6	10–14	18–20	17–22
Lignin (%)	<1	8–12	2–3	3–8
Pectin (%)	0.7–1.2	2–3	1–1.5	0.9–1.2
Wax and fats (%)	0.4–1.2	2–3	1–1.5	0.8–1.5
pH Level	Neutral (6–7)	Neutral to Alkalin(7–8)	Neutral (6–7)	Neutral (6–7)
Biodegradability	Low	Good	Moderate	Good
Moisture Resistance	Low	Medium to High	Medium	High

2.2.4.2   physico_mechanic properties
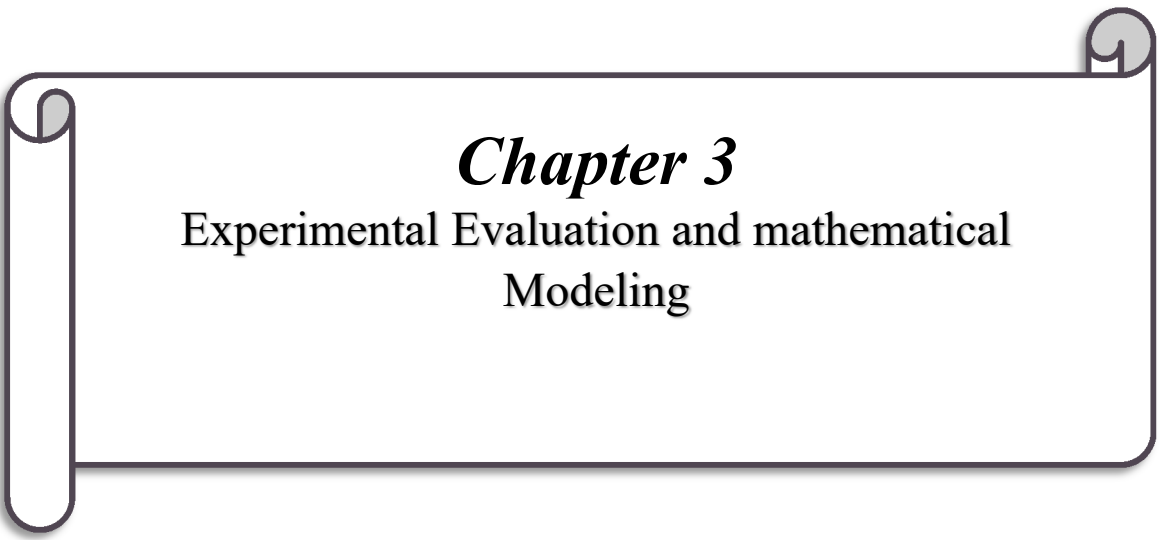
The geographical location of the plant, maturity, size, chemical composition, and part of the plant from which the fiber is extracted may vary in the properties of natural fibers. While the strength of the fiber is related to the angle of the fiber and its physical properties, the high strength of kenaf and ramie fibers, and the low strength of coconut fibers, can be attributed to high and low cellulose content. Natural fibers have a high amount of moisture content, which affects their mechanical properties. High cellulose content, high relative humidity, high pore size, and low crystallinity in the fibers are directly proportional to high moisture content [112].

Table 2 Natural fibers physico_mechanic properties

Physical Property	Cotton	Sisal	Flax	Hemp
Water Absorption (%)	24–27	10–12	12–15	12–14
Moisture Regain (%)	~8.5	~11	~12	~12
Density (g/cm³)	1.50–1.55	1.45–1.50	1.40–1.50	1.48–1.55
Thermal Conductivity (W/m·K)	~0.04	~0.045	~0.035	~0.042
Cooling Performance Index[1]	High	Medium	Medium	High
Air Permeability	High	Medium	High	High
Durability in Wet State	Low	Good	Moderate	Good
Surface Texture	Soft	Coarse	Smooth	Slightly Rough

2.3 Conclusion

This chapter detailed the chemical and physical properties of various natural plant fibers suitable for evaporative cooling pads. Sisal and cotton emerged as promising candidates due to their high cellulose content, moisture retention capacity, and air permeability. These insights guide the material selection for the experimental phase of the project.

Chapter 3
Experimental Evaluation and mathematical Modeling

Chapter 3

Experimental Evaluation and mathematical Modeling

3.1 Introduction

This chapter presents the practical aspect of the research, aiming to test the theoretical hypotheses and evaluate the extent to which the specified objectives have been achieved. The applied work includes designing the experimental methodology, identifying the tools and equipment used, explaining the implementation steps, and methods for collecting and analyzing data.

The procedures followed to ensure the accuracy and reliability of the results are also clarified, along with a detailed description of the samples or models studied. This section is essential for linking the theoretical framework to the results achieved in the field, contributing to a deeper understanding of the phenomena under investigation and evaluating the effectiveness of the proposed solutions or hypotheses.

A structured methodology was adopted to ensure objectivity, while adhering to the scientific and technical standards relevant to the field. It also clarifies any challenges encountered and how to address them.

Thus, this chapter represents a practical embodiment of what was theoretically addressed in the previous chapters and lays the foundation for the results and analyses that will be discussed later.

3.2 Experimental Study

After reviewing the theoretical principles related to direct evaporative cooling systems, the re-search moved to the practical side of the research by conducting a practical experiment aimed at evaluating the performance of a simple air cooler. The experiment employed a fan to enhance airflow and accelerate the evaporation process, allowing for more pronounced results in a shorter period of time. This section aims to validate the theoretical concepts in practice and analyze the factors affecting cooling efficiency under realistic operating conditions.
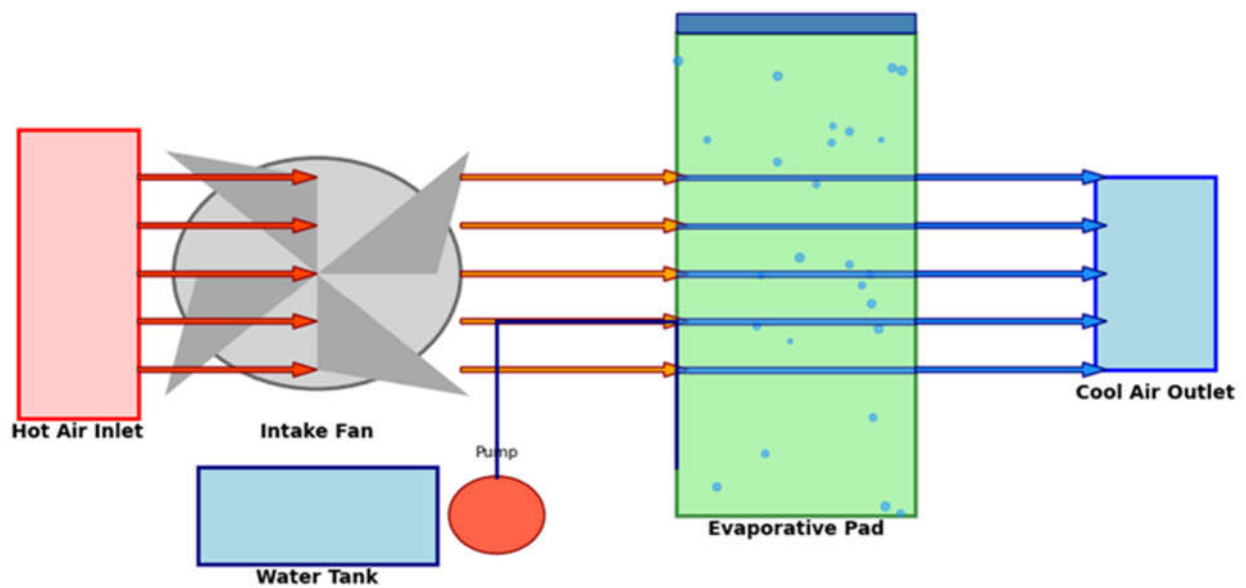
Figure 0-1 Schematic Diagram of the Direct Evaporative Cooling System

3.2.1 Experimental Setup

The experimental setup consisted of a custom-made evaporative cooling device built from transparent glass, externally insulated with 3 cm thick polystyrene to reduce heat exchange with the surroundings. The device had an overall surface area of approximately 0.24 m² and a height of 0.34 m. It was functionally divided into two sections: an inlet chamber measuring 0.111 m², where warm air enters the system, and an outlet chamber of 0.09 m², where the cooled air exits. A vertical evaporative pad with a width of 10 cm was installed between the two sections, serving as the active cooling interface. To maintain continuous moisture on the pad, a water irrigation system powered by a small pump was used. Additionally, a side-mounted fan was employed to force warm air through the wet pad, accelerating the evaporation process and enhancing the cooling effect. This configuration enabled controlled testing of direct evaporative cool-ing under forced convection conditions.
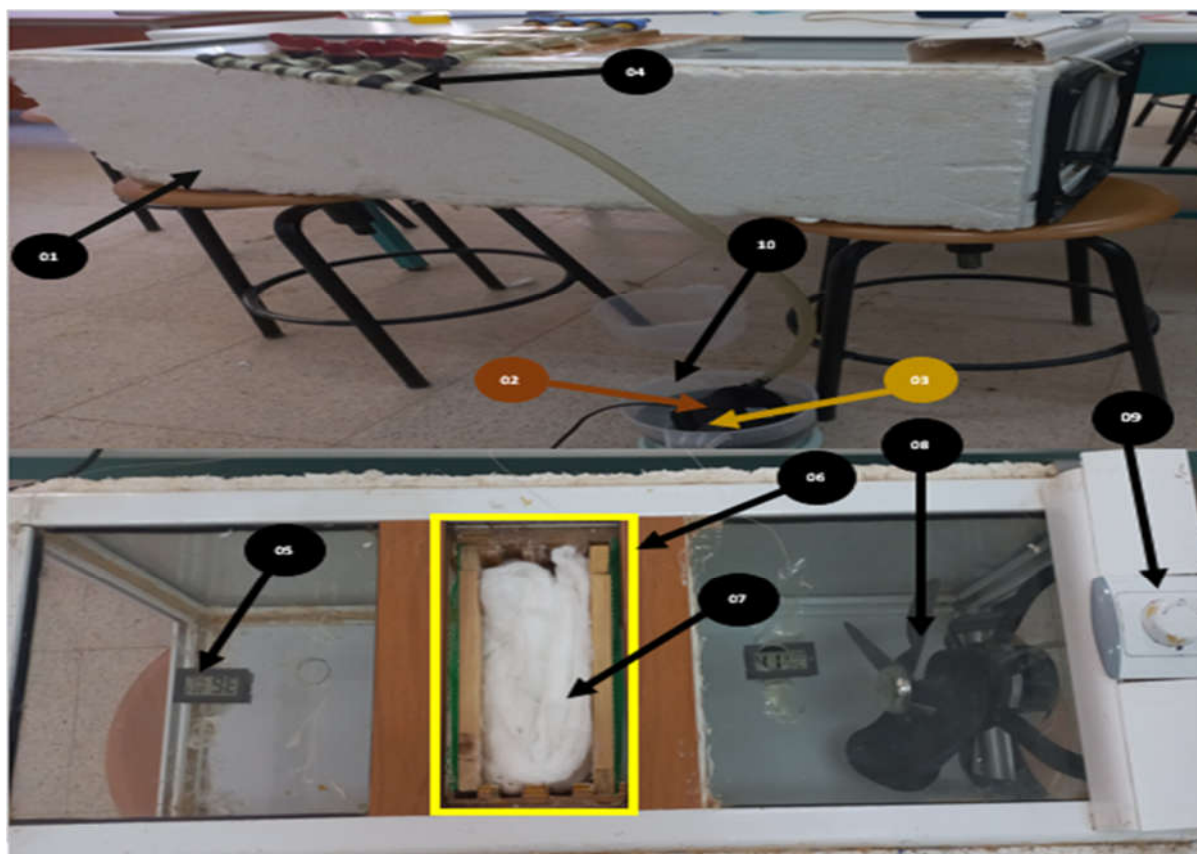
Figure 0-2   experimental evaporaive cooler structure

Table 3 experimental evaporaive cooler composents

Element	Name	Element	Name
01	Main Structure	06	Evaporation Pad Location
02	Water Pump	07	Cellulose Fibers (Cotton)
03	Thermometer	08	Fan
04	Irrigation System	09	DC adapter
05		10	Water Tank

3.2.1.1 Tools used

Table 4 Tools used

Main Structure	Configuration: Horizontal rectangular tunnel. 🞣 Tunnel material: • Direct evaporative cooler - DEC • Plexiglas (thickness 0.004 m). • Polystyrene (thickness 0.02 m). • Rectangular tunnel length: • 0.8 (m). • ✓ Rectangular tunnel width: 0.3 • ✓ Pad dimensions (fibers): (0.3 x 0.3) m² • (m). • ✓ Rectangular tunnel height: 0.3 m	
Axial fan, 12V DC, 0.25 A, 120 mm diameter	• Model: L300 • ✓ Voltage: 220 V • ✓ Power: 130 W • ✓ Rotation speed: 1400 rpm • ✓ Frequency: 50 Hz • ✓ Dimensions: 0.3 x 0.3 (m²)	
Mini water pump, 5W, 220V, max flow rate: 3 L/min	MSD • AC:220V/50-60HZ • Qmax:1200L/H • Hmax:3M • Power: 45W • 45W • 50HZ • 220V	

Digital sensors, ±0.5°C accuracy	- Model: Digital LCD Thermometer Hygrometer 10% to 99% Relative Humidity Temperature and Pyrometer - Humidity Controller - Transit Sensor - Weather Measurement - Temperature Range: -50°C ~ +70°C - Temperature Accuracy: ±1°C - Humidity Measurement: 10% RH-99% RH - Humidity Resolution: 1% RH - Humidity Accuracy: ±5%	
Digital thermometer	- Digital kitchen thermometer with probe - Displays °C and °F - Range: -50+200°C / -58+392°F - Probe length: 125 mm - Probe diameter: 3.5 mm - Display resolution: 0.1°	
DC adapter, 12V/2A for fan and sensors	- Input voltage: 220V - Output voltage: AC0-220V - Maximum power: 4000W - Size: 10.1 x 9.6 x 4.5 cm; 80 grams - Weight: 80 g	

Sisal Fiber	- Walnut Fiber - Coarse, golden fiber - Highly porous to air and water - Low water storage capacity	
Cotton Fiber	- Seed Fiber - White, soft fiber - Low porosity to air and water - High water storage capacity	
Activated Charcoal	585 mg hard tablets - Activated charcoal 5850 mg used	

3.2.1.2 Key measured parameters

The experimental study focused on evaluating the effect of fiber type, pad thickness, and airflow rate on the performance of a direct evaporative cooling device. Two types of natural fibers—sisal and cotton—were used as evaporative media. For each fiber type, the pad thickness

was varied between 9 cm and 5 cm, forming four distinct test configurations. Each configuration was tested under three different levels of airflow rate, adjusted using a lateral fan. For every airflow level, the experiment was conducted for a total duration of 90 minutes, with measurements taken at 10-minute intervals.

The key parameters measured included:

• Inlet and outlet air temperatures

• Relative humidity at the outlet

• Remaining water volume at the end of the test

• Temperature of the remaining water

This approach allowed for a comparative analysis of cooling performance under various physical and oper-ational conditions, enabling the identification of optimal material and system parameter.

The experimental study was conducted to evaluate the impact of varying thickness (tp), fiber type, and airflow rate ($\dot{m}$) on the performance of an evaporative cooling device. Two types of natural fibers—cotton and sisal—were tested at two different thicknesses (tp = 0.1m and 0.05m), under three distinct airflow rates: $\dot{m}$ = 0.236 kg/s, 0.334 kg/s, and 0.410 kg/s, respectively.

All experiments were performed in a controlled environment at a room temperature of 32 °C. . The collected data provide insight into the thermal performance and moisture ex-change efficiency of the system. The results are summarized in the following tables for detailed comparison and analysis.

Table 5   Experiment results

Time (min)	Sisal 0.263 Tin (℃)	Sisal 0.263 Tout (℃)	Sisal 0.334 Tin (℃)	Sisal 0.334 Tout (℃)	Sisal 0.410 Tin (℃)	Sisal 0.410 Tout (℃)	cotton 0.263 Tin (℃)	cotton 0.263 Tout (℃)	cotton 0.334 Tin (℃)	cotton 0.334 Tout (℃)	cotton 0.410 Tin (℃)	cotton 0.410 Tout (℃)
00 :00	26.3	23.4	26.3	23.1	25.8	25.8	25.6	23.5	25.6	24.2	25.4	25.4
00 :10	26.4	23.3	26.2	23.1	25.7	24	25.5	23.4	25.6	24.1	25.2	25.3
00 :20	26.4	23.4	26.3	23.8	25.9	23.1	25.4	23.4	25.6	23.9	25.3	25
00 :30	26.4	23.2	26.3	23.6	26.1	23.3	25.5	23.3	25.5	23.8	25.4	24.6
00 :40	26.4	23.3	26.3	23.6	26.1	23.3	25.7	23.5	25.6	23.6	25.5	24.6
01 :50	26.4	23.3	26.4	23.5	26.3	23.2	25.7	23.5	25.5	23.5	25.6	24.5
01 :00	26.4	23.3	26.3	23.4	26.3	23.2	25.6	23.1	25.6	23.4	25.5	24.7
01 :10	26.3	23.3	26.4	23.4	26.3	23.4	25.8	22.9	25.7	23.3	25.5	24.5
01 :20	26.4	23.2	26.3	23.4	26.3	23.4	25.8	22.7	25.8	23.1	25.6	24.4
01 :30	26.4	23.2	26.3	23.4	26.3	23.4	25.8	22.8	25.8	23.1	25.6	24.2
01 :40	26.4	23.1	26.3	23.1	26.3	23.4	25.9	22.7	25.7	23.4	25.6	24.3

t_p=0.05 m

T(℃)

tp=0.1 m											
τ(°C)	00 :00	22.4	20.8	22.3	20.8	21.9	21	24.6	22.1	23.2	21.4	23.4	23
	00 :10	22.5	20.9	22	20.8	21.8	19.6	24.2	22.1	23.5	21.5	23.6	22.8
	00 :20	22.5	20.1	22.3	20.7	21.9	19.5	24.4	22.2	23.1	21.3	23.8	22.3
	00 :30	22.5	20.1	22	20	22.1	19.9	23.9	22	23.1	21.3	23.5	22
	00 :40	22.5	20.6	22.3	20.7	22.2	20.6	23.6	21.8	23.1	21.2	24	22.1
	01 :50	22.6	20.1	22	20.7	22.5	20.8	23.4	21.6	23.1	21.1	24	22
	01 :00	22.5	20.1	22.4	20.7	22.6	20.9	23.4	21.6	23.3	21.1	24.3	22.1
	01 :10	22.5	20.9	22.4	20.7	22.5	21.3	23.3	21.4	23.2	21.1	24.2	22.1
	00 :20	22.5	20.9	22.4	20.7	22.5	21.5	23.3	21.3	23.1	21.1	24	22
	01 :30	22.4	20.8	22.3	20	22.4	21	23.3	21.3	22.9	21.1	24.6	22.1
	01 :40	22.4	20.8	22.4	20.8	22.3	20.8	23.3	21.3	23.1	21	24	22

tp=0.05 m											
HUMIDITY(%)	RH in	RH out	RH in	RH out	RH in	RH out	RH in	RH out	RH in	RH out	RH in	RH out
Time (min												
00 :00	37	43	39	53	37	36	36	42	37	42	37	36

	mv (kg)	Tv	mv	Tv	mv	Tv	mv (kg)	Tv	Mv	Tv	Mv	Tv
00 :10	38	54	39	53	37	38	37	45	37	42	37	38
00 :20	38	52	39	53	37	39	37	46	37	43	37	39
00 :30	38	54	39	52	36	39	37	45	37	43	36	38
00 :40	38	53	39	54	36	38	37	45	37	45	36	40
01 :50	38	53	39	55	37	40	37	45	37	45	37	41
01 :00	39	54	39	56	37	41	37	45	37	45	37	41
01 :10	39	56	40	55	37	41	37	46	37	45	37	41
01 :20	39	56	39	56	37	41	36	47	37	45	37	41
01 :30	39	55	40	55	37	42	36	47	37	45	37	42
01 :40	39	57	40	55	37	42	37	48	37	44	37	42

RH(%) (row label for the above section)

$t_p=0.1$ m												
00 :00	38	44	41	47	40	41	35	48	36	46	37	37
00 :10	37	43	41	47	40	49	36	48	35	46	39	46
00 :20	37	45	40	46	40	50	36	47	36	47	38	45
00 :30	37	44	40	45	40	50	37	48	36	47	38	46
00 :40	37	43	39	46	40	46	37	47	36	46	38	47
01 :50	37	44	38	45	40	49	36	47	36	47	**38**	47
01 :00	37	44	38	44	41	47	37	48	37	47	37	47
01 :10	36	43	38	45	42	48	37	49	37	47	37	47
01 :20	36	43	38	44	43	48	37	48	37	47	37	47
01 :30	36	43	38	44	42	48	37	49	36	47	37	47
01 :40	36	43	38	44	41	47	37	48	36	48	35	46

RH(%) (row label for the above section)

$t_p=0.05$ m												
	mv (kg)	Tv	mv	Tv	mv	Tv	mv (kg)	Tv	Mv	Tv	Mv	Tv

Time (min		(°C)	(kg)	(°C)	(kg)	(°C)		(°C)	(kg)	(°C)	(kg)	(°C)
00 :00	00	22.7	00	22.4	00	22.1	00	24.7	00	24	00	24
00 :10	0.1	22.3	0.1	22.1	0.08	22.1	0.35	24.3	0.1	23.8	0.15	23.7
00 :20	0.06	22.3	0.05	22	0.04	21.8	0.1	24.1	0.07	23.4	0.1	23.4
00 :30	0.06	22.2	0.05	21.7	0.04	21.4	0.09	23.6	0.08	23.1	0.09	22.8
00 :40	0.14	21.7	0.12	21.4	0.06	21.1	0.04	23.4	0.1	22.9	0.09	22.7
01 :50	0.04	21.1	0.04	21.2	0.12	19.7	0.07	22.9	0.09	22.4	0.1	22.4
01 :00	0.04	20.6	0.04	20.7	0.08	19.4	0.09	22.5	0.07	22.2	0.04	21.9
01 :10	0.03	20	0.07	20.3	0.06	19.7	0.07	21	0.07	22	0.07	21.7
01 :20	0.07	19.9	0.03	20.1	0.06	18.8	0.07	21	0.09	21.8	0.07	21.5
01 :30	0.02	19.7	0.05	19.4	0.04	18.4	0.03	20.7	0.04	21.3	0.06	21.3
01 :40	0.08	19.4	0.06	19.1	0.04	18.2	0.05	20.1	0.04	20.9	0.05	20
t_p=0.1 m												
00 :00	00	23.9	00	24.1	00	24	00	23.7	00	24	00	24.3
00 :10	0.1	23	0.07	23.6	0.1	23.7	0.4	23.1	0.1	23.6	0.1	24.1
00 :20	0.06	22.7	0.07	22.4	0.07	21.9	0.09	23	0.09	23.5	0.08	23.8
00 :30	0.06	22.4	0.04	22.2	0.07	21.7	0.08	22.8	0.09	23.4	0.07	23.2
00 :40	0.06	21.9	0.01	20.9	0.05	21.4	0.08	22.6	0.09	23	0.06	22.7

01 :50	0.07	21.7	0.14	20.7	0.07	20.6	0.07	22.4	0.05	22.7	0.04	22.4
01 :00	0.07	21.3	0.05	19.9	0.09	20.2	0.1	22.1	0.04	22.4	0.03	22.1
01 :10	0.03	21.1	0.05	19.6	0.04	19.7	0.05	21.8	0.09	22.3	0.07	21.9
01 :20	0.07	19.9	0.04	19.4	0.03	19.5	0.08	21.6	0.15	21.8	0.09	21.7
01 :30	0.04	19.7	0.03	19.3	0.07	18.9	0.07	21.1	0.09	21.7	0.08	21.1
01 :40	0.04	19.4	0.05	19.1	0.06	18.8	0.05	20.7	0.07	21.4	0.09	20.8

3.2.1.3   Experimental Observations :

• The tests were carried out in a closed laboratory environment under mild to relatively low ambient temperatures, typical of a spring-like climate.

• It was observed that cotton fibers required approximately twice as much water to become fully sat-urated compared to sisal fibers, indicating a higher absorption capacity.

• The laboratory remained thermally stable at around 32 °C, minimizing external interference with the results.

• Despite the controlled conditions, evaporation rates varied significantly depending on fiber type, thickness, and airflow rate, highlighting the influence of material properties on cooling efficiency.

3.2.2 Mathematical Modeling

The following mathematical model focuses on the heat and mass transfer processes in a DEC system where cooling pads are composed of locally sourced natural fibers. To simplify the analysis, the following assump-tions are considered:

• The water-air interface temperature is uniform and constant.

• The convective heat transfer coefficient (h_c) between humid air and the water film surface re-mains constant.

• The pad material is fully and continuously wetted.

• The air near the water-air interface is saturated, and its temperature equals that of the dripping water.

• The thermophysical properties of water and air are assumed constant.

• Surrounding heat flux interactions are neglected.

• Air temperature varies only along the flow direction

3.2.2.1 DEC Performance Analysis

Experimental Setup and Parameters Prior to deriving the governing equations, the following parameters were measured and recorded during experimentation:

• Inlet and outlet air and water temperatures.

• Air humidity (inlet and outlet).

• Airflow rate through the system.

• Surface area of natural fiber pads.

• Volume of evaporated water.

• Duration of the experiment.

• Specific heat capacities of air and water.

• Ambient conditions (temperature and humidity).

3.2.2.2 Key Equations and Concepts

3.2.2.2.1 Heat Transfer Calculations

3.2.2.2.1.1 Heat absorbed by air: Q_{air}

$$\mathbf{Q_{air}} = \mathbf{m_{air}} \times \mathbf{c_{air}} \times \mathbf{\Delta T_{air}} \times \mathbf{t)}$$

where:

Q_{air} : Heat absorbed by air (J).

m_{air} : Mass of air (derived from airflow rate and air density, kg).

c_{air} : Specific heat capacity of air (J/kg·°C).

ΔT_{air} : Air temperature change (°C).

3.2.2.2.1.2 Heat required for water evaporation:

$$\mathbf{Q\,L} = \mathbf{m\,water} \times \mathbf{L\,v} \qquad (3.2)$$

where:

Q evap : Heat for evaporation (J).

m water : Mass of evaporated water (kg).

L v : Latent heat of vaporization of water (J/kg).

Evaporation Rate The evaporation rate is determined by:

$$\dot{m}_{evap} = \frac{m\,water}{t} \qquad (3.3)$$

where:

$\dot{m}_{ev}$: Evaporation rate (kg/min).

t : Experiment duration (min).

3.2.2.2.1.3 Sensible Cooling Capacity of DEC

$$\boldsymbol{Q\,s} = \dot{m}\,air \times \boldsymbol{C\,p\,air} \times (\boldsymbol{Tin} - \boldsymbol{T\,out}) \qquad (3.4)$$

where:

$\dot{m}$ air : Mass flow rate of inlet air (kg/s).

C p,air : Specific heat of inlet air (kJ/kg·°C).

3.2.2.2.1.4 Air Mass Flow Rate : $\dot{m}\,air$

$$\dot{m}\boldsymbol{air} = \boldsymbol{\rho\,air} \times \boldsymbol{V\,air} \times \boldsymbol{S} \qquad (3.5)$$

where:

ρ_{air} ρ air : Air density (kg/m³).

V_{air} V air : Volumetric airflow rate (m/s).

S: Cross-sectional area (m²).

The air velocity can be derived from pressure difference (ΔP):

$$V = \sqrt{\frac{2\Delta P}{\rho}} \qquad (3.6)$$

3.2.2.2.2 Efficiency and Performance Metrics Cooling Efficiency

3.2.2.2.2.1 The cooling efficiency is defined as:

$$\eta \text{ cooling} = \frac{Qair}{Qevap} \times 100\ \% \qquad (3.7)$$

3.2.2.2.2.2 System Cooling Effectiveness

The effectiveness is the ratio of actual temperature drop to the maximum possible (wet-bulb depression):

$$\epsilon = \frac{Tin - Tout}{Tint - Tweb} \qquad (3.8)$$

(III.8) where:

T in : Inlet air temperature (°C).

T out : Outlet air temperature (°C).

T web : Wet-bulb temperature of inlet air (°C).

3.2.2.2.2.3 Energy Efficiency Ratio (EER) EER

$$EER = \frac{Qs}{Wf + Wp} \qquad (3.9)$$
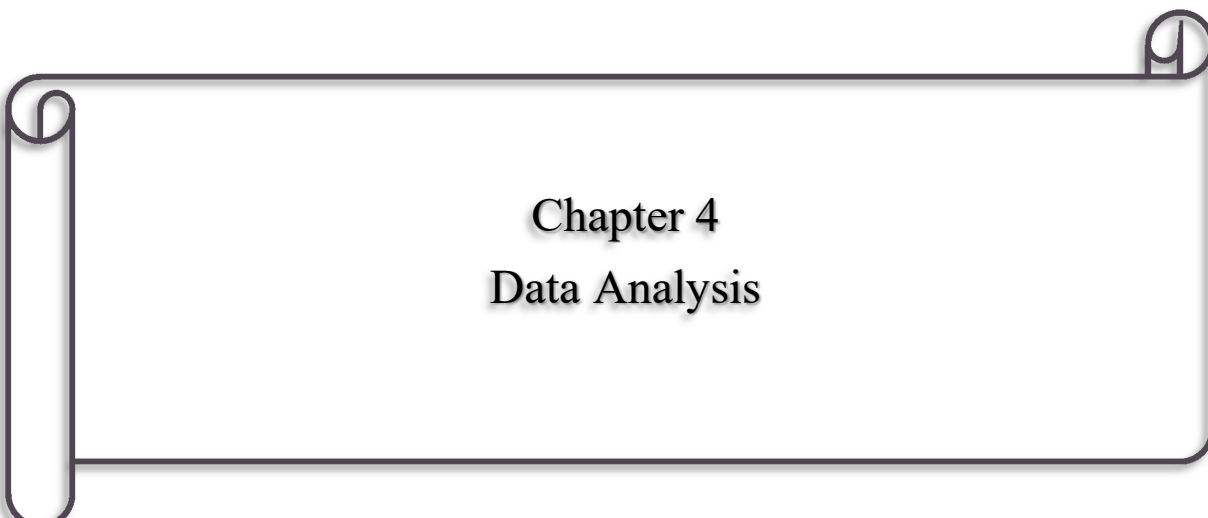
where:

W f : Fan power consumption (W).

W p : Pump power consumption (W).

3.3   Conclusion

The experimental evaluation confirmed the influence of fiber type, pad thickness, and airflow rate on the performance of the evaporative cooling system. Cotton and sisal demonstrated distinct thermal behaviors under varied configurations, providing valuable insights into optimizing material combinations for maximum efficiency. These findings serve as a foundation for further development and refinement of the proposed cooling system.

Chapter 4
Data Analysis

Data Analysis

4.1 Introduction

The evaluation of thermal performance is a critical step in validating the design and effectiveness of passive evaporative cooling systems. This chapter presents a comprehensive analysis of heat transfer mechanisms—namely, sensible, latent, and total heat flux—over time, using natural fiber pads (sisal and cotton) of varying thicknesses and subjected to different air mass flow rates. Through a rigorous experimental protocol, temperature and humidity data were collected at fixed intervals over 1 hour and 40 minutes. The purpose of this analysis is to extract meaningful trends that highlight the thermal behavior of the tested materials under realistic operating conditions.

In order to ensure accuracy and consistency in data processing, the calculations were carried out using Python programming language. Libraries such as pandas, matplotlib, and psychrolib were employed to organize, visualize, and compute psychrometric properties. The dry-bulb and wet-bulb temperatures were used to derive the sensible and latent heat fluxes, which were subsequently summed to determine total heat flux. Furthermore, system efficiency (η) was calculated as a function of total heat removed compared to the theoretical heat input from the air stream.

This chapter not only presents raw data in the form of plots but also dives into deep comparative analysis, examining the impact of fiber type, pad thickness, and airflow rate on the thermal exchange capabilities of the system. The purpose is twofold: first, to assess the most efficient material and configuration, and second, to provide insights that can guide future design improvements of the passive evaporative cooling prototype. The performance of each configuration is examined across multiple dimensions—instantaneous thermal response, overall heat transfer trends, and temporal decay in system efficiency—giving a nuanced picture of system behavior.

4.2 Numerical Analysis

To calculate the wet-bulb temperature, sensitive flow, total flow, efficiency, and various parameters for each tested sample, we used the Python libraries psychrolib, matplotlib.pyplot, pandas, numpy, time_points, and matplotlib.lines, which are based on equations approved by the American Society of Heating, Refrigerating, and Air-Conditioning Engineers (ASHRAE). The results are listed in the following table.

Table 6 Numerical Analysis results

	Fibre	Sisal			cotton		
	Air flow(kg /s)	0.263	0.334	0.410	0.263	0.334	0.410
	t_p=0.05 m						
	00 :00	16,91	17,26	16,51	16,17	17,21	14,59
	00 :10	17,17	17,18	16,43	16,27	17,21	15,08
	00 :20	17,17	17,26	16,59	16,19	17,38	15,08
	00 :30	17,17	17,26	16,56	16,27	17,3	14,84
	00 :40	17,17	17,26	16,56	16,43	17,71	15,24
	01 :50	17,17	17,35	16,91	16,43	17,63	15,67
	01 :00	17,35	17,26	16,91	16,35	17,71	15,31
	01 :10	17,26	17,52	16,91	16,51	17,79	15,23
	01 :20	17,35	17,26	16,91	16,33	18,21	15,07
	01 :30	17,35	17,44	16,91	16,33	18,21	15,55
	01 :40	17,35	17,44	16,91	16,59	18,28	14,73
	t_p=0.1 m						
	00 :00	13,96	14,34	13,86	15,2	14,27	14,59
	00 :10	13,88	14,34	13,78	15,2	14,27	14,59
	00 :20	13,88	14,34	13,86	15,2	14,27	14,59
	00 :30	13,88	14,34	14,03	15,2	14,27	14,59
T web (°C)	00 :40	13,88	14,34	14,11	15,2	14,27	14,59
	01 :50	13,96	14,34	14,35	15,2	14,27	14,59
	01 :00	13,88	14,34	14,59	15,2	14,27	14,59
	01 :10	13,72	14,34	14,66	15,2	14,27	14,59
	01 :20	13,72	14,34	14,81	15,2	14,27	14,59
	01 :30	13,64	14,34	14,58	15,2	14,27	14,59
	01 :40	13,64	14,34	14,34	15,2	14,27	14,59
	t_p=0.05 m						
	00 :00	766,510	1074,144	0	555,0615	469,938	0
	00 :10	819,37649	1040,577	819,3764	555,0615	503,505	41,205
	00 :20	792,945	839,175	700,485	528,63	570,639	123,615

Qs(W)	00 :30	845,808	906,309	1153,74	581,493	570,639	123,615
	00 :40	819,376	906,309	1153,74	581,493	671,34	329,639
	01 :50	819,3764	973,443	1153,74	581,493	671,34	370,844
	01 :00	819,3764	973,443	1277,355	581,493	738,474	329,64
	01 :10	792,945	1007,01	1277,355	660,7875	805,608	412,05
	01 :20	845,808	973,443	1194,945	766,513	906,309	494,46
	01 :30	845,808	973,443	1194,945	819,3765	906,309	576,870
	01 :40	872,239	1107,711	1194,945	792,945	772,041	535,665
t_p=0.1 m							
Qs (W)	00 :00	422,903	503,505	370,844	660,7875	604,206	164,819
	00 :10	422,904	402,804	906,51	555,0614	671,34	329,64
	00 :20	634,356	537,072	988,919	581,493	604,206	618,075
	00 :30	634,356	671,34	906,510	502,1985	604,206	618,075
	00 :40	502,1985	537,072	659,279	475,767	637,77	782,894
	01 :50	660,7875	436,371	700,485	475,7669	671,34	824,1
	01 :00	634,356	570,639	700,4850	475,766	738,474	906,51
	01 :10	422,904	570,639	494,46	502,1985	704,906	865,304
	01 :20	422,904	570,639	412,05	528,63	671,34	824,1
	01 :30	422,904	772,041	576,8699	528,63	604,205	1030,125
	01 :40	422,903	537,071	618,075	528,63	704,907	824,1
t_p=0.05 m							
Qair (KJ)	00 :00	45,99081	64,44864	0	33,30369	28,19628	0
	00 :10	49,16259	62,43462	42,0291	33,30369	30,2103	2,4723
	00 :20	47,5767	50,3505	69,224399	31,7178	34,238340	0
	00 :30	50,74848	54,37854	69,2244	34,88958	34,23834	19,7783
	00 :40	49,16259	54,37854	69,2244	34,88958	40,2804	22,2507
	01 :50	49,16259	58,40658	76,6413	34,88958	40,2804	27,1953
	01 :00	49,16259	58,4065	76,6413	39,64725	44,30844	19,7784
	01 :10	47,5767	60,4206	71,69670000	45,99081	48,33648	24,723
	01 :20	50,74848	58,406580	71,69670001	49,16259	54,37854	29,6676
	01 :30	50,74848	58,4065801	71,69670001	47,5767	54,37854	34,61220
	01 :40	52,33437	64,44864	71,696700	50,74848	46,32246	32,1399
t_p=0.1 m							
Qair (KJ)	00 :00	25,37424	30,2103	7,41689	39,64725	36,25236	2,472299
	00 :10	25,37424	28,19628	54,3906	33,30369	40,2804	19,7784
	00 :20	38,06136	32,22432	59,3352	34,88958	36,25236	37,0845
	00 :30	38,06136	30,2103	54,39060	26,96013	36,25236	29,6676
	00 :40	30,13191	32,22432	39,5568	28,54602	38,26638	51,9183
	01 :50	39,64725	30,2103	42,0291	28,54602	40,2804	51,9183
	01 :00	38,06136	34,23834	42,0291	28,54602	44,30844	54,3906
	01 :10	25,37424	34,23834	29,6676	30,13191	42,29442	51,9183
	01 :20	25,37424	34,23834	24,723	31,7178	40,2804	51,9183
	01 :30	25,37424	32,22432	27,1953	31,7178	36,25236	61,8075
	01 :40	25,37424	32,22432	37,0845	31,7178	40,2804	51,9183
t_p=0.05 m							

	00 :00	0	0	0	0	0	0
	00 :10	0,00166	0,00166667	0,00133333	0,005	0,0016666	0,0025
	00 :20	0,00166	0,000833	0,0006667	0,0016666	0,001167	0,001
	00 :30	0,00166	0,0008333	0,000666667	0	0,001333	0,0015
	00 :40	0,002333	0,002	0,001	0,0006666	0,001666	0,0015
	01 :50	0,000667	0,00066667	0,002	0,0011666	0,0015	0,00166
	01 :00	0,000666	0,00066666	0,0013333	0,0015	0,001166	0,00016
	01 :10	0,0005	0,00116667	0,001	0,0011666	0,001166	0,0011
	01 :20	0,001166	0,0005	0,001	0,0011667	0,0015	0,001
	01 :30	0,0003333	0,000833	0,00066666	0,0005	0,0006	0,001
	01 :40	0,0013333	0,001	0,00066666	0,0008333	0,000666	0,00083
$\dot{m}$ $evap$ (Kg/s)				t_p=0.1 m			
	00 :00	0	0	0	0	0	0
	00 :10	0,0016667	0,00116666	0,0016666	0,0066666	0,001666	0,00166
	00 :20	0,001	0,00116666	0,00116666	0,0015	0,0015	0,00133
	00 :30	0,001	0,00066666	0,00116666	0,001333	0,0015	0,001166
	00 :40	0,001	0,0001666	0,00083333	0,0013333	0,0015	0,001
	01 :50	0,0011666	0,0023333	0,0011666	0,0011666	0,000833	0,000666
	01 :00	0,0011666	0,00083333	0,0015	0,0016666	0,0006667	0,0005
	01 :10	0,0005	0,00083333	0,00066666	0,0008333	0,0015	0,00116
	01 :20	0,0011666	0,00066666	0,0005	0,0013333	0,0025	0,0015
	01 :30	0,0006666	0,0005	0,00116666	0,00116	0,0015	0,001333
	01 :40	0,00066	0,0008333	0,001	0,0008333	0,00116	0,0015
				t_p=0.05 m			
	00 :00	0	0	0	0	0	0
	00 :10	245	245	196	735	245	367,5
	00 :20	122,5	122,5	98	245	171,5	245
	00 :30	98	122,5	98	98	196	220,5
	00 :40	343	294	147	98	245	220,5
	01 :50	98	98	294	171,5	220,5	245
QL(KJ)	01 :00	98	98	196	220,5	171,5	98
	01 :10	73,5	171,5	147	171,5	171,5	171,5
	01 :20	171,5	73,5	147	171,5	220,5	171,5
	01 :30	49	122,5	98	73,5	98	147
	01 :40	196	147	98	122,5	98	122,5
				t_p=0.1 m			
QL(KJ	00 :00	0	0	0	0	0	0
	00 :10	245	171,5	245	980	245	245
	00 :20	147	171,5	171,5	220,5	220,5	196
	00 :30	147	98	171,5	196	220,5	171,5
	00 :40	147	24,5	122,5	196	220,5	147
	01 :50	171,5	343	171,5	171,5	122,5	98
	01 :00	171,5	122,5	220,5	245	98	73,5
	01 :10	73,5	122,5	98	122,5	220,5	171,5

	01 :20	171,5	98	73,5	196	367,5	220,5
	01 :30	98	73,5	171,5	171,5	220,5	196
	01 :40	98	122,5	147	122,5	171,5	220,5
η				t_p=0.05 m			
	00 :00	0	0	0	0	0	0
	00 :10	20,0663	25,48	21,44	4,53	12,33	0,672
	00 :20	50,16	41,10	70,63	12,94	19,96	0
	00 :30	29,59	44,39	70,63	0	17,46	8,96
	00 :40	14,33	18,49	47,09	35,60	16,44	10,091
	01 :50	50,16	59,59	26,068	20,34	18,26	11,10
	01 :00	50,16	59,59	39,102	17,98	25,83	20,182
	01 :10	64,73	35,23	48,77	26,81	28,18	14,41
	01 :20	29,59	79,46	48,77	28,66	24,66	17,29
	01 :30	103,56	47,67	73,15	64,73	55,48	23,54
	01 :40	26,70	43,84	73,15	41,42	47,267	26,236
				t_p=0.1 m			
	00 :00	0	0	0	0	0	0
	00 :10	10,35	16,44	22,20	3,39	16,44	8,07
	00 :20	25,89	18,78	34,59	15,82	16,44	18,92
	00 :30	25,89	30,82	31,71	13,75	16,44	17,29
	00 :40	20,49	11,52	32,29	14,56	17,35	35,31
	01 :50	23,11	8,80	24,50	16,64	32,88	52,97
	01 :00	22,19	27,94	19,06	11,65	45,21	74,00
	01 :10	34,52	27,94	30,27	24,59	19,18	30,27
	01 :20	14,795	34,93	33,63	16,18	10,96	23,54
	01 :30	25,89	43,84	15,85	18,49	16,44	31,53
	01 :40	25,89	26,30	25,22	25,89	23,48	23,54
ERR				t_p=0.05 m			
	00 :00	4,380	6,13796571	0	3,17178	2,68536	0
	00 :10	4,6821514	5,9461548	4,002771428	3,17178	2,8771	0,235457
	00 :20	4,5311142	4,79528571	6,592799999	3,020	3,26079	0,235457
	00 :30	4,8331885	5,17890857	6,5928	3,3228	3,26079	1,883657
	00 :40	4,6821514	5,17890857	6,5928	3,32281	3,8362285	2,119114
	01 :50	4,6821514	5,56253142	7,299171	3,32281	3,836228	2,590028
	01 :00	4,6821514	5,56253142	7,2991714	3,775928	4,2198514	1,883657
	01 :10	4,5311142	5,75434285	6,8282571	4,380077	4,603474	2,35457
	01 :20	4,8331885	5,562531	6,8282571	4,68215	5,1789085	2,825485
	01 :30	4,8331885	5,56253142	6,8282571	4,5311	5,17890	3,29640
	01 :40	4,9842257	6,13796571	6,8282571	4,83318	4,411662	3,060942
				t_p=0.1 m			
	00 :00	2,41659	2,877171	0,706371	3,775	3,4526	0,235
	00 :10	2,416599	2,68536	5,1800	3,17178	3,8362	1,88365
	00 :20	3,6248914	3,068	5,650	3,3228	3,45260	3,531857
	00 :30	3,624891	2,8771	5,180057	2,56763	3,4526	2,8254

	00 :40	2,8697057	3,068982	3,76731	2,718668	3,6444	4,944599
	01 :50	3,775928	2,877171	4,002771	2,718668	3,83622	4,944599
	01 :00	3,624891	3,2607942	4,002771	2,718668	4,219851	5,1800
	01 :10	2,4165942	3,26079428	2,82548	2,869705	4,02804	4,944599
	01 :20	2,4165942	3,2607942	2,35457	3,020742	3,836228	4,944599
	01 :30	2,4165942	3,06898	2,5900285	3,020746	3,4526	5,886428
	01 :40	2,4165942	3,0689	3,53185	3,020742	3,83622	4,944599
				t_p=0.05 m			
ε	00 :00	0,3088	0,354	0	0,2227	0,1669	0
	00 :10	0,3359	0,3437	0,1834	0,2275	0,1788	0,0099
	00 :20	0,325	0,2765	0,3115	0,2172	0,2068	0,0294
	00 :30	0,3467	0,2987	0,2935	0,2384	0,2073	0,0758
	00 :40	0,3359	0,2987	0,2935	0,2373	0,2535	0,0877
	01 :50	0,3359	0,3204	0,3301	0,2373	0,2541	0,1108
	01 :00	0,3425	0,3208	0,3301	0,2703	0,2788	0,0785
	01 :10	0,3319	0,3378	0,3088	0,3122	0,3034	0,0974
	01 :20	0,3536	0,3208	0,3088	0,3273	0,3557	0,114
	01 :30	0,3536	0,3273	0,3088	0,3168	0,3557	0,1393
	01 :40	0,3646	0,3612	0,3088	0,3437	0,31	0,1196
				t_p=0.1 m			
	00 :00	0,1896	0,1884	0,1119	0,266	0,2016	0,0454
	00 :10	0,1856	0,1567	0,2743	0,2333	0,2167	0,0888
	00 :20	0,2784	0,201	0,2985	0,2391	0,2039	0,1629
	00 :30	0,2784	0,2611	0,2726	0,2184	0,2039	0,1684
	00 :40	0,2204	0,201	0,1978	0,2143	0,2152	0,2019
	01 :50	0,2894	0,1697	0,2086	0,2195	0,2265	0,2125
	01 :00	0,2784	0,2109	0,2122	0,2195	0,2436	0,2266
	01 :10	0,1822	0,2109	0,1531	0,2346	0,2352	0,2185
	01 :20	0,1822	0,2109	0,13	0,2469	0,2265	0,2185
	01 :30	0,1826	0,201	0,1407	0,2469	0,2086	0,2498
	01 :40	0,1826	0,1985	0,1884	0,2469	0,2265	0,2498

4.2.1 Data Analysis

4.2.1.1 Heat Flux Analysis (Sensible, Latent, Total)

Heat flux measurements provide valuable insights into the heat transfer dynamics within the evaporative cooling system. The heat flux was measured in three components: sensible, latent, and total, across different fiber materials (cotton and sisal), thicknesses (0.05 m and 0.1 m), and mass flow rates (0.263, 0.334, and 0.41 kg/s).

The top graph in Figure Figure 4 2 shows how the sensible heat flux varies with time
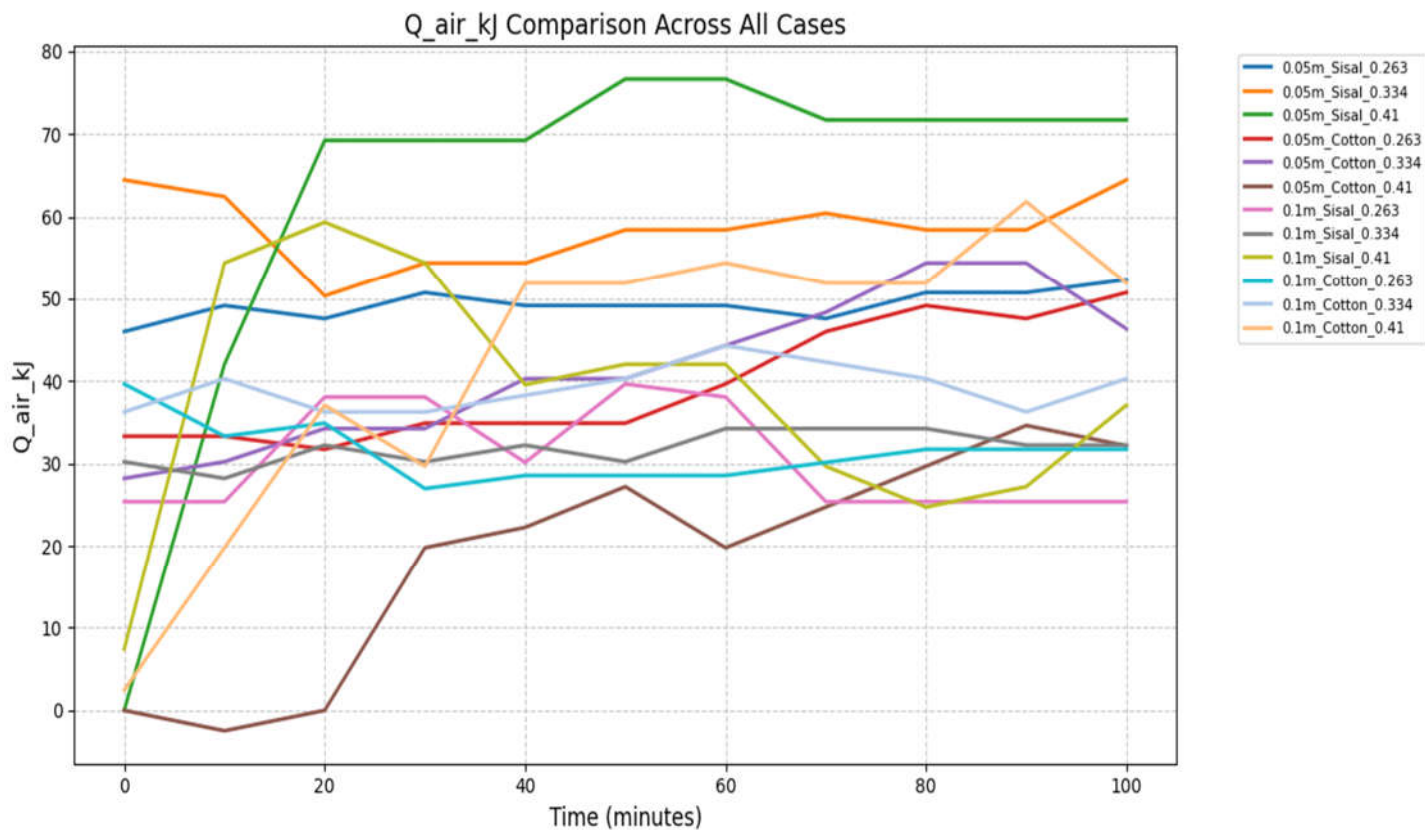
Figure 0-1 Air heat flow changes comparison over time
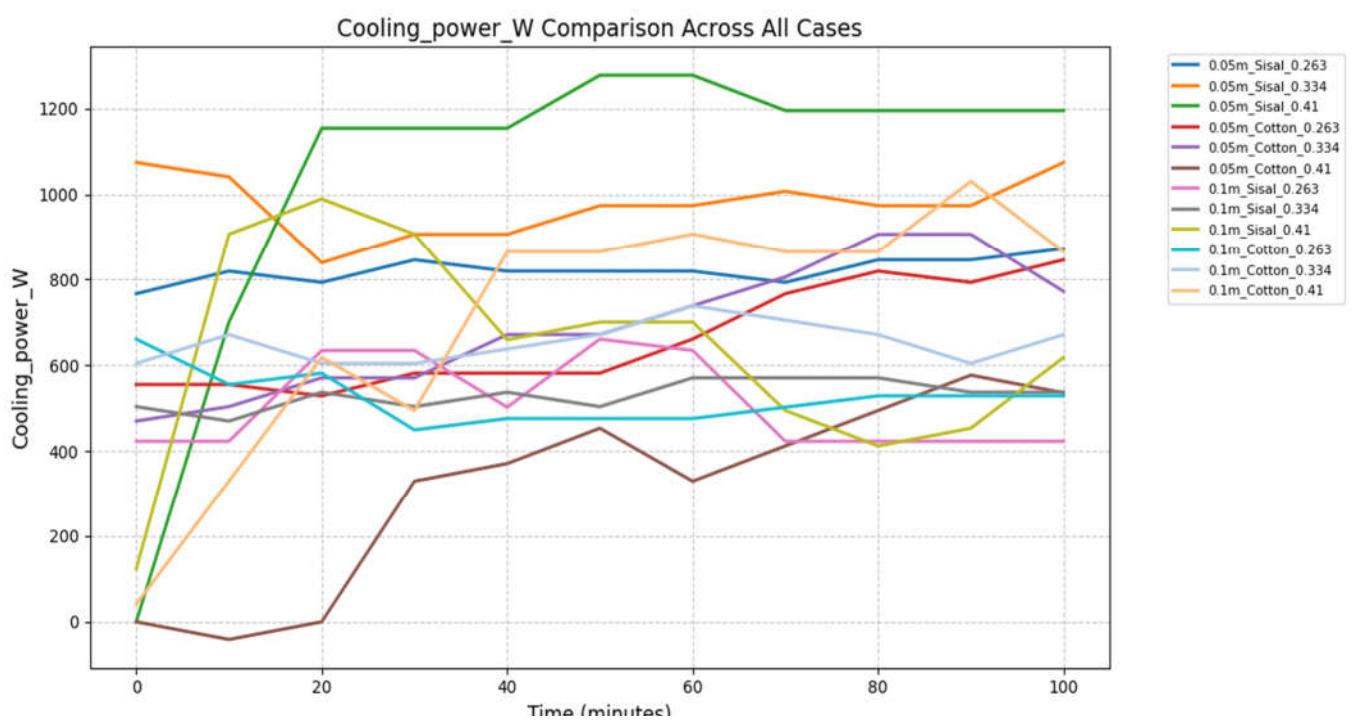
Figure 0-2 sensible heat changes comparison over time
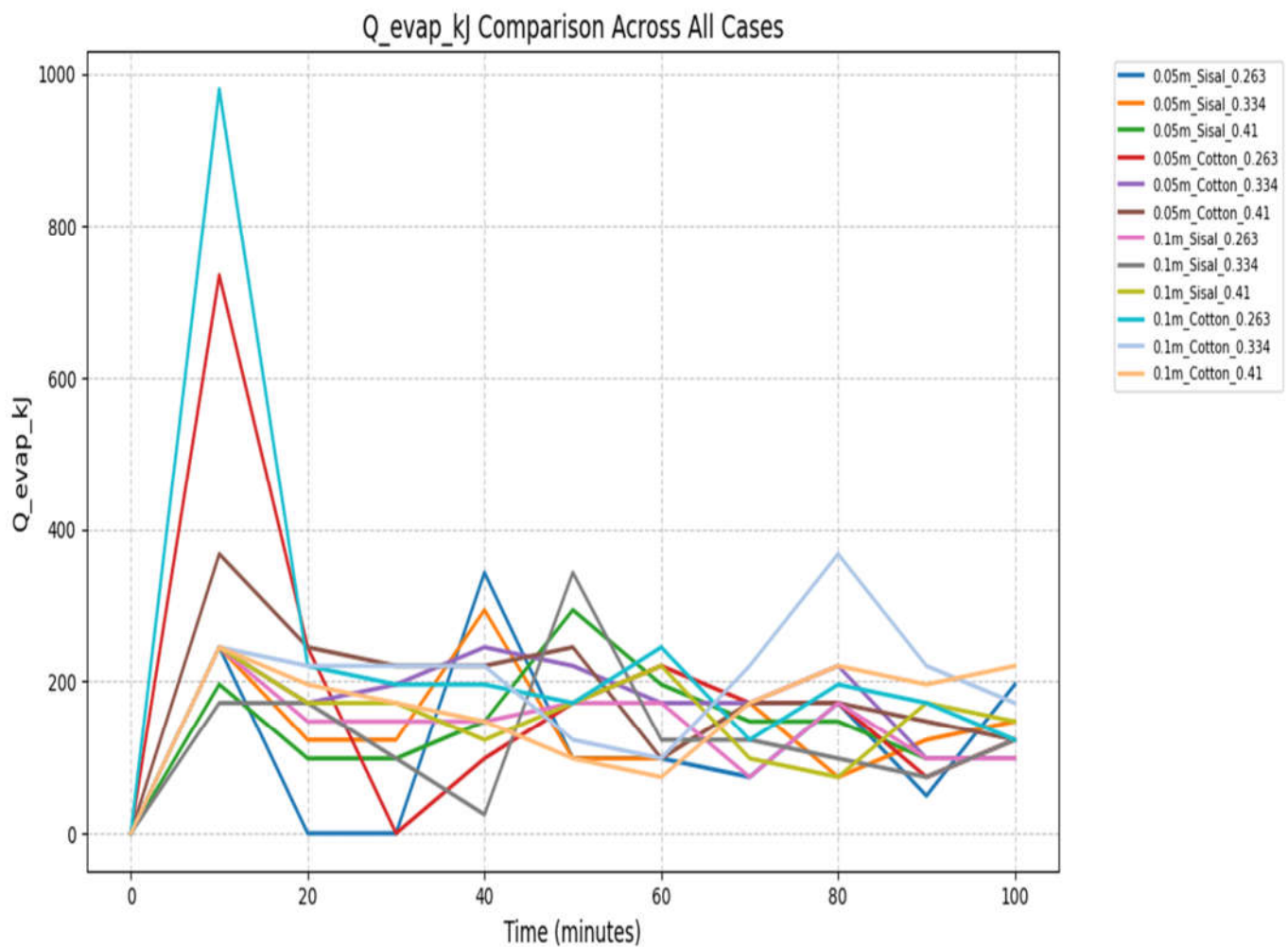
Figure 0-3   evaporaive heat flow changes comparison over time

4.2.1.2   System Efficiency

Energy efficiency analysis is an essential component of evaporative cooling system performance evaluation, particularly in areas where sustainability, water use, and thermal comfort are critical. This analysis aims to determine how effectively a system converts available energy—particularly from airflow and water evaporation—into useful cooling output. The results are represented in Figure 4 4:
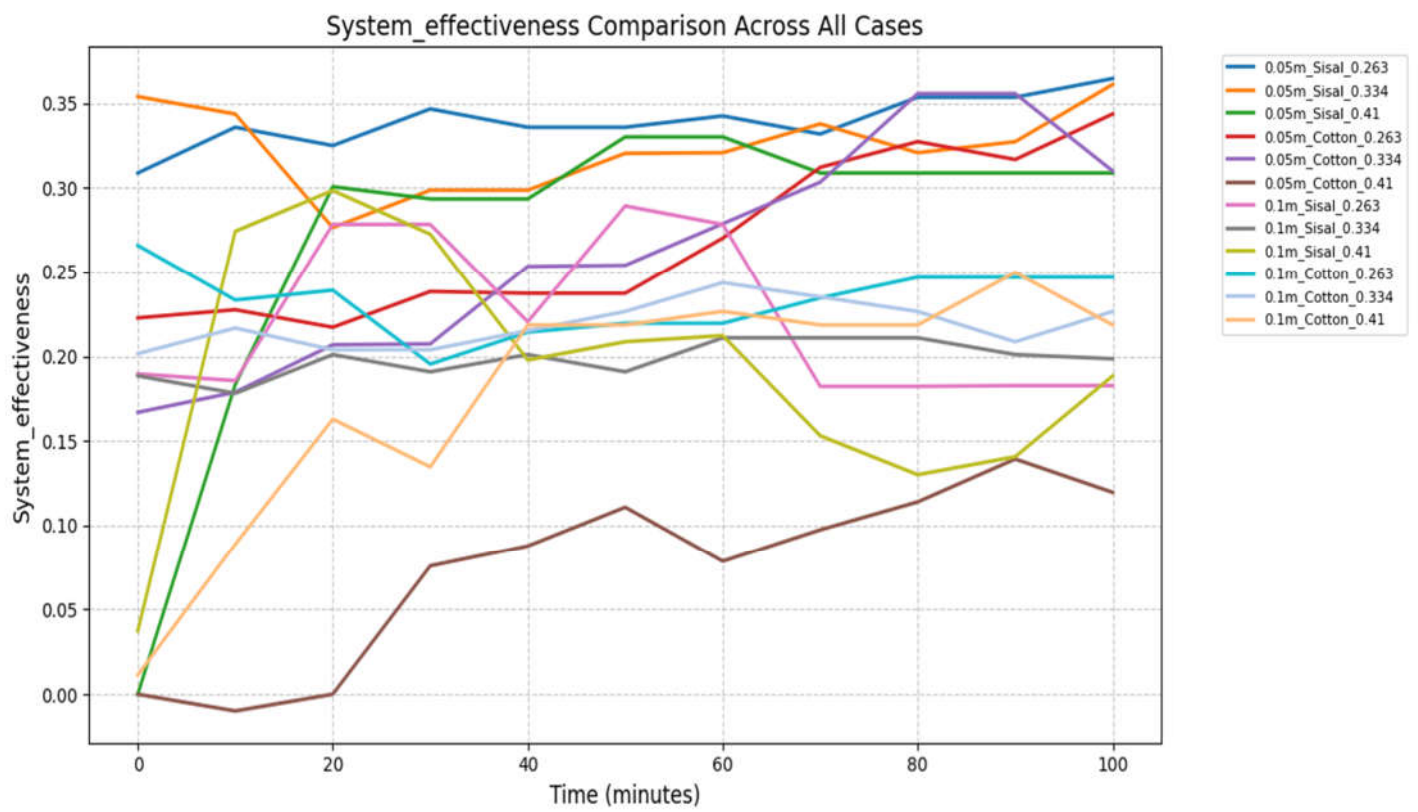
Figure 0-4 cooling effectiveness changes comparison over time
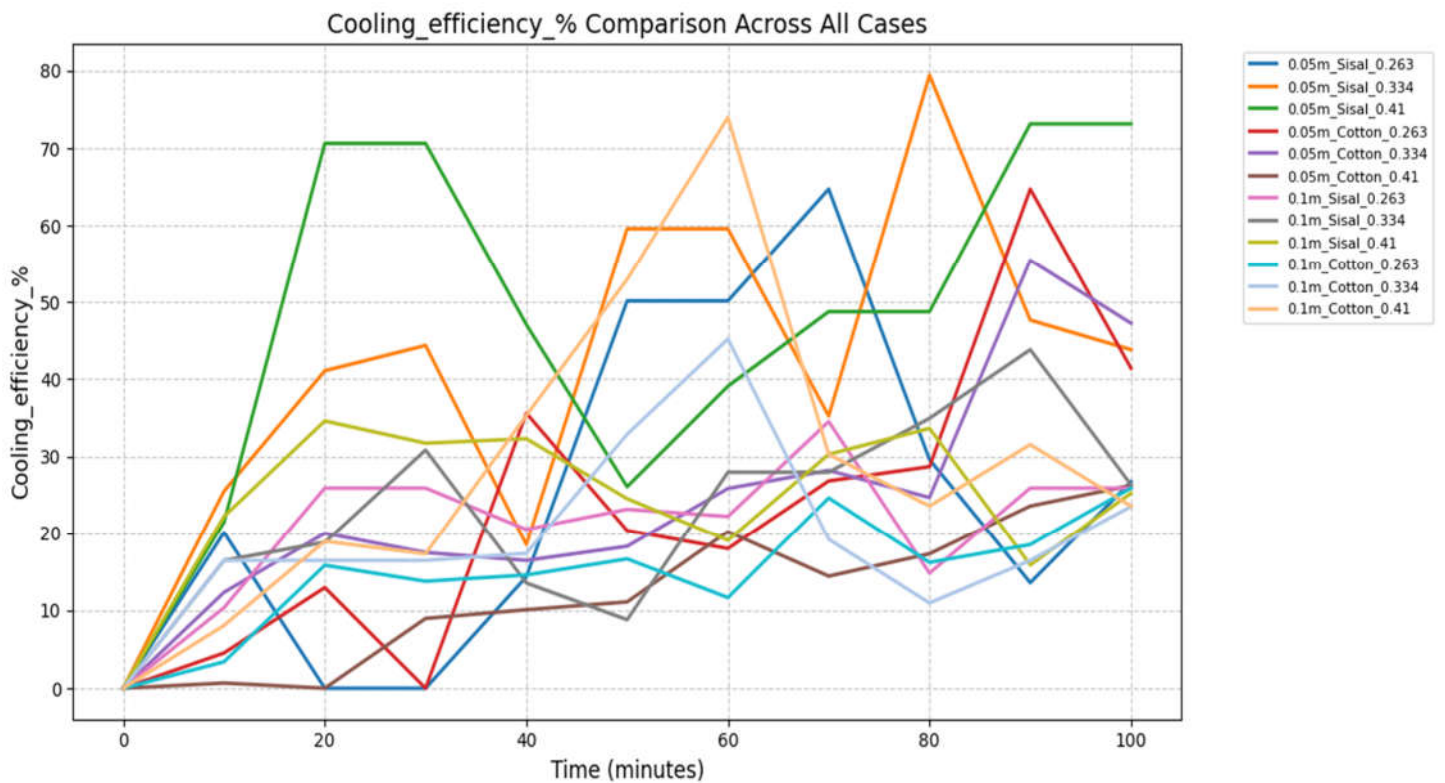
Figure 0-5 cooling efficiency changes comparison over time

4.2.2 Results Interpretation

Figure 1 represents changes in air heat flux over time. We observed that the sisal fibers, **0.05** m thick, and an air flow rate of approximately **0.410 kg/s**, reached their peak, maintaining the same result for an hour and occasionally decreasing. We attribute this to the permeability of the sisal fibers and their constant need for water.

Sisal fibers of the same thickness maintained the same performance, but with a slight difference in the results.

We observed that cotton fibers maintained increasing results over time and maintained the same performance. This is explained by the cotton fibers' ability to retain water and their low air porosity. Similar observations were recorded for Figure 2 .

We recorded the same observations for Figure 3 , but this time we observed a significant increase in the latent heat flux of cotton at a thickness of **0.1** meters and a flow rate of **0.410 kg/s**. This is explained by the cotton's poor air permeability, the higher outside air temperature, and the increased flow. This suggests that cotton production is higher in hotter environments. The same results were recorded for the total flow, but completely different results were recorded for the document, which represents changes in vapor flow over time.

We observed a peak for cotton at thicknesses of **0.1** m and **0.05 m**, respectively. This is explained by cotton's high water-holding capacity, as it required twice the volume of sisal to saturate, unlike sisal, which recorded the exact opposite.

We see in Figure 4 3 that sisal fibers with thickness 0.05 and air flow 0.410 recorded the highest efficiency, followed by sisal fibers with the same thickness at air flow à, which also achieved the same cooling efficiency with slight variations. Sisal fibers outperformed in efficiency but maintained consistent, sometimes decreasing, results. We note a significant increase in the cooling efficiency of cotton fibers over time. After the 80th minute, cotton recorded cooling efficiency rates that differed depending on the sisal fiber. This is what we see in the document at the intersection of the curves. We also observe the same results for Figure Figure 4 4 .

4.3 Conclusion :

Based on the data recorded during the third semester, the results obtained were calculated and analyzed, where we noticed that the performance of the system varied according to the air flow, the nature of the evaporating pad and the different thicknesses, in general, the system

consisting of a sisal evaporating pad recorded better performance, while the system consisting of a cotton evaporating pad recorded a more stable performance.

Chapter 5

Artificial Intelligence as a Tool for System Evaluation and Design Optimization

Chpter 5

Artificial Intelligence as a Tool for System Evaluation and Design Optimization

5.1 Introduction

The focus shifts from experimental evaluation to the optimization and development of a passive evaporative cooling system. Based on the detailed thermal and efficiency analyses conducted in this chapter, several limitations and performance gaps in the current system are identified, particularly with regard to heat flow consistency, system efficiency, and material response to varying airflow rates and thicknesses.

5.2 Design Development Towards a Hybrid Cooling System

Based on the previous results and analyses, it was concluded that both the thickness and area of the evaporative pad, in addition to the type of materials used, contribute directly to influencing the system performance, taking into account the effect of air flow, which helped in testing better solutions that contribute to raising the device's performance.

In addition, the evaporative pad was developed using a hybrid of sisal and cotton fibers, combining the water absorption and sustainability properties of sisal with the moisture-retaining properties of cotton, providing an effective evaporation surface. This combination helped improve moisture distribution within the pad and increase cooling efficiency without negatively impacting water consumptionThe pad is made of 80% sisal and 20% cotton, with a thickness of 0.1 m and a flow rate of 0.10 kg/s. The outer surface of the pad is provided with a quantity of activated charcoal to filter the outside air and absorb excess moisture.. The results obtained are recorded in the following table

Figure 0-1 Top view of the hybrid evaporative pad

Table 7 Hybrid pad system experimenal results

Time (min)	T(℃)		RH(%)		Vv(kg)	Tv (℃)	Tw(°C)
	T_in	T_out_no_cond	RH_in	RH_out_no_cond			
00 :00	25.7	25.8	30	33	0	0	18.0
00 :10	25.9	25	31	39	0.2	25	18.3
00 :20	25.9	24.2	31	40	0.1	23	17.8
00 :30	25.9	23.5	31	41	0.07	22.7	17.4
00 :40	26	23	31	43	0.04	22.1	17.1
00 :50	26	22.7	32	46	0.02	21.9	16.9
01 :00	26.1	22.4	32	46	0.01	21.4	16.6
01 :10	26	22.3	32	50	0.03	21.4	16.6
01 :20	26	22.1	32	51	0.02	21	16.5

	26.1	22	32	50	0.01	20.9	16.4
01 :30							

Table 8 Hybrid bad system analysis results

TIME(min)	Q_air (kJ)	Q_evap (kJ)	m_evap_rate (kg/min)	Qs (W)	EER	Effective-ness
0	0	0	0	0	0	
10	222,507	490	0,02	370,84	2,06025	0,1184210
20	420,291	245	0,01	700,48	3,8915833	0,2098765
30	593,352	171,5	0,007	988,92	5,494	0,282352
40	741,69	98	0,004	1236,15	6,8675	0,337078
50	815,859	49	0,002	1359,76	7,55425	0,36263
60	914,75100000	24,5	0,001	1524,59	8,4699166	0,389473
70	914,751	73,5	0,003	1524,58	8,4699166	0,39361
80	964,197	49	0,002	1606,99	8,92774	0,410526
90	1013,643	24,5	0,001	1689,41	9,38558333	0,422680
100	988,92	24,5	0,001	1648,2	9,156666	0,41666

5.2.1 Data Analysis

The data recorded in the table was analyzed and plotted in curves to compare sisal and cotton fibers in different variables to monitor, interpret, and compare the results for different experimental environments as shown in the figure   **0-2 , 0-3, 0-4, 0-5, 0-6 .**

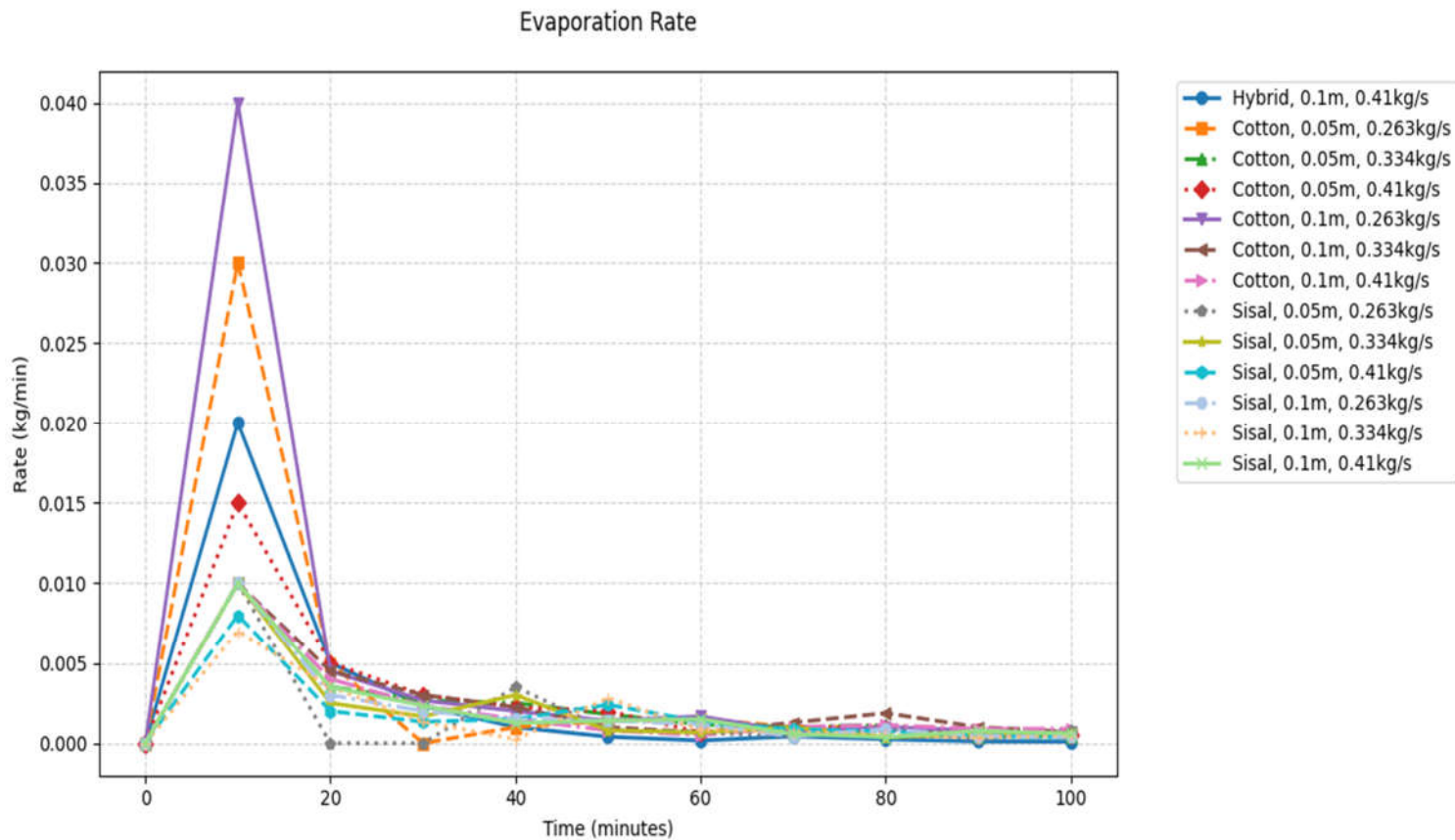**Figure 0-2 Evaporation rate changes for all systems over time**
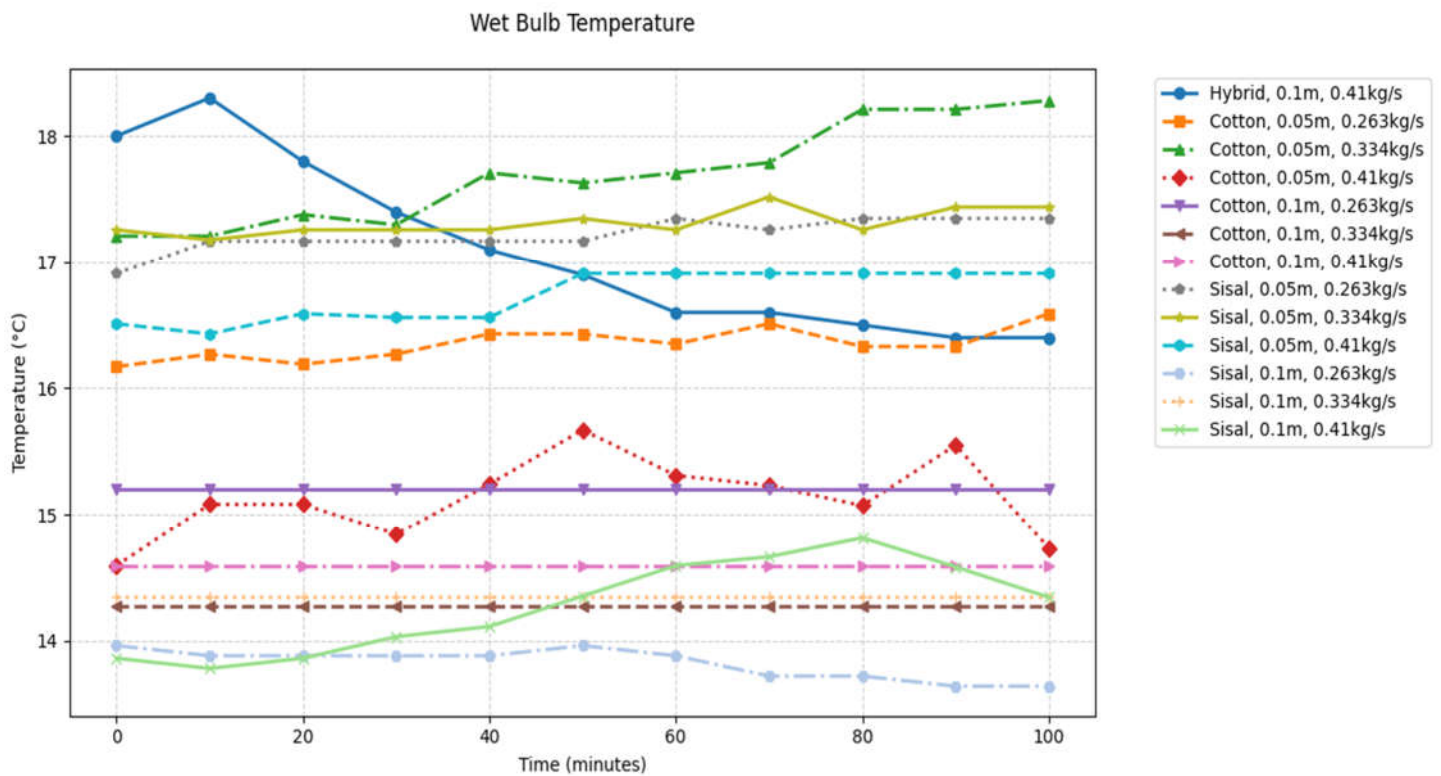
Figure 0-3 Wet bulb temperature changes over time
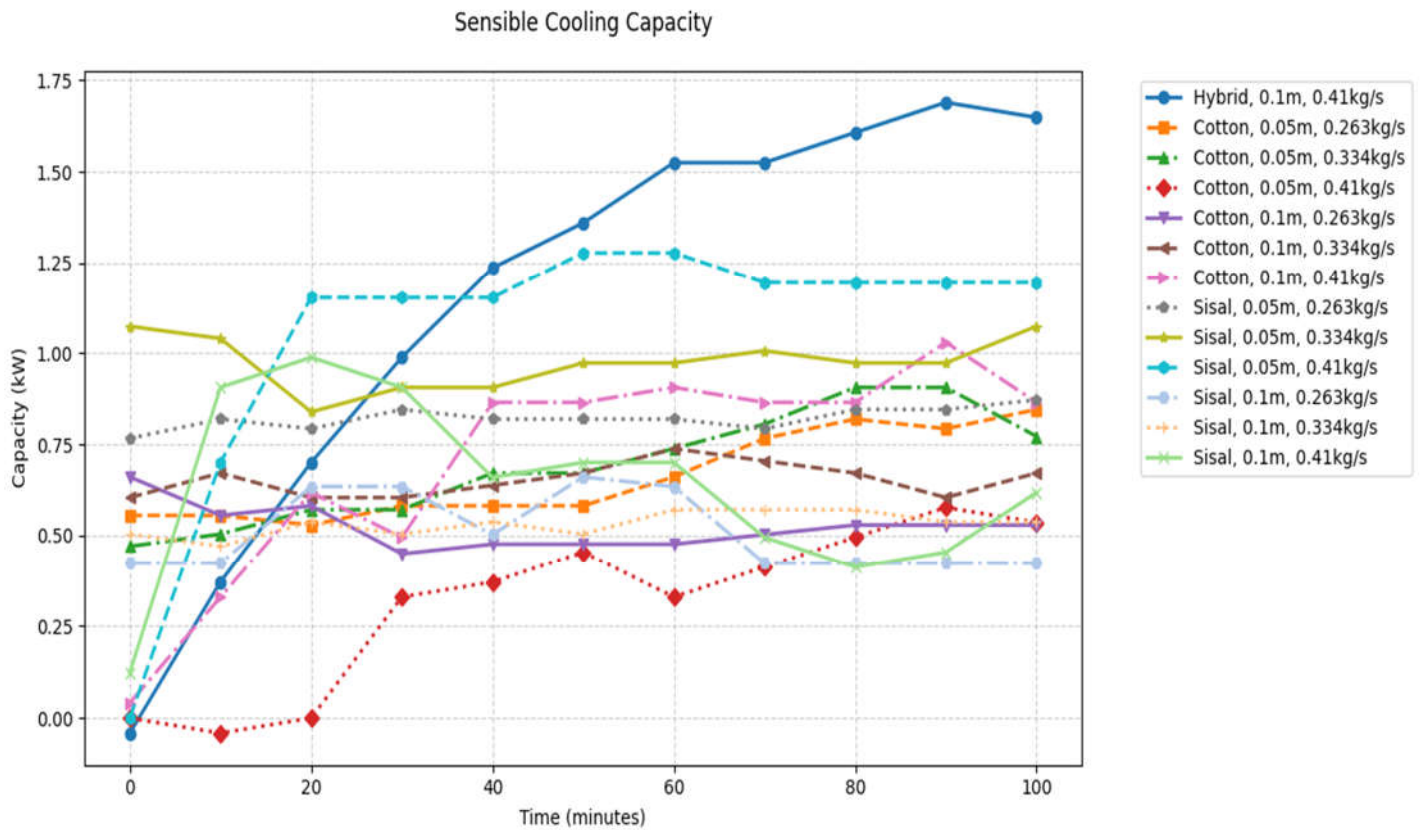
Figure 0-4 Sensible heat flow changes over time
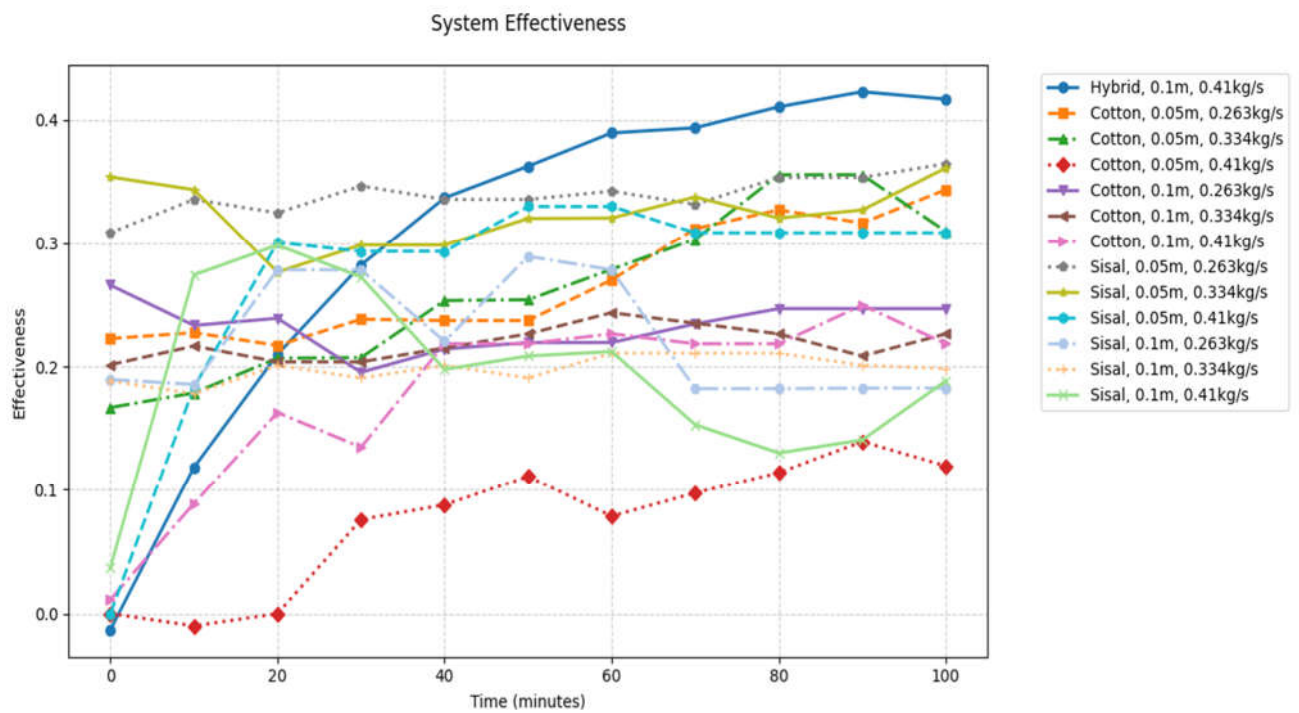
Figure 0-5 system effectiveness for all systems changes over time

Energy Efficiency Ratio
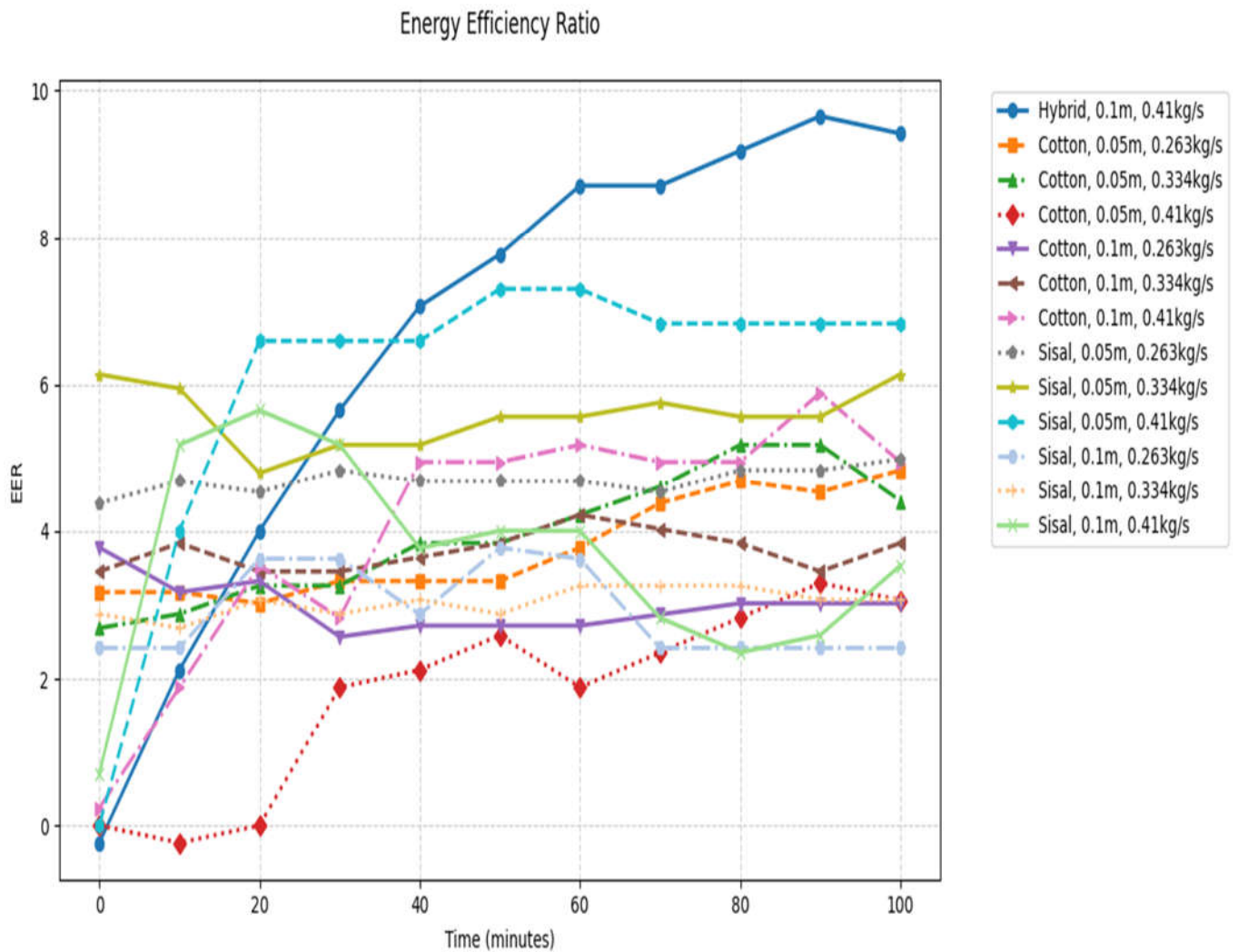
Figure 0-6 ERR changes for all systems over time

5.2.2 Results Interpretation

Figure 2 shows a comparative curve of sensitive flow changes for cotton, sisal, and hybrid evaporative pads. We observed significant improvements in device performance, not only in flow, but also in energy efficiency, cooling efficiency, and even temperature. At the same time, we observed reasonable water consumption, which is expected given the low porosity of cotton, which does not exceed 20%, and the low water-holding capacity of sisal. We observed a significant increase in performance of the device equipped with the hybrid pad. Therefore, the hybrid pad was considered the optimal choice among these experimental phases for inclusion in the new system, paving the way for the next steps.

5.2.3 3D modeling and visualization of evaporative cooling systems for buildings

Based on the previous results, a 3D model was designed using AutoCAD, specifically FreeCAD, and then exported to Blender for clearer results, as both are open source 3D technical drawing programs. The device's body was designed to **1.6 m³** in size, with a **2 m²,** 0.4 m thick hybrid evaporative pad in the center. It was equipped with a **45** watt pump, a **135**-watt fan, and a system water tank with ventilation holes and temperature and humidity sensors. The following figure was obtained:
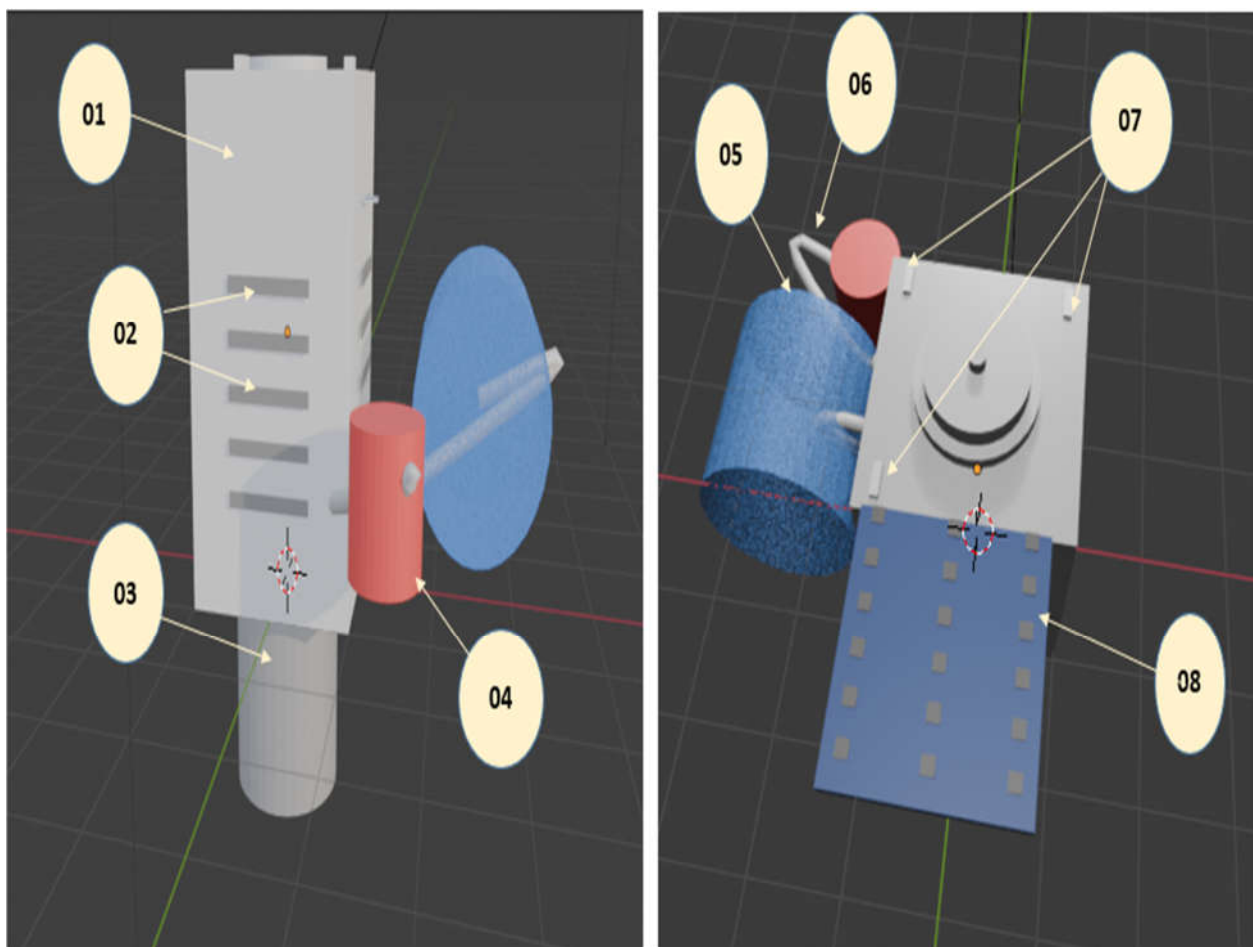
Figure 0-7 Exterior view of a 3D AutoCAD structure
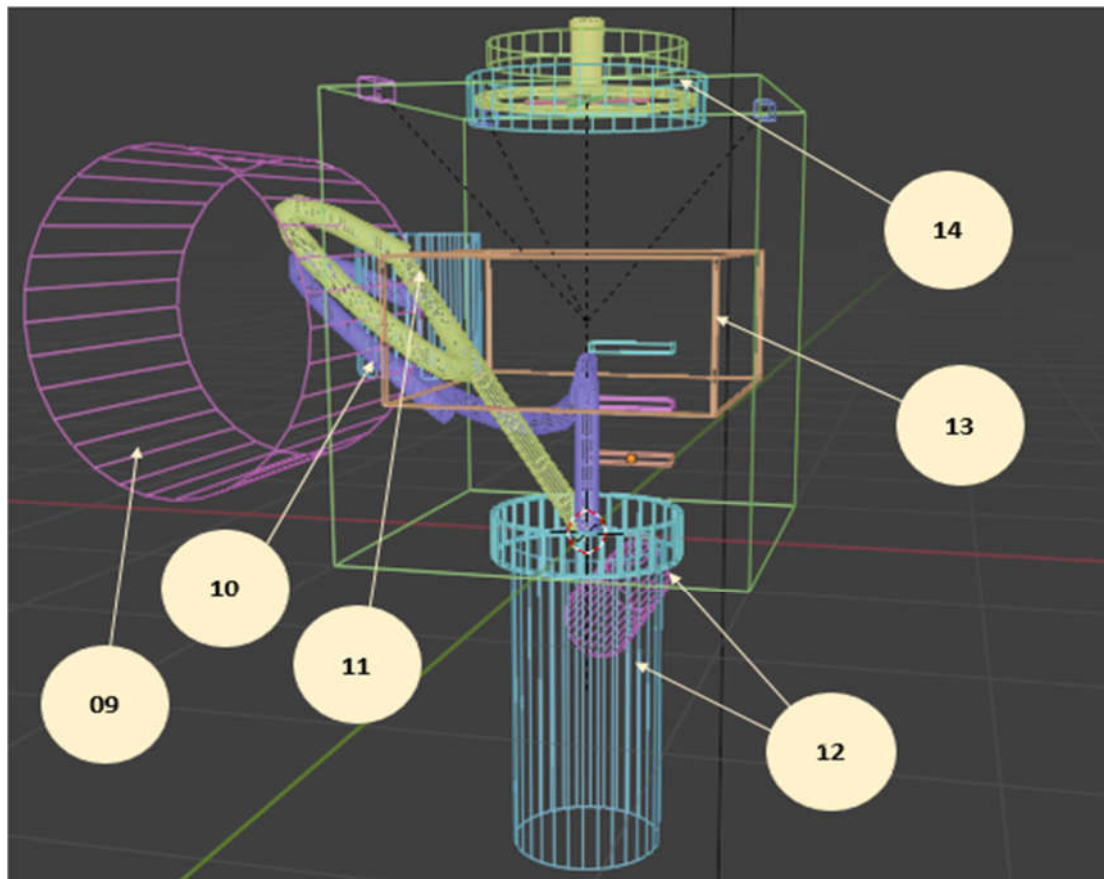
Figure 0-8 Internal components of DEC

Table 9   Definition of the components of the 3D drawing of the device

Element	Name	Element	Name
01	Evaporative cooler	08	Solar panel
02	Distribution duct	09	Water tank
03	Air vents	10	Water distribution pipe
04	Water pump	11	Water recovery pipe
05	Water tank	12	Cold air distribution ducts
06	Water pipe	13	Evaporative hybrid pad
07	Sensors	14	Fan

5.2.4 System simulation using artificial intelligence

Dynamic Simulation of a Hybrid Cooling System and Artificial Intelligence Applications in a Python Programming Environment. An advanced numerical model was developed to simulate the dynamic performance of a hybrid evaporative cooling system using the Python programming environment, combining analytical and experimental methodologies. The model is based on a reference dataset extracted from preliminary experiments (hybrid, sisal, and cotton). Artificial intelligence algorithms were employed to predict the system's behavior under different operating conditions. The methodology combines fundamental principles of thermofluid dynamics with supervised machine learning techniques to build a predictive model capable of simulating the complex, nonlinear relationships between operating variables (such as temperature, relative humidity, and airflow rate) and performance indicators (energy efficiency, temperature drop, and outlet relative humidity). The Random Forest Regression algorithm was chosen as the primary predictive tool due to its superior ability to process multidimensional data, its resistance to overfitting, and its accuracy in handling nonlinear relationships between variables. This algorithm works by building hundreds of decision trees on partial data samples, then combining their results to obtain more stable and accurate predictions.

This study features an integrated methodology that includes:

- Primary physical modeling based on the laws of conservation of mass and energy
- Generating comprehensive simulation data covering wide operating ranges
- Applying data preprocessing techniques such as normalization
- Evaluating model performance using multiple statistical measures (MAE, R^2)
- Three-dimensional analysis of the relationships between variables

This methodology represents a practical model for how artificial intelligence techniques can be employed to improve the efficiency of cooling systems. It provides a powerful tool for predicting performance and determining optimal operating conditions, which contributes to rationalizing energy consumption and improving the thermal efficiency of the system. The results obtained were recorded in Figure 09 Figure 10; Figure 11.

Tout (°C)		RH_out (%)		Cooling Effect		m_evap (kg)	
MSE	R^2	MSE	R^2	MSE	R^2	MSE	R^2

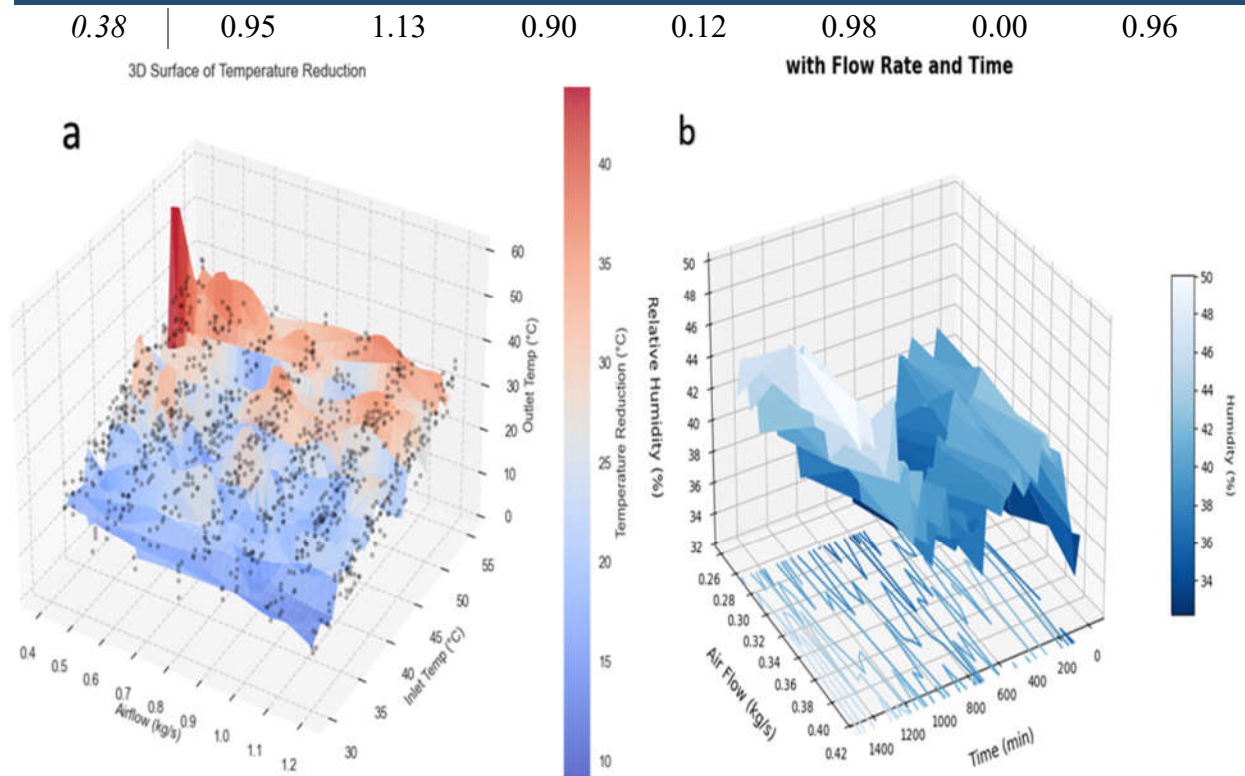| *0.38*	0.95	1.13	0.90	0.12	0.98	0.00	0.96

Figure 0-9 (a) The effect of airflow changes on temperature changes over time (b) The effect of airflow changes On humidity changes over time

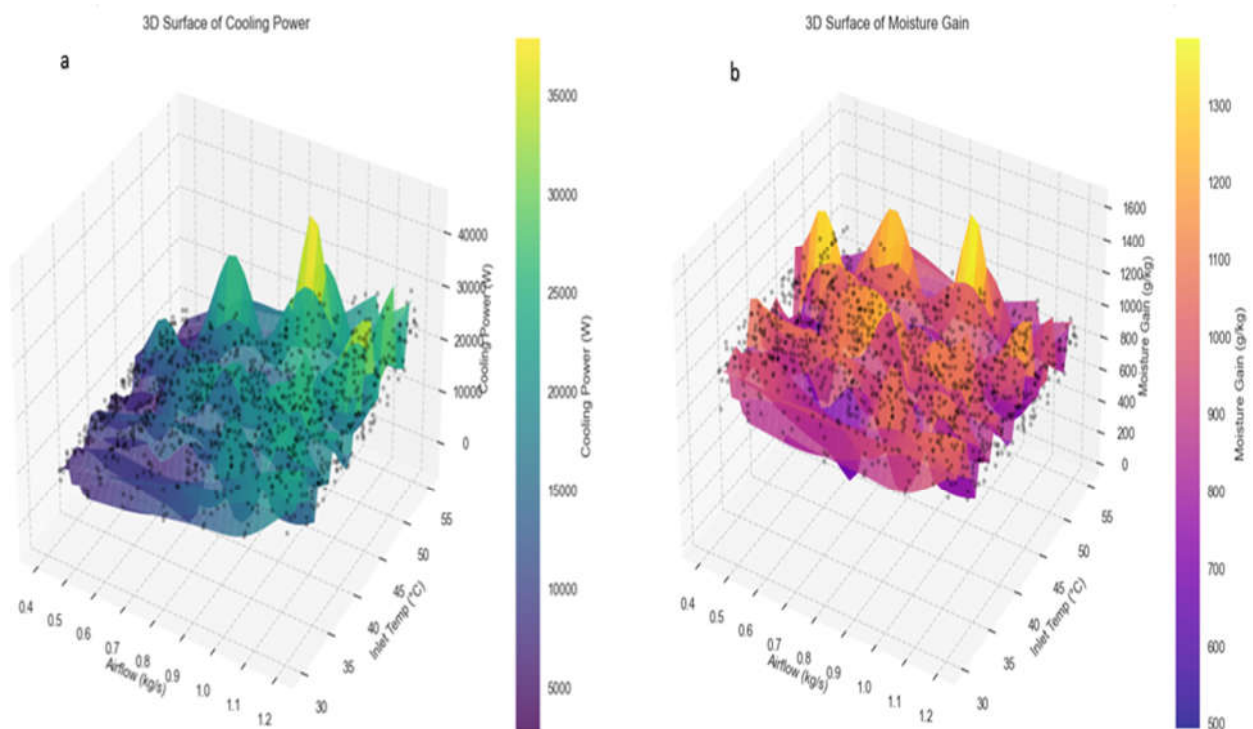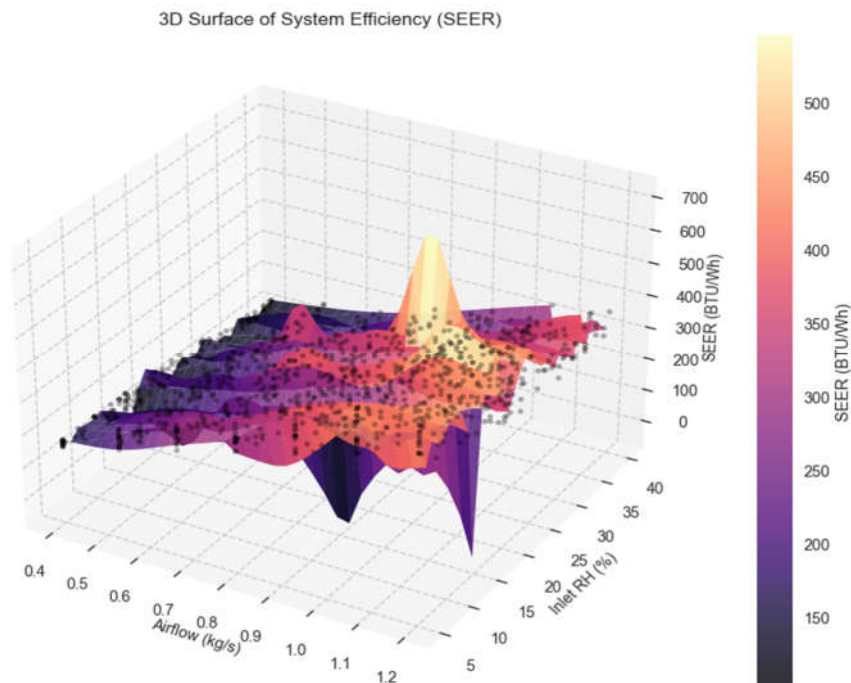**Figure 0-10 (a) sensible heat flow changes over time (b) moisture Gain changes over time**

Figure 0-12 Hybrid system efficiency SEER changes over time
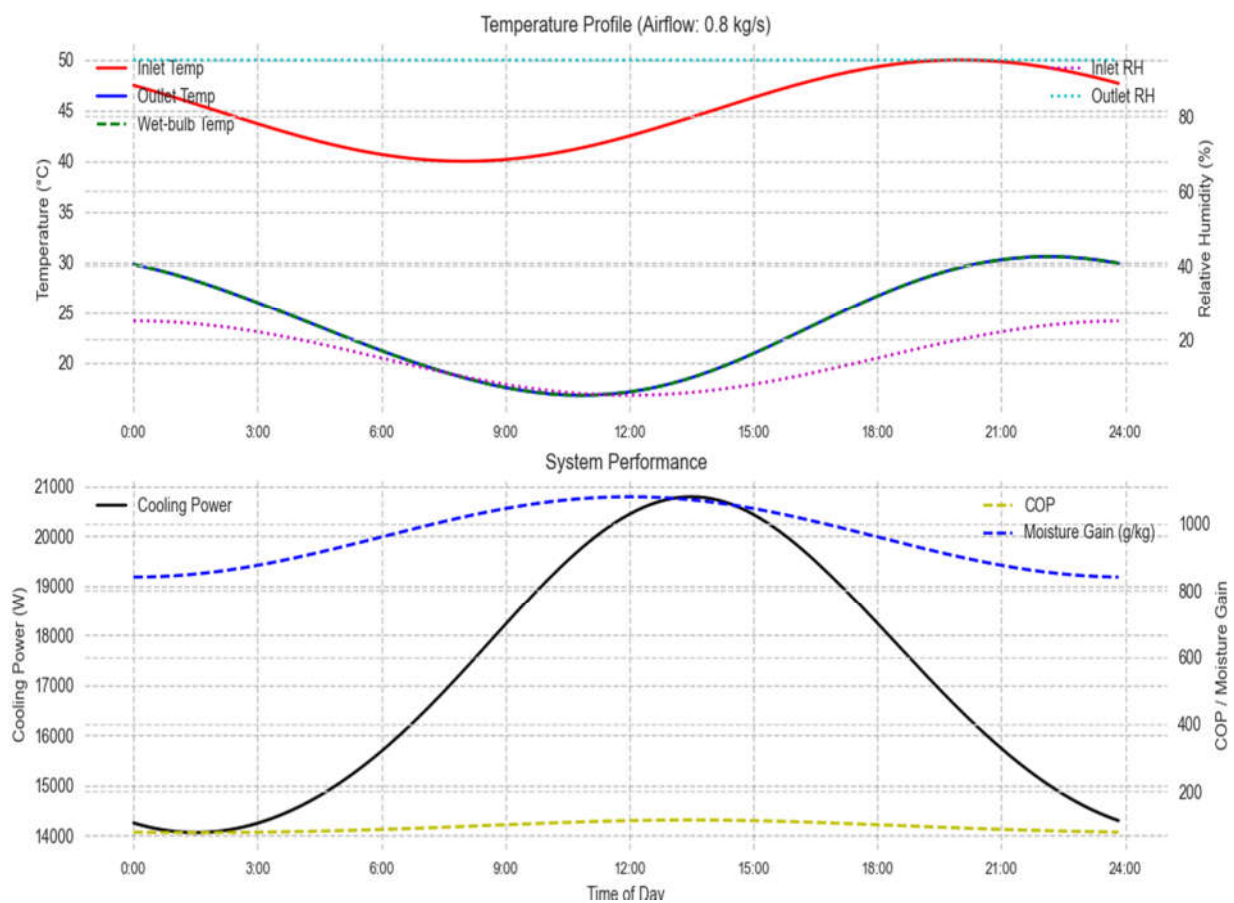

Figure 0-11 DEC Physical ingredients changes over 24 hours

5.2.5 Decisions and Analysis

The statistical metrics analysis demonstrates the outstanding performance of the predictive model in simulating the behavior of the cooling system, as demonstrated by the following indicators:

5.2.5.1 Outlet Temperature (Tout - °C)

Mean Square Error (MSE): 0.38 , Coefficient of Determination (R^2): 0.95 ; These results indicate high accuracy in predicting outside temperatures, with the model explaining 95% of the variance in the data, with a small margin of error not exceeding 0.38°C². We observe the effect of airflow on temperature changes over time, as documented in Figure **0-9**, where we observe an inverse relationship between airflow values and changing temperature.

5.2.5.2 Outlet Relative Humidity (RH_out - %)

MSE: 1.13 , R^2: 0.90 ; The model demonstrates good ability to predict humidity, explaining 90% of the variance. Note that the relatively higher MSE value reflects the greater challenges in modeling humidity behavior compared to temperature.

Humidity values are also inversely affected by changes in airflow. As airflow increases, the recorded humidity decreases.

5.2.5.3 Cooling Effect (Cooling_Effect) and seer

MSE: 0.12 , R^2: 0.98 ;These results demonstrate exceptional performance in predicting the cooling effect, indicating that the model accurately captures the relationship between operating variables and the amount of cooling delivered. We also observe the direct impact of temperature, humidity, and direct airflow on the performance of the system. As the temperature increases, humidity decreases, and airflow increases, the system performance increases. This demonstrates the effectiveness of evaporative cooling systems in hot and dry regions. To ensure better learning of the system, a prediction of the above values was created throughout the day in a hot and dry environment, as represented in the curves in the document. Therefore, the results confirm the validity of the previously proposed hypotheses, which include the effects of inlet temperatures, airflow, and the nature and size of the evaporative pad on the performance of evaporative cooling systems.

5.2.6   Fabrication of the New Prototype

The prototype was constructed using transparent glass sheets, wooden panels, a water circulation system, and built-in measuring devices. The construction was directly inspired by the improved design features of the digital model. The device measures 60 cm in length and is 2 cm thick. The device was tested and its performance verified in a closed, thermally insulated space. Figure **0-10-** show images of the prototype construction.

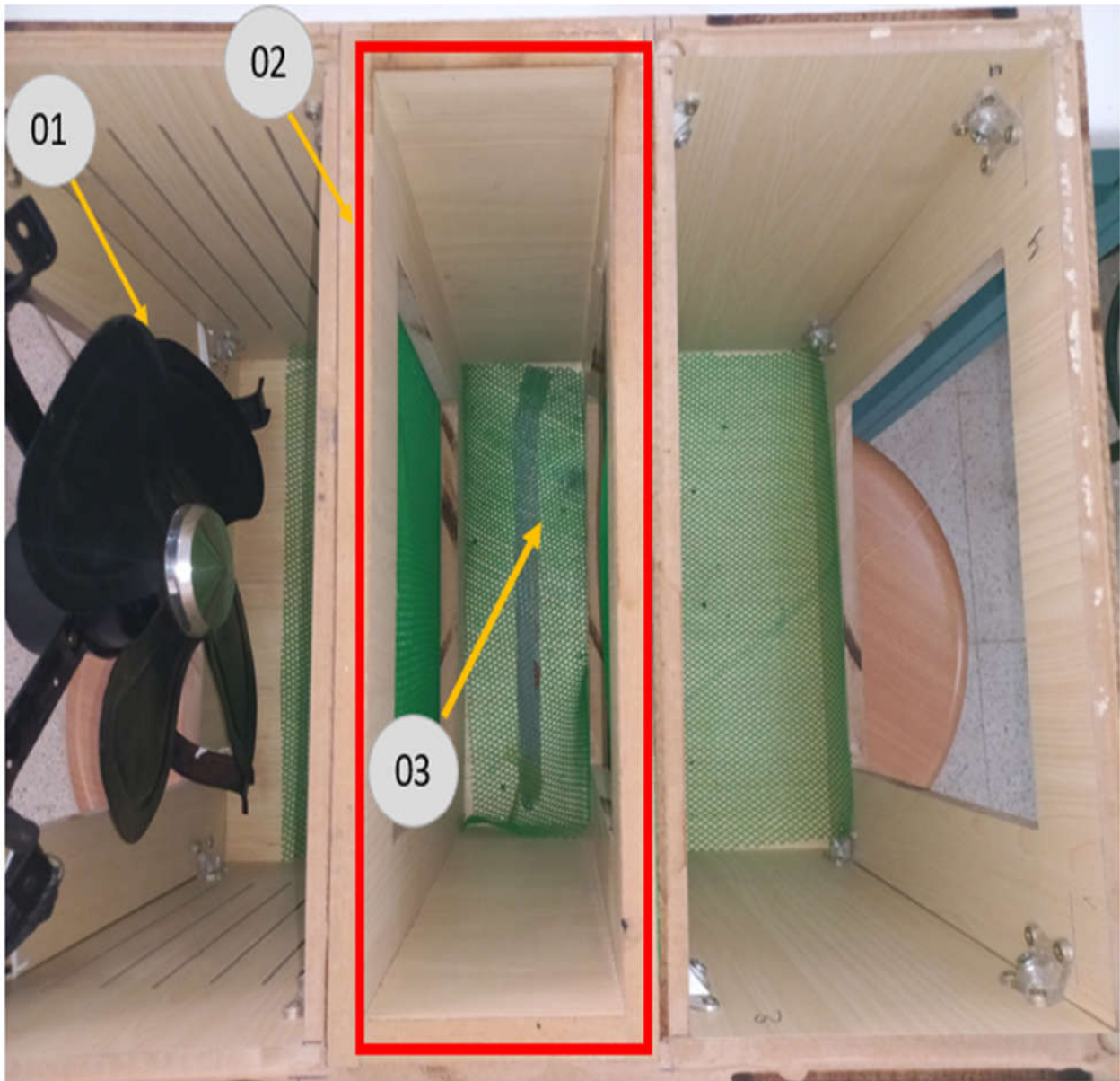**Figure 0-13 Top view of the internal structure of the prototype**
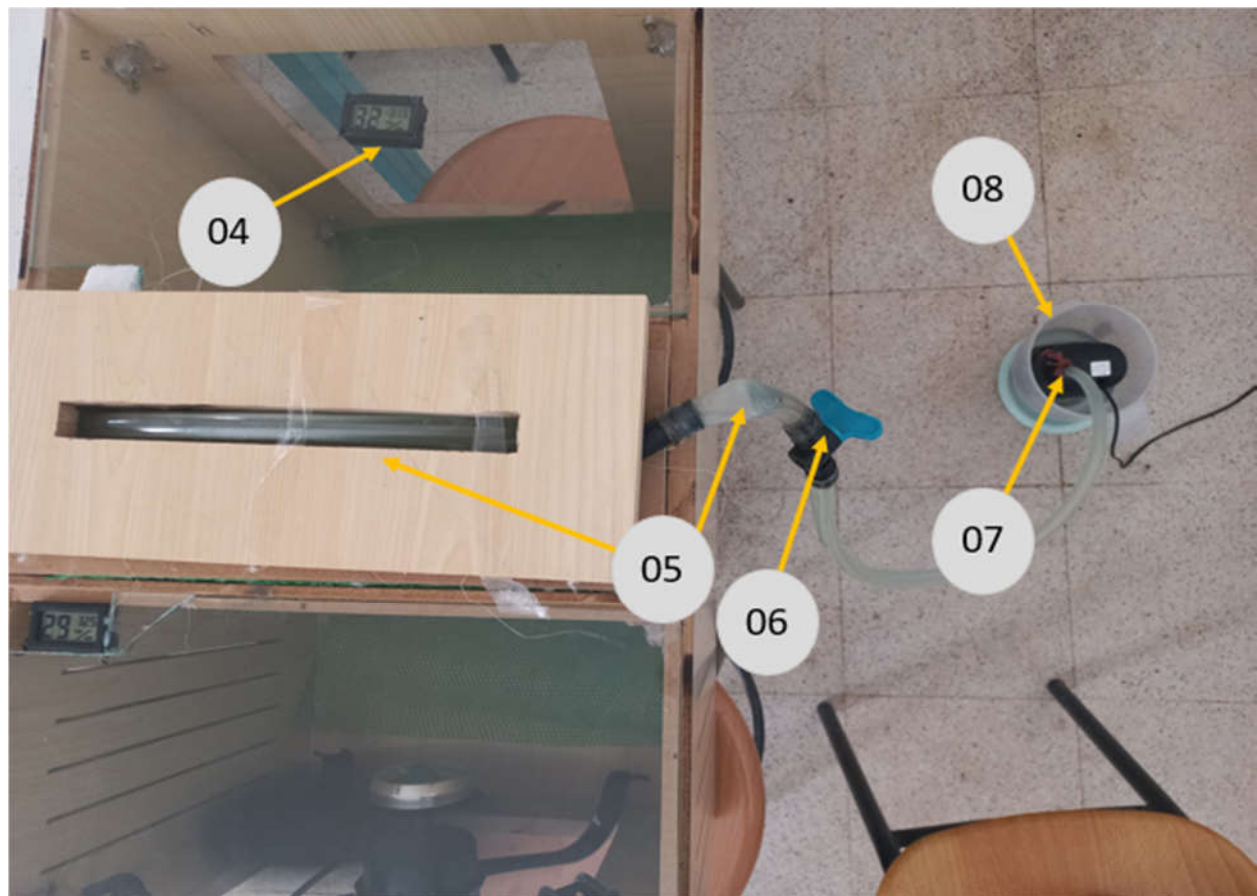
Figure 0-14 Top view of the prototype's components

Table 10 Definition of prototype components

No.	Component Description
01	Axial fan
02	Evaporative pad location
03	Water return pipe
04	Temperature and humidity sensors
05	Irrigation system
06	Valve
07	Water pump

08	Water tank

5.2.7 Reference Notes on Thermal and Humidity Response

An initial test was conducted using the prototype in indoor ambient conditions. After just one minute of operation, the system showed a significant thermal effect: 2°C decrease in air temperature and 4% increase in relative humidity. The evaporative pad was only 0.16 m thick and the performance continued to improve, with the temperature difference reaching 4°C while the humidity difference increased to 6%, representing a promising design for improving the performance of a vapor air cooler.

5.3 Advantages and Recommendations

- The system falls within the framework of sustainable development systems
- Environmentally friendly
- Proven effective in hot and dry environments
- The system is subject to further development in the future using artificial intelligence algorithms
- The system is energy independent by connecting it to renewable energy systems
- Simple and uncomplicated construction, ensuring easy maintenance
- Lower energy consumption compared to other systems

5.4 Conclusion

In this chapter, a comprehensive numerical analysis supported by Python programming and psychrometric computations was conducted to evaluate the thermal performance of the cooling device. By leveraging experimental data, we assessed sensible, latent, and total heat fluxes, and derived key performance indicators such as efficiency and EER. Additionally, preliminary steps toward AI integration were implemented, enabling the prediction of system performance over extended periods. These findings validate the experimental approach and open the path toward intelligent, self-adaptive passive cooling systems.

General conclusion

General conclusion

This thesis presented a comprehensive study on the design, development, and optimization of a passive evaporative cooling system for buildings, integrating natural materials and artificial intelligence. Through a structured approach combining theoretical analysis, experimental validation, numerical simulation, and intelligent prediction, the work addressed both environmental and technical challenges associated with traditional cooling systems.

The research began by establishing a solid theoretical foundation of passive cooling principles and the physics of heat transfer, followed by an in-depth investigation of natural plant fibers, particularly cotton and sisal as sustainable evaporative pad materials. These fibers were selected not only for their ecological and economic advantages but also for their thermal and hygroscopic properties, which proved critical for enhancing system performance.

A meticulously designed experimental setup enabled the testing of multiple configurations under controlled conditions, evaluating the influence of fiber type, pad thickness, and airflow rate. The findings highlighted cotton's superior water and moisture retention capacity, especially at higher airflow rates, while sisal offered benefits in airflow permeability, structural durability, and greater cooling efficiency. Therefore, a hybrid evaporative pad consisting of 80% sisal and 20% cotton was tested, with activated carbon added to the cotton to filter air and absorb moisture, achieving the best results.

In parallel, a numerical analysis using Python and psychrometric modeling provided deeper insight into the system's thermal behavior, validating experimental trends and supporting performance optimization. Notably, the integration of AI-based predictive models demonstrated the potential for real-time monitoring and performance forecasting, marking a key step toward intelligent and adaptive cooling systems for smart buildings.

The prototype developed in the final phase successfully embodied the project's core objectives: sustainability, simplicity, cost-effectiveness, and adaptability to varying environmental conditions. The system's design not only reduced reliance on mechanical HVAC systems but also showcased the feasibility of combining traditional cooling concepts with modern digital tools.

In conclusion, this work contributes meaningfully to the field of sustainable building technologies by demonstrating that passive cooling can be reimagined through the lens of modern materials and intelligent modeling.

Future research may focus on expanding the AI integration for autonomous system control, exploring additional natural fiber composites, and scaling the system for larger architectural applications. With the growing urgency of climate change and energy efficiency, such innovations are more relevant than ever.

References

References
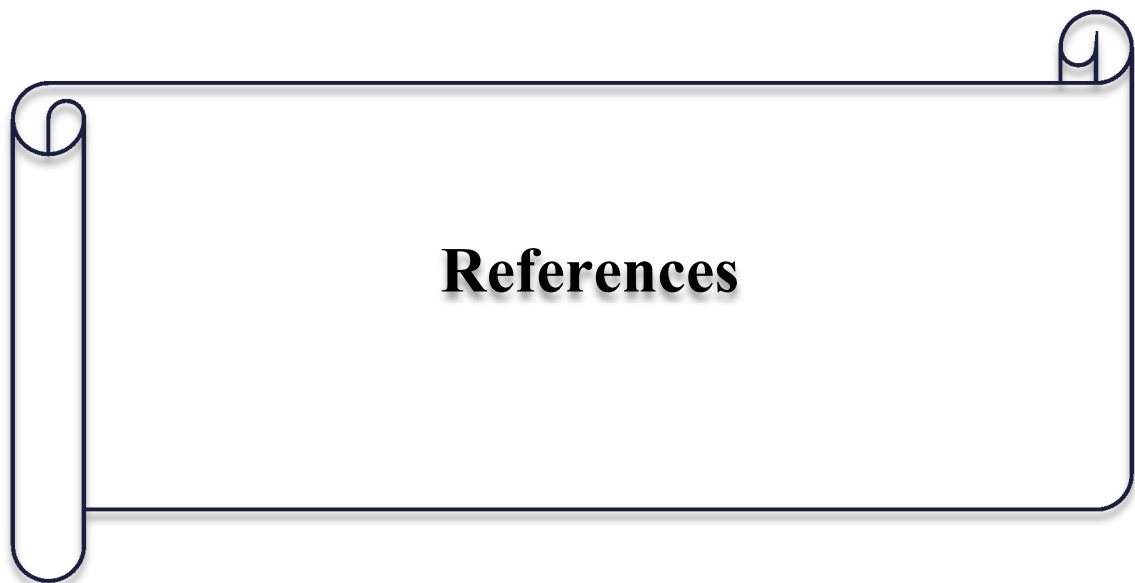
[[1]] H. M. Taleb, "Using passive cooling strategies to improve thermal performance and reduce energy consumption of residential buildings in U.A.E. buildings," *Front. Archit. Res.*, vol. 3, pp. 154–165, Jun. 2014, doi: 10.1016/j.foar.2014.01.002.

[2] Ł. Stefaniak, S. Szczęśniak, J. Walaszczyk, K. Rajski, K. Piekarska, and J. Danielewicz, "Challenges and future directions in evaporative cooling: Balancing sustainable cooling with microbial safety," *Build. Environ.*, vol. 267, Jan. 2025, doi: 10.1016/j.buildenv.2024.112292.

[3] A. M. Hassan, H. Lee, and S. Oh, "Challenges of passive cooling techniques in buildings: A critical review for identifying the resilient technique," Jun. 2016, *Penerbit UTM Press*. doi: 10.11113/jt.v78.5748.

[4] H. Farzaneh, L. Malehmirchegini, A. Bejan, T. Afolabi, A. Mulumba, and P. P. Daka, "Artificial intelligence evolution in smart buildings for energy efficiency," Jan. 2021, *MDPI AG*. doi: 10.3390/app11020763.

[5] "Knowledge hub," https://communes-vertes.org/reseaux-ee/knowledge-hub/climatisation/le-refroidissement-passif/.

[6] G. van Rossum, Python Tutorial, CWI. msterdam, 1991.

[7] J. VanderPlas, "Python Data Science Handbook," https://jakevdp.github.io/PythonDataScienceHandbook/.

[8] P. S. Foundation, "Python Documentation." [Online]. Available: https://docs.python.org

[9] M. Lutz, Learning Python, 4th Edition, vol. 78, no. 1. 2009.

[10] S. R. and V. Mirjalili, Python Machine Learning: Machine Learning and Deep Learning with Python, Scikit-learn, and TensorFlow 2. UK, 2019.

[11] "Armstrong Air And Electric," https://armstrongairinc.com/passive-cooling-hvac-system-will-save-money/.

[12] "Refroidissement passif | Guide Bâtiment Durable," https://guidebatimentdurable.brussels/construction-dun-commerce-dune-creche-projet-cameleon/refroidissement-passif.

[13] F. Flourentzou, J. Van Der Maas, and C. A. Roulet, "Natural ventilation for passive cooling:

References

Measurement of discharge coefficients," *Energy Build.*, vol. 27, pp. 283–292, 1998, doi: 10.1016/s0378-7788(97)00043-1.

[14] H. Y. Woo, Y. Choi, H. Chung, D. W. Lee, and T. Paik, "Colloidal inorganic nano- and microparticles for passive daytime radiative cooling," Dec. 2023, *Korea Nano Technology Research Society*. doi: 10.1186/s40580-023-00365-7.

[15] A. Mohammed *et al.*, "Reducing the Cooling Loads of Buildings Using Shading Devices: A Case Study in Darwin," *Sustain.*, vol. 14, Apr. 2022, doi: 10.3390/su14073775.

[16] "Shading technology," https://energyeducation.ca/encyclopedia/Shading_technology.

[17] "Thermal mass," https://www.yourhome.gov.au/passive-design/thermal-mass.

[18] "The Importance of Thermal Mass – By Eco-Expert Tim Pullen," https://acarchitects.biz/self-build-blog/thermal-mass.

[19] "Earth Tubes - Climate Action Accelerator," https://climateactionaccelerator.org/solutions/earth-tubes/.

[20] Z. Emdadi, N. Asim, M. A. Yarmo, R. Shamsudin, M. Mohammad, and K. Sopian, "Green material prospects for passive evaporative cooling systems: Geopolymers," 2016, *MDPI AG*. doi: 10.3390/en9080586.

[21] "What is evaporative cooling and how does it work?," https://www.oxy-com.com/what-is-evaporative-cooling.

[22] "Your Guide to Evaporative Cooling and Energy Savings," https://www.condair.com/humidifiernews/blog-overview/your-guide-to-evaporative-cooling-and-energy-savings.

[23] "Natural, mechanical and hybrid ventilation compared," https://ves.co.uk/hvac-solutions/school-ventilation/insights/natural-mechanical-hybrid-ventilation-compared/.

[24] N. Kapilan, A. M. Isloor, and S. Karinka, "A comprehensive review on evaporative cooling systems," Jun. 2023, *Elsevier B.V.* doi: 10.1016/j.rineng.2023.101059.

[25] "Direct vs Indirect Evaporative Cooling: What is the Difference," https://www.evapoler.com/difference-between-direct-and-indirect-evaporative-cooling/.

[26] P. Glanville and A. Kozlov, "(PDF) Dew point evaporative cooling: Technology review and fundamentals,"

References

https://www.researchgate.net/publication/279718773_Dew_point_evaporative_cooling_T echnology_review_and_fundamentals.

[27] "Indirect Evaporative Cooling," https://www.drenergysaver.com/cooling-systems/evaporative-cooling/indirect-evaporative-cooling.html.

[28] E. Kozubal and S. Slayzak, "Coolerado 5 Ton RTU Performance: Western Cooling Challenge Results (Revised)," Nov. 2010. doi: 10.2172/965116.

[29] C. Kian Jon, M. R. Islam, N. Kim Choon, and M. W. Shahzad, "Dew-Point Evaporative Cooling Systems," in *Green Energy and Technology*, Springer Science and Business Media Deutschland GmbH, 2021, pp. 53–130. doi: 10.1007/978-981-15-8477-0_3.

[30] V. Vakiloroaya, M. Khatibi, Q. P. Ha, and B. Samali, "New integrated hybrid evaporative cooling system for HVAC energy efficiency improvement," in *2011 IEEE/SICE International Symposium on System Integration, SII 2011*, 2011, pp. 772–778. doi: 10.1109/SII.2011.6147546.

[31] "15.1: Structure of Water," https://chem.libretexts.org/Bookshelves/Introductory_Chemistry/Introductory_Chemistry_ (CK-12)/15%3A_Water/15.01%3A_Structure_of_Water.

[32] "Physical and Chemical Properties of Water," https://unacademy.com/content/neet-ug/study-material/chemistry/physical-and-chemical-properties-of-water/.

[33] "Heat transfer | Definition & Facts | Britannica," https://www.britannica.com/science/heat-transfer.

[34] "Convection - Définition et Explications," https://www.techno-science.net/glossaire-definition/Convection.html.

[35] "Convection Diagram," https://quizlet.com/gb/513798227/convection-diagram/.

[36] "Natural Convection."

[37] K. Nagesha, K. Srinivasan, and T. Sundararajan, "Heat transfer characteristics of single circular jet impinging on a flat surface with a protrusion," *Heat Mass Transf. und Stoffuebertragung*, vol. 56, pp. 1901–1920, Jun. 2020, doi: 10.1007/s00231-020-02814-z.

[38] "Forced convection," https://energyeducation.ca/encyclopedia/Forced_convection.

[39] U. K. Merbah -Ouargla, "République algérienne Démocratique et populaire Ministère de

References

l'Enseignement Supérieur et de la Scientifique."

[40] U. C. for S. Education, "Center forScience Education," https://scied.ucar.edu/learning-zone/earth-system/conduction.

[41] "Conduction, Convection and Radiation – Science Ready," https://scienceready.com.au/pages/conduction-convection-and-radiation.

[42] "What is heat conduction?," https://phys.org/news/2014-12-what-is-heat-conduction.html.

[43] I. Cartagenas, "Radiation Heat Transfer - Definition and Examples," https://thermtest.com/examples-of-radiation-heat-transfer.

[44] "What Is Heat Transfer (Heat Flow)? Complete Guide | SimScale," https://www.simscale.com/docs/simwiki/heat-transfer-thermal-analysis/what-is-heat-transfer/.

[45] "Heat of Vaporization," https://chem.libretexts.org/Bookshelves/Physical_and_Theoretical_Chemistry_Textbook_Maps/Supplemental_Modules_(Physical_and_Theoretical_Chemistry)/Thermodynamics/Energies_and_Potentials/Enthalpy/Heat_of_Vaporization.

[46] A. BenGaid, Et, and O. Ben Dehina, "Évaluation des Performances du Système De Refroidissement par Evaporation d'Eau dans les Régions Arides Utilisant des Fibres Naturelles," 2024.

[47] M. R. Sanjay, G. R. Arpitha, L. L. Naik, K. Gopalakrishna, and B. Yogesha, "Applications of Natural Fibers and Its Composites: An Overview," *Nat. Resour.*, vol. 07, pp. 108–114, 2016, doi: 10.4236/nr.2016.73011.

[48] "What are Natural Fiber Composites? Basics Applications and Future Potentials," https://www.addcomposites.com/post/what-are-natural-fiber-composites-basics-applications-and-future-potentials.

[49] "Natural fiber | Definition, Uses, & Facts | Britannica," https://www.britannica.com/topic/natural-fiber.

[50] "Untitled Document," https://iopscience.iop.org/article/10.1088/1757-899X/736/5/052017/pdf.

[51] "International Fiber Journal," https://www.fiberjournal.com/author/jasonfinnis/.

References

[52] R. H. Marchessault and P. R. Sundararajan, "Cellulose," 1983. doi: 10.1016/b978-0-12-065602-8.50007-8.

[53] J. Koh, "Dyeing of cellulosic fibres," in *Handbook of Textile and Industrial Dyeing*, Elsevier, 2011, pp. 129–146. doi: 10.1533/9780857094919.1.129.

[54] I. F. H. AI-Jawhari, "Nanocellulose for Sustainable Future Applications," in *Handbook of Nanomaterials and Nanocomposites for Energy and Environmental Applications*, Springer International Publishing, 2020, pp. 1–12. doi: 10.1007/978-3-030-11155-7_16-1.

[55] S. Paramjeet, P. Manasa, and N. Korrapati, "Biofuels: Production of fungal-mediated ligninolytic enzymes and the modes of bioprocesses utilizing agro-based residues," Apr. 2018, *Elsevier Ltd*. doi: 10.1016/j.bcab.2018.02.007.

[56] M. J. Peña, S. T. Tuomivaara, B. R. Urbanowicz, M. A. O'Neill, and W. S. York, "Methods for structural characterization of the products of cellulose- and xyloglucan-hydrolyzing enzymes," in *Methods in Enzymology*, vol. 510, Academic Press Inc., 2012, pp. 121–139. doi: 10.1016/B978-0-12-415931-0.00007-0.

[57] F. Xu, "Structure, Ultrastructure, and Chemical Composition. Fundamentals and Applications.," in *Cereal Straw as a Resource for Sustainable Biomaterials and Biofuels: Chemistry, Extractives, Lignins, Hemicelluloses and Cellulose*, Elsevier, 2010, pp. 9–47. doi: 10.1016/B978-0-444-53234-3.00002-X.

[58] S. W. Cui, Q. Wang, and M. Zhang, "β-Glucans," *RSC Polym. Chem. Ser.*, pp. 319–345, 2011, doi: 10.3390/encyclopedia1030064.

[59] Z. Usmani *et al.*, "Ionic liquid based pretreatment of lignocellulosic biomass for enhanced bioconversion," May 2020, *Elsevier Ltd*. doi: 10.1016/j.biortech.2020.123003.

[60] "5.2c Hemicellulose," https://www.e-education.psu.edu/egee439/node/664.

[61] "Hemicelluloses: major sources, properties and applications, in "Monomers, polymers and composites from renewable resources," https://www.researchgate.net/publication/290440728_Hemicelluloses_major_sources_properties_and_applications_in_Monomers_polymers_and_composites_from_renewable_resources/citations.

[62] R. Vanholme, B. Demedts, K. Morreel, J. Ralph, and W. Boerjan, "Lignin biosynthesis and structure," *Plant Physiol.*, vol. 153, pp. 895–905, 2010, doi: 10.1104/pp.110.155119.

References

[63]   H. Nishimura, A. Kamiya, T. Nagata, M. Katahira, and T. Watanabe, "Direct evidence for α ether linkage between lignin and carbohydrates in wood cell walls," *Sci. Rep.*, vol. 8, Dec. 2018, doi: 10.1038/s41598-018-24328-9.

[64]   S. K. Ramamoorthy, M. Skrifvars, and A. Persson, "A review of natural fibers used in biocomposites: Plant, animal and regenerated cellulose fibers," Jan. 2015, *Taylor and Francis Inc.* doi: 10.1080/15583724.2014.971124.

[65]   "The Fiber and Hurd Council | Hemp Industries Association," https://thehia.org/the-fiber-council/.

[66]   D. Jones, G. O. Ormondroyd, S. F. Curling, C. M. Popescu, and M. C. Popescu, "Chemical compositions of natural fibres," in *Cereal Straw as a Resource for Sustainable Biomaterials and Biofuels: Chemistry, Extractives, Lignins, Hemicelluloses and Cellulose*, Elsevier, 2010, pp. 23–58. doi: 10.1016/B978-0-08-100411-1.00002-9.

[67]   T. Fatma, "Surface Modification of Bast-Based Natural Fibers through Environment Friendly Methods," in *Generation, Development and Modifications of Natural Fibers*, IntechOpen, 2020. doi: 10.5772/intechopen.85693.

[68]   Y. Li, L. Xie, and H. Ma, "Permeability and mechanical properties of plant fiber reinforced hybrid composites," *Mater. Des.*, vol. 86, pp. 313–320, Dec. 2015, doi: 10.1016/j.matdes.2015.06.164.

[69]   K. Suzuki, I. Kimpara, H. Saito, and K. Funami, "Cross-sectional area measurement and monofilament strength test of kenaf bast fibers," *Zair. Soc. Mater. Sci. Japan*, vol. 54, pp. 887–894, Aug. 2005, doi: 10.2472/jsms.54.887.

[70]   M. Preisner, W. Wojtasik, A. Kulma, M. Żuk, and J. Szopa, "Flax Fiber," in *Kirk-Othmer Encyclopedia of Chemical Technology*, Wiley, 2014, pp. 1–32. doi: 10.1002/0471238961.0612012401110914.a01.pub2.

[71]   "Flax | Description, Fiber, Flaxseed, Uses, & Facts | Britannica," https://www.britannica.com/plant/flax.

[72]   "Linen," https://oecotextiles.blog/2010/06/30/linen/.

[73]   textile-engineering, "Flax Fibre: Types, Chemical Composition, Properties and Uses," https://textileengineering.net/flax-fibre-types-properties-and-uses/.

[74]   "Flax Fiber | Chemical Composition | Physical Properties and Chemical Properties | Uses

References

and Application of Flax Fiber | Textile Study Center," https://textilestudycenter.com/flax-fiber-properties/.

[75] P. Madhu, J. Praveenkumara, M. R. Sanjay, S. Siengchin, and S. Gorbatyuk, "Introduction to bio-based fibers and their composites," in *Advances in Bio-Based Fiber: Moving Towards a Green Society*, Elsevier, 2021, pp. 1–20. doi: 10.1016/B978-0-12-824543-9.00014-1.

[76] A. Hiremath and T. Sridhar, "Use of Bio-Fibers in Various Practical Applications," in *Encyclopedia of Renewable and Sustainable Materials: Volume 1-5*, vol. 1–5, Elsevier, 2020, pp. 931–935. doi: 10.1016/B978-0-12-803581-8.11116-6.

[77] H. Savastano, S. F. Santos, and V. Agopyan, "Sustainability of vegetable fibres in construction," in *Sustainability of Construction Materials*, Elsevier Ltd., 2009, pp. 55–81. doi: 10.1533/9781845695842.55.

[78] W. Wang, Z. Cai, and J. Yu, "Study on the Chemical Modification Process of Jute Fiber," *J. Eng. Fiber. Fabr.*, vol. 3, p. 155892500800300, Jun. 2008, doi: 10.1177/155892500800300203.

[79] R. Mia, M. A. Islam, B. Ahmed, and J. I. A. Mojumdar, "Woolenization of Jute Fibre," *Eur. Sci. Journal, ESJ*, vol. 13, p. 314, Oct. 2017, doi: 10.19044/esj.2017.v13n30p314.

[80] M. I. Kiron, "Types, Classification and Chemical Composition of Jute Fiber," https://textilelearner.net/types-and-classification-of-jute-fiber/.

[81] T. K. G. Roy, D. Sur, and D. Nag, "Chemistry of Jute and Its Applications," 2022, pp. 37–51. doi: 10.1007/978-3-030-91163-8_3.

[82] textileblog, "Physical, Chemical and Mechanical Properties of Jute Fibre," https://www.textileblog.com/properties-of-jute-fibre/.

[83] R. A. Majid, H. Ismail, and N. Hayeemasae, "Poly(Vinyl Chloride)/Epoxidized Natural Rubber/Kenaf Powder Composites," in *Natural Fiber Reinforced Vinyl Ester and Vinyl Polymer Composites: Development, Characterization and Applications*, Elsevier, 2018, pp. 283–312. doi: 10.1016/B978-0-08-102160-6.00015-9.

[84] M. M. A. Sayeed *et al.*, "Assessing Mechanical Properties of Jute, Kenaf, and Pineapple Leaf Fiber-Reinforced Polypropylene Composites: Experiment and Modelling," *Polymers (Basel).*, vol. 15, Feb. 2023, doi: 10.3390/polym15040830.

References

[85]   G. Tronci and S. J. Russell, "Raw materials and polymer science for nonwovens," in *Handbook of Nonwovens, Second Edition*, Elsevier, 2022, pp. 49–88. doi: 10.1016/B978-0-12-818912-2.00005-7.

[86]   J. P. Manaia, A. T. Manaia, and L. Rodriges, "Industrial hemp fibers: An overview," *Fibers*, vol. 7, 2019, doi: 10.3390/fib7120106.

[87]   A. K. Both, D. Choudhry, and C. L. Cheung, "Valorization of hemp fibers into biocomposites via one-step pectin-based green fabrication process," *J. Appl. Polym. Sci.*, vol. 140, Mar. 2023, doi: 10.1002/app.53586.

[88]   S. N. Pandey, "Ramie fibre: Part I. Chemical composition and chemical properties. A critical review of recent developments," *Text. Prog.*, vol. 39, pp. 1–66, Mar. 2007, doi: 10.1080/00405160701580055.

[89]   M. Cai *et al.*, "Mechanical Stability of Carbon/Ramie Fiber Hybrid Composites Under Hygrothermal Aging," *Appl. Compos. Mater.*, 2024, doi: 10.1007/s10443-024-10211-6.

[90]   *Dietary Reference Intakes for Energy, Carbohydrate, Fiber, Fat, Fatty Acids, Cholesterol, Protein, and Amino Acids (Macronutrients)*. National Academies Press, 2005. doi: 10.17226/10490.

[91]   "- Physiochemical Properties of Wheat Bran and Related Application Challenges," in *Dietary Fiber and Health*, CRC Press, 2012, pp. 388–403. doi: 10.1201/b12156-29.

[92]   A. Kamal-Eldin *et al.*, "Dietary fiber components, microstructure, and texture of date fruits (Phoenix dactylifera, L.)," *Sci. Rep.*, vol. 10, Dec. 2020, doi: 10.1038/s41598-020-78713-4.

[93]   S. N. Sarmin, "Anatomical structure of coir fibers," in *Coir Fiber and its Composites: Processing, Properties and Applications*, Elsevier, 2022, pp. 43–54. doi: 10.1016/B978-0-443-15186-6.00033-3.

[94]   Y. Guo, P. Tataranni, and C. Sangiorgi, "The use of fibres in asphalt mixtures: A state of the art review," Aug. 2023, *Elsevier Ltd*. doi: 10.1016/j.conbuildmat.2023.131754.

[95]   M. A. Esmeraldo *et al.*, "Dwarf-green coconut fibers: A versatile natural renewable raw bioresource. Treatment, morphology, and physicochemical properties," *BioResources*, vol. 5, pp. 2478–2501, Nov. 2010, doi: 10.15376/biores.5.4.2478-2501.

[96]   M. Raji, S. Nekhlaoui, C. A. Kakou, H. Essabir, R. Bouhfid, and A. el kacem Qaiss,

References

"Thermal properties of coir fiber-reinforced polymer composites," in *Coir Fiber and its Composites: Processing, Properties and Applications*, Elsevier, 2022, pp. 191–220. doi: 10.1016/B978-0-443-15186-6.00099-0.

[97] A. K. Both, J. A. Linderman, G. Madireddy, M. A. Helle, and C. L. Cheung, "Valorization of coco coir into biocomposite materials through water-based chemistry," *Ind. Crops Prod.*, vol. 178, Apr. 2022, doi: 10.1016/j.indcrop.2022.114563.

[98] "Comprehensive Guide to Plant Fibers: Types, Properties, and Examples | Wikifarmer," https://wikifarmer.com/library/en/article/comprehensive-guide-to-plant-fibers-types-properties-and-examples.

[99] F. G. B. Los, A. A. F. Zielinski, J. P. Wojeicchowski, A. Nogueira, and I. M. Demiate, "Beans (Phaseolus vulgaris L.): whole seeds with complex chemical composition," Feb. 2018, *Elsevier Ltd*. doi: 10.1016/j.cofs.2018.01.010.

[100] textile-engineering, "Cotton Fibre: Types, Properties and Uses," https://textileengineering.net/cotton-fibre-types-properties-and-uses/.

[101] M. Razavi, "Bio-based nanostructured materials," in *Nanobiomaterials: Nanostructured Materials for Biomedical Applications*, Elsevier Inc., 2018, pp. 17–39. doi: 10.1016/B978-0-08-100716-7.00002-7.

[102] S. Khandaker, M. M. Bashar, A. Islam, M. T. Hossain, S. H. Teo, and M. R. Awual, "Sustainable energy generation from textile biowaste and its challenges: A comprehensive review," Apr. 2022, *Elsevier Ltd*. doi: 10.1016/j.rser.2021.112051.

[103] "Cotton fibers: Review of structure, properties, types and uses," https://sootter.com/blog/cotton-fibers-review-of-structure-properties-types-and-uses/.

[104] A. V. Kiruthika, "A review of leaf fiber reinforced polymer composites," Dec. 2024, *Institute for Ionics*. doi: 10.1186/s44147-024-00365-2.

[105] M. Siti Alwani, A. Khalil, N. Islam, W. O. W. Nadirah, and R. Dungani, "Fundamental approaches for the application of pineapple leaf fiber in high performance reinforced composites", doi: 10.14314/polimery.2014.7.

[106] textile-engineering, "Chemical Composition, Properties and Uses of Sisal Fibres," https://textileengineering.net/properties-and-uses-of-sisal-fibres/.

[107] O. S. Abiola, W. K. Kupolati, E. R. Sadiku, and J. M. Ndambuki, "Utilisation of natural

References

fibre as modifier in bituminous mixes: A review," Mar. 2014. doi: 10.1016/j.conbuildmat.2013.12.037.

[108] S. M. Hejazi, M. Sheikhzadeh, S. M. Abtahi, and A. Zadhoush, "A simple review of soil reinforcement by using natural and synthetic fibers," May 2012. doi: 10.1016/j.conbuildmat.2011.11.045.

[109] "Recent Advances on Coal Ash Particulates' Fortified Glossy Finish Polymer Composites," https://www.researchgate.net/publication/277304586_Recent_Advances_on_Coal_Ash_P articulates'_Fortified_Glossy_Finish_Polymer_Composites#pf9.

[110] Y. Li and Y. O. Shen, "The use of sisal and henequen fibres as reinforcements in composites," in *Biofiber Reinforcements in Composite Materials*, Elsevier Inc., 2015, pp. 165–210. doi: 10.1533/9781782421276.2.165.

[111] J. A. Lolo, S. Nikmatin, H. Alatas, D. D. Prastyo, and A. Syafiuddin, "Fabrication of biocomposites reinforced with natural fibers and evaluation of their physio-chemical properties," *Biointerface Res. Appl. Chem.*, vol. 10, pp. 5803–5808, 2020, doi: 10.33263/BRIAC104.803808.

[112] J. K. Fink, "Unsaturated Polyester Resins," in *Reactive Polymers Fundamentals and Applications*, Elsevier, 2013, pp. 1–48. doi: 10.1016/B978-1-4557-3149-7.00001-2.

الجمهورية الجزائرية الديمقراطية الشعبية

وزارة التعليم العالي والبحث العلمي

<table>
<tr><td>Université de Ghardaïa</td><td>جامعة غرداية</td></tr>
<tr><td>Faculté des Sciences</td><td>كلية العلوم والتكنولوجيا</td></tr>
<tr><td>et de la technologie</td><td>قسم :الآلية والكهروميكانيك</td></tr>
</table>

غرداية في: .2025 / 07 / 02

شعبة :......... ميكانيكية ....

تخصص:......... طاقة متجددة في الميكانيك ....

شهادة ترخيص بالتصحيح والايداع:

انا الاستاذ(ة)......... بكريجمعة جوزير ....

بصفتي المشرف المسؤول عن تصحيح مذكرة تخرج (ليسانس/ماستر/دكتورا) المعنونة ب:

Design and optimization of a new passive building cooling system
using water evaporation : A numerical and experimental approach
Guided by artificial intelligence

من انجاز الطالب (الطلبة):

.... بوزكينة شمس الدين ....

....

التي نوقشت بتاريخ : ....24 / 06 / 2025.........

اشهد ان الطالب/الطلبة قد قام /قاموا بالتعديلات والتصحيحات المطلوبة من طرف لجنة المناقشة وقد تم التحقق من ذلك من طرفنا

وقد استوفت جميع الشروط المطلوبة.

مصادقة رئيس القسم

قسم الآلية والكهروميكانيك

عزاوي محمد

امضاء المسؤول عن التصحيح